THE UNIVERSITY OF CALGARY

A FREQUENCY DOMAIN MEASUREMENT SYSTEM FOR INDOOR ULTRAHIGH FREQUENCY RADIO PROPAGATION STUDIES

BY

GERALD DALE MORRISON

A THESIS

SUBMITTED TO THE FACULTY OF GRADUATE STUDIES

IN PARTIAL FULFILLMENT OF THE REQUIREMENTS FOR THE

DEGREE OF MASTER OF SCIENCE

DEPARTMENT OF ELECTRICAL AND

COMPUTER ENGINEERING

CALGARY, ALBERTA

DECEMBER, 1991

ISBN 0-315-75150-9

THE UNIVERSITY OF CALGARY

FACULTY OF GRADUATE STUDIES

The undersigned certify that they have read, and recommend to the Faculty of Graduate Studies for acceptance, a thesis entitled, *" A Frequency Domain Measurement System for Indoor Ultrahigh Frequency Radio Propagation Studies"*, submitted by Gerald Dale Morrison in partial fulfillment of the requirements for the degree of Master of Science.

Supervisor - Dr. M. Fattouche
Dept. of Elec. and Comp. Engg.

Dr. R. H. Johnston
Dept. of Elec. and Comp. Engg.

Dr. M. R.Smith
Dept. of Elec. and Comp. Engg.

Dr. E. J. Krakiwsky
Dept. of Surveying Engineering

Date: December 3rd, 1991.

ABSTRACT

The rapid growth and successful implementation of cellular communications have caused service providers to look at new systems. These systems will need to be portable, light weight, handle a large number of users, and provide a wide variety of services. One area that can meet these demands and is therefore receiving considerable attention is digital inbuilding communications. It is expected that over the next several years indoor wireless will be heavily used by providers of such services as wireline, cellular, paging, local area networks, personal communications networks, and cordless phones.

A vital factor in the development and implementation of any indoor wireless system is a comprehensive knowledge of radio frequency propagation behavior in different types of buildings. The most direct method for determining this behavior is to apply a radio frequency signal to the environment and make empirical observations. This method requires an experimental measurement system and has been applied successfully by several researchers in two types of propagation studies known as narrowband and wideband.

This thesis describes the implementation of a frequency domain measurement system that performs both narrowband and wideband measurements. The focus of this study is to evaluate the performance of the measurement system and to examine results from different measurements .

The measurement system collects the transfer function of the indoor channel and the impulse response is obtained from the Fourier transform. It will be shown that the frequency domain measurement system has a straight forward implementation that is available to any researcher with access to a network analyzer. The measurement system is not restricted to a

specific frequency and yields accurate magnitude and phase information. It will also be shown that the system has a dynamic range and an equivalent temporal resolution that would be difficult to achieve with current time domain systems. Additionally, the system has good rejection to interfering transmissions.

The information reported in this thesis provides a tool that will hopefully assist communication system engineers and manufacturers in obtaining a better understanding of the complex indoor radio environment.

ACKNOWLEDGEMENTS

I would like to acknowledge the following people and organizations for their contributions to this thesis project:

Dr. Michel Fattouche, my supervisor, whose complete involvement in the project provided me with encouragement, support, and helpful suggestions. TR*Labs* provided me with a scholarship as well as office space, computer equipment, and word processing facilities. The University of Calgary also provided financial support in the form of a graduate teaching assistantship. NovAtel Communications Limited provided access to the measurement equipment and to the measurement area reported in this project. AGT Limited supported the project and provided access to their office for the purpose of conducting measurements. Hatim Zaghloul of AGT Limited initially conceived the idea for the project and provided encouragement, suggestions, and support throughout the project. To all above I would like to express my gratitude.

Throughout my thesis research the following individuals provided me with thought provoking discussions: Dr. Spencer Nichols, Dr. Mike Smith, Dr. Abu Sesay, and Dr. Ron Johnston.

This thesis is dedicated to my Wife and Children

for their patience with me and my long hours

and also to my Parents for their support

TABLE OF CONTENTS

LIST OF TABLES

LIST OF FIGURES

LIST OF SYMBOLS AND ABBREVIATIONS

α_k	Attenuation of the kth path.
a_m	Amplitude of the mth plane wave.
A	Amperes.
AOA	Angle-of-Arrival.
ARMA	Auto Regressive Moving Average.
AWGN	Additive White Gaussian Noise.
B	Window bandwidth (frequency domain).
B_c	Coherence Bandwidth.
BW	Bandwidth.
c	Speed of light.
CW	Continuous Wave.
D	Distance.
Δ	Excess Delay.
δ	The delta function.
D_a	Interelement distance.
dB	Decibel.
D_f	Dynamic range of a frequency response.
DFT	Discrete Fourier Transform.
D_I	Dynamic range of an impulse response.
D_N	Dynamic sensitivity of the network analyzer..
Δt	Increment of sample time.
DUT	Device Under Test.
EM	Electromagnetic.
ϕ	Phase.
$F(\tau)$	Narrowband response of the channel.

f_c	Center frequency.
f_d	Difference frequency.
FFT	Fast Fourier Transform.
ϕ_m	Angle-of-Arrival of the mth plane wave.
f_o	Initial frequency in a sweep.
GPIB	General Purpose Interface Bus.
$H(x,f)$	The channel transfer function as a function of position.
$h(x, \tau)$	The channel impulse response as a function of position.
η	Number of profiles.
Hz	Hertz.
I	Inphase.
IDFT	Inverse Discrete Fourier Transform.
IF	Intermediate Frequency.
IIR	Infinite Impulse Response.
ISI	Intersymbol Interference.
L	Code length.
λ	Wavelength.
LAN	Local Area Network.
LOS	Line-of-Sight.
m	Gradient (slope).
Mr	Magnitude of the channel response.
N	Number of points in a sample.
$v(f)$	Noise (frequency domain).
$v(t)$	Noise (time domain).
N_B	Noise bandwidth reduction.
N_f	Noise floor.

Np	The number of paths received.
OBS	Obstructed path.
P	Received Power.
PCN	Personal Communications Network.
P_L	Path loss.
Pr	Phase of the channel response.
PRBS	Pseudo Random Binary Sequence.
Q	Quadrature.
θ_k	Phase of the kth path.
θ_m	Electrical phase angle.
R	Chip rate.
$R(f)$	Received signal (frequency domain).
$r(t)$	Received Signal (time domain).
RF	Radio Frequency.
RMS	Root Mean Square.
s	Second.
$S(f)$	Transmitted signal (frequency domain).
$s(n,m)$	Signal at the nth element by the mth plane wave.
$s(t)$	Transmitted signal (time domain).
$S_m(\phi)$	Angle-of-Arrival Spectrum.
SNR	Signal to Noise Ratio.
T	Total time of impulse response period.
t_a	Arrival time of the first path.
TERA	Transient Error Reconstruction Analysis.
τ_g	Group delay.
t_k	Arrival time of the kth path.

τ_k	Individual path delay.
τ_m	The mean excess delay.
τ_{rms}	RMS delay Spread.
UHF	Ultrahigh Frequency.
VSWR	Voltage Standing Wave Ratio.
ω	Frequency in radians.
Ω	Ohms.
W(f)	Window function (frequency domain).
w[n]	Window coefficients
w(t)	Window function (time domain).
W_L	Window loss.
x	A point in space in the channel.
X(f)	Comb filter (frequency domain).
x(t)	Comb filter (time domain).

Multiplier Prefixes

n	nano	$\bullet 10^{-9}$
μ	micro	$\bullet 10^{-6}$
m	milli	$\bullet 10^{-3}$
c	centi	$\bullet 10^{-2}$
k	kilo	$\bullet 10^{3}$
M	Mega	$\bullet 10^{6}$
G	Giga	$\bullet 10^{9}$

CHAPTER ONE

INTRODUCTION

1.1 Objective

The rapid growth and successful implementation of cellular communications have caused service providers to look at new systems. One area that is receiving considerable attention is digital inbuilding communications. Currently, outdoor cellular communications work within buildings but the quality of reception is often poor due to signal attenuation on penetrating into the building. Also, the capacity of outdoor cells is inadequate for the number of users in a typical office building. Evidently more sophisticated systems will be needed to accommodate more users. These systems will need to be portable, light weight, and provide a large variety of services. The revenue generating potential for indoor wireless communications is tremendous [Slekys, 1990]. It is expected that over the next several years the indoor wireless market will be heavily used by providers of wireline, cellular, paging, personal communications networks (PCN), computer local area networks (LAN), and cordless phones. This is due to the realization of the convenience and cost effectiveness in providing speech and data services by radio frequency (RF) communications. Wireless systems have several advantages over traditional wireline systems. These include: i) elimination of wiring or rewiring in and around buildings, ii) giving the user uninhibited movement, iii) flexibility in moving terminals (telephone, computer, etc.), iv) cost effective maintenance, and v) better immunity to natural and man made disasters. These advantages have prompted the manufacturing industry to start development of

high performance wireless systems. For now, it appears that the future of telecommunications is in digital wireless systems.

A vital factor in the development and implementation of any indoor wireless system is a comprehensive knowledge about the electromagnetic (EM) propagation behavior of different types of building environments. These environments are usually referred to as indoor or inbuilding RF channels. The most direct method for determining the characteristic of an indoor RF channel is to apply an RF signal to it and make an empirical evaluation. This method has been successfully applied by many researchers in two types of propagation studies known as narrowband and wideband. Both methods are valuable for indoor channel characterization but typically researchers' measurement systems use one method or the other. This limits characterization of inbuilding channel parameters to one type of propagation behavior.

This thesis describes the implementation of a measurement system that performs both narrowband and wideband measurements over a wide range of frequencies. The measured data can be used to characterize the indoor RF propagation channel. The thrust of this study is to evaluate the performance of the measurement system and to examine the results from different measurement techniques. The information reported here provides a tool that will hopefully assist communication system engineers and manufacturers in obtaining a better understanding of the complex indoor radio channel environment.

1.2 The Multipath Channel

The inbuilding radio environment is very complicated. This is primarily a result of a phenomenon known as multipath fading.

Multipath fading is due to the transmitted signal being reflected off several scatterers and arriving at the receiving antenna with different time delays. This concept is depicted in figure 1.1.

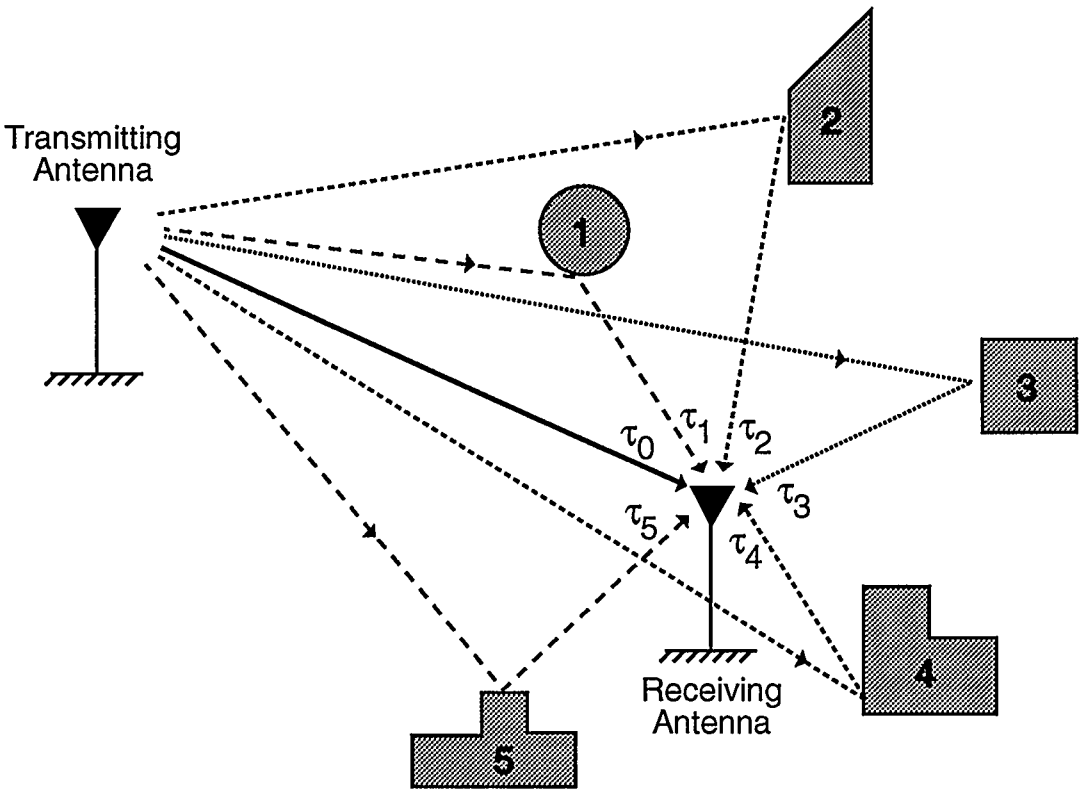

Figure 1.1: The Multipath Channel

Each delay, τ_n, comes from a different path that has an amplitude and phase associated with it. The amplitude is due to varying attenuations of the paths and phase is introduced upon reflection and if the medium of the path is different. The resultant signal at the receiving antenna is the vector sum of the multiple path signals. Fading results when the individual path phases lead to destructive interference.

The complex impulse response is a characteristic of the channel that describes the nature of multiple reflections present in the environment. It contains information about the number of reflectors in the channel as well as their associated amplitudes and phases. The impulse response is the response of the channel to a very short duration pulse (ideally a delta function) and is shown in figure 1.2 and expressed by the following equation:

$$h(x, \tau) = \sum_{k=0}^{N_p(x)-1} \alpha_k(x)\, e^{j\theta_k(x)} \bullet \delta(\tau - \tau_k(x))$$

where:

α_k is the amplitude of the k^{th} path,

θ_k is the phase of the k^{th} path,

τ_k is the delay of the k^{th} path,

N_p is the number of paths received,

x is a point in space in the channel.

This expression is based on a model pioneered by Turin [Turin,1956] and has been used in several mobile radio applications [Hashemi, 1979; Turin et al., 1972; Suzuki, 1977; Saleh and Valenzuela, 1987]. The above channel model assumes stationarity (time invariance). This assumption is used by several researchers and measurements demonstrating acceptable channel time invariance will be given in section 3.6. The effect of receiving multiple, spread-out pulses from a single transmitted pulse as depicted in figure 1.2 is known as channel spreading.

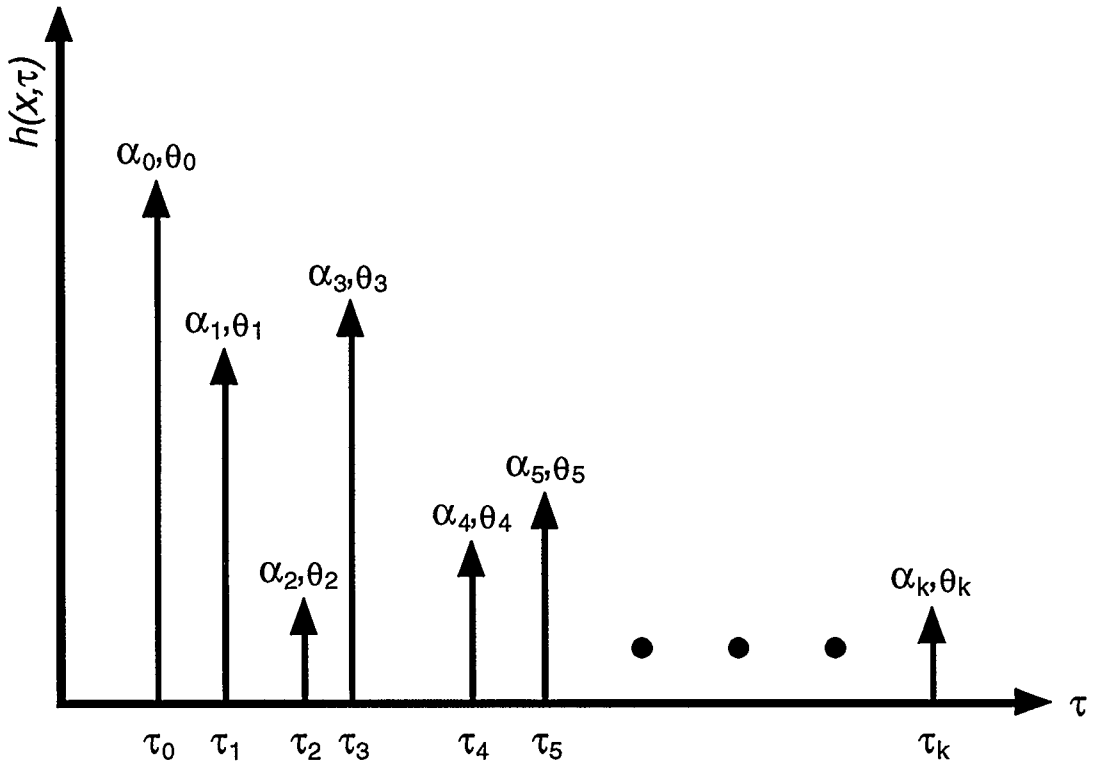

Figure 1.2: Theoretical Channel Impulse Response

The indoor environment may be assumed to be a time invariant linear channel [Turin et al.,1972; Saleh and Valenzuela,1987; Rappaport, 1989] and is modeled well by the previous expression. Time invariance means that the characteristics of the channel do not change during the transmission through it. Additionally, the channel is corrupted by additive white Gaussian noise (AWGN) [Proakis, pp. 702]. Therefore, the indoor radio propagation channel can be modeled by figure 1.3 where s(t) is the transmitted signal, ν(t)is the AWGN, and r(t) is the received signal. Note that the received signal is a result of the transmitted signal being convolved with the channel when noise is present.

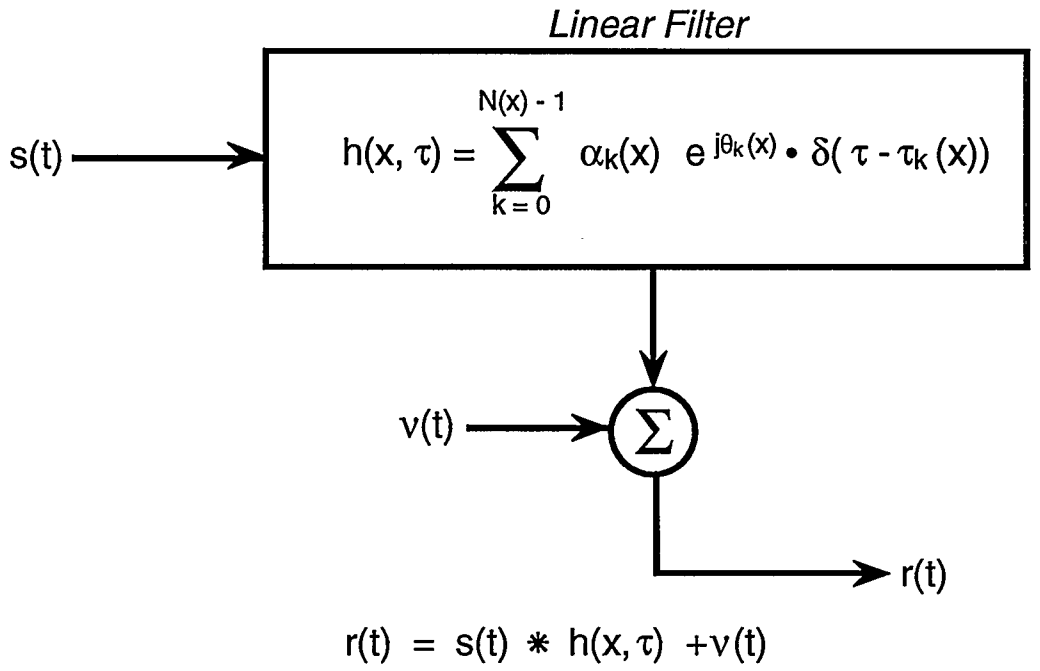

Figure 1.3: A Time Domain Indoor RF Propagation Channel Model

1.3 Channel Characterization

The way in which channel characterization is accomplished largely depends on the nature of the measurement system. Factors such as system sampling rate and frequency of operation must be considered before measurements are taken. Systems that employ the technique of measuring the channel response to a pulse of long duration are known as continuous wave (CW) systems and measure the narrowband behavior of the channel. Systems that excite the channel with a short duration pulse (a delta) measure the wideband response of the channel

There are many areas of channel characterization. Several questions a system designer may need answered include: how often a channel fades; what speeds can data be transmitted through the channel; what effects do partitions, furniture, walls, heavy equipment, etc., have on the transmission;

what differences exist among buildings of differing construction; and are both transmitter and receiver inside the building. Attempts to answer these and other pertinent questions about the indoor channel fall into the category of characterization.

1.3.1 Narrowband Measurements

When the data rate of a measurement system is below the coherence bandwidth of the channel, the narrowband response is of concern. The coherence bandwidth or correlation, B_C, is related to channel spreading. Basically it is the maximum frequency difference between two frequencies having a strong potential for correlation [Lee, pp. 18]. In terms applicable to the measurement system, the duration of the probing pulse (the system data rate) must be long enough to ensure that the channel's frequency response is flat for the required bandwidth of the pulse. There is no strict definition for B_C, but is approximated by the following expression:

$$B_c \approx \frac{1}{\Delta}$$

where Δ is the excess delay (a rigorous method for determining the spread of a channel is given in section 1.3.2).

Statistics that are generally studied with this type of measurement are small scale amplitude fluctuations, power law gradient, and path loss. For example, it has been shown that when there is not a direct path between the transmit and receive antennas, the envelope of the received signal follows a Rayleigh distribution [Proakis, pp. 706; Lee, pp. 228-230]. These statistics are

useful in predicting the area of coverage for a transmitter and outage time of a signal due to fading.

1.3.2 Wideband Measurements

Wideband measurements are of concern when the system data rate is more than the coherence bandwidth of the channel. According to Molkdar, all wideband measurements regarding the indoor channel have been conducted in the time domain [Molkdar, 1991]. This demonstrates the rarity of indoor frequency domain measurements.

The useful results from wideband measurements include: coherence bandwidth, root mean square (RMS) delay spread, average delay, excess delay (the time it takes until there is no further spreading of the pulse), and arrival time distribution. Of these, RMS delay spread is the most common form of characterization and will be defined here.

The RMS delay spread is denoted by the symbol τ_{rms} and is defined by the following equation:

$$\tau_{rms} = \left[\frac{\sum_k (t_k - \tau_m - t_a)^2 \alpha_k^2}{\sum_k \alpha_k^2} \right]^{\frac{1}{2}}$$

$$\tau_m = \frac{\sum_k (t_k - t_a)\alpha_k^2}{\sum_k \alpha_k^2}$$

where:

τ_m is the mean excess delay

t_k is the arrival time of the kth path

t_a is the arrival time of the first path

τ_{rms} is the square root of the second central moment of the power delay profile $|h(x,\tau)|^2$. It is an accurate measure of the multipath spread as it indicates the potential for intersymbol interference (ISI). ISI is related to the maximum data rate that can be placed on a channel.

There is a problem in determining τ_{rms}, however. There is no way to decide when t_k is a valid reflection or an artifact of the AWGN. Solutions to this problem have been to: i) use only the data above a specified power level, and ii) use only the data within a specified time. Neither of these methods are appropriate for removing the most noise while preserving the most data because they assume either uniform signal to noise ratios (SNR) or uniform excess delays. Consequently, a different method was developed for the analysis presented in this thesis.

1.3.2.1 A Deterministic Method for τ_{rms}

The intention in calculating τ_{rms} is to sum the powers of the multipath reflections and not the noise, so a deterministic method for calculating τ_{rms} for delay profiles with differing SNR's would be of value.

The method proposed here (and used for the results of this thesis) is statistically based. The procedure is given on the following page.

1). Calculate the mean value and the standard deviation of the AWGN. This is obtained from the known noise level that exists on the tail of an impulse response profile.

2). Assign a power level that is 2.5 to 3.5 standard deviations above the mean power value of the noise as a reference level.

3). Calculate τ_{rms} ignoring all information below the assigned reference level.

This method requires no *apriori* information about either the excess delay or the SNR of the impulse response. Additionally, it preserves the largest available SNR. By using 2.5 to 3.5 standard deviations above the mean value of the noise as a cutoff level, between 99.38% and 99.98% of the noise is removed (assuming AWGN). This does not guarantee that reflections will not be removed but if their power is low enough to be considered below the cutoff level, it cannot be decided whether it is a true reflection or a noise artifact. The only limitation to this method is that it requires a segment of the impulse response that is only noise. This is not difficult to obtain as this segment always appears beyond the excess delay.

1.4 History of Indoor UHF Propagation Studies

Propagation studies in the mobile multipath environment date back to 1952 when Young performed a narrowband comparison study at 150 MHz, 450 MHz, 900 MHz, and 3700 MHz. The measurement procedure consisted of fixing a transmitter to the top of a building and recording the magnitude of the received signal envelope from a moving vehicle [Young, 1952].

Young was able to show that the statistical distribution of the signal envelope closely agreed with a Rayleigh distribution. Young observed this phenomenon for each of the tested frequencies. By use of the central limit theorem, Young was able to conclude that the received signal envelope consisted of a large number of reflected signals. This early work pioneered what is now an intense interest in mobile communications.

Propagation studies did not move into buildings until 1958 when Rice measured the signal attenuation of 35 MHz and 150 MHz narrowband transmissions into office buildings [Rice, 1958]. Rice found that losses of more than 20 dB between the RF level inside a building and the median RF level outside the building can occur. He defined this loss as *penetration loss* and is the same as what is currently called *path loss*. This may be confusing as there is always a loss associated with the path whether there is penetration or not .

Rice's work was not expanded on until 1973 when Durante examined path loss into buildings at 900 MHz [Durante, 1973] and Shefer did the same at 450 MHz and 900 MHz [Shefer, 1973]. Durante suggested a relationship between path loss and building material when he was able to show that path loss could be reduced on floors with large areas of glass. Studies in this area were not aggressively pursued until the early 1980's when Cox along with others released several reports on path loss into buildings in the 800 MHz [Cox, Murray, and Norris, 1983, 1984, 1985] and 900 MHz range [Hoffman and Cox., 1982]. The apparent lack of interest in the indoor environment before 1982 can be attributed to: i) the interest in improving outdoor mobile radio telephone systems, ii) the lack of suitable technology for developing indoor radio systems, and iii) cellular phones were introduced in the early 1980's and much of the interest was focused on them.

The first wholly indoor channel characterization experiments were reported by Kiyoyuki and Kuwabara in 1977 [Kiyoyuki and Kuwabara, 1977] and Alexander in 1982 [Alexander, 1982,1983]. In the Kiyoyuki-Kuwabara experiment, the propagation frequencies were 250 MHz and 450 MHz. This experiment was used for preliminary microcellular evaluations for digital cordless telephones. The Alexander experiment was conducted at 900 MHz and was done to evaluate the inbuilding environment for existing cellular systems. In both experiments the envelope statistics of the channel were characterized using narrowband measurements.

The first indoor characterizations using wideband measurements were reported by Devasirvatham in 1984 [Devasirvatham, 1984]. These measurements were performed at 850 MHz and gave the magnitude of the indoor channel impulse response. Devasirvatham used these measurements to study the delay spread of the channel.

Devasirvatham's work was extended in 1987 by Bultitude to include both magnitude and phase information for wideband measurements [Bultitude, 1987].

There are many other researchers that have reported important results and have not been included in this discussion. This is because this section is intended to highlight the chronological progress of measurements for indoor channel characterization and not provide a comprehensive report of work to date. A good evaluation of indoor studies up to 1990 is found in the reference [Molkdar, 1991].

1.5 Measurement Systems

The need for high data rate systems has prompted researchers to develop new measurement systems that more accurately characterize the multipath phenomenon in the indoor environment. This suggests that improvement of dynamic range and temporal resolution would be of value. Also, depending on the nature of the study, systems that yield phase information might be more appropriate.

In this section different types of measurement systems are described. This is not a comparison of the systems but is a review of the basic principles in the measurement techniques.

1.5.1 Time Domain Measurement

Time domain measurements are overwhelmingly the most popular type of measurements when characterizing the indoor channel. In the past (before 1984), this characterization was done exclusively by measuring the envelope of a CW RF signal. This method is still applicable for determining the statistical distribution of a fading envelope and therefore an important technique. Recently, there has been an increased interest in obtaining the impulse response of the channel because it contains more information than the envelope of a CW signal.

1.5.1.1 Envelope Detection

Envelope detection systems yield amplitude information only. These systems operate by finding either the CW envelope or impulse response of a channel. The CW method was mentioned in section 1.3. The methods

described in this section are not restricted to envelope detection only but have been implemented as such by the researchers involved.

There are two methods for determining the impulse response of the channel. One method is to directly measure the impulse response by sounding the channel with a pulse of short duration and collecting the response. This method is used by Saleh and Valenzuela [Saleh and Valenzuela, 1987] and Rappaport [Rappaport and McGillem, 1987]. Both systems obtained temporal resolutions of 10 ns. A second method is to transmit a wideband signal through the channel and deconvolute this signal out of the received response. The wideband signal is generally generated by a pseudo random binary sequence (PRBS). In this case, the operation of deconvolution reduces to correlation because the auto correlation function of a PRBS approximates a delta function [Proakis, pp. 832-833]. Measurement systems that use this method are sometimes referred to as *Sliding Correlator* systems. This system was used by Cox [Cox,1972] for outdoor channel characterization and by Devasirvatham [Devasirvatham, 1984] for characterization of the indoor channel. The temporal resolution in the Devasirvatham system was 25 ns.

1.5.1.2 Inphase and Quadrature Detection

Inphase (I) and Quadrature (Q) detection is important when phase information is required. The magnitude (M_r) and phase (P_r) of the channel response is determined by the follow equations:

$$M_r = \sqrt{I^2 + Q^2}$$

$$P_r = atan\left(\frac{Q}{I}\right)$$

A sliding correlator system that has I and Q detection is used by Bultitude [Bultitude,1987]. This system has a temporal resolution of 25 ns.

Phase information has not typically been measured in the past. This is due to the assumption that the phase from multiple random scatterers is uniformly distributed on the interval $[0,2\pi)$. This assumption is used by several researchers [Turin et al., 1972; Saleh and Valenzuela, 1987; Seidel and Rappaport, 1990].

1.5.2 Frequency Domain Measurement

There is not a large contribution by researchers using frequency domain measurements. By the linear relationship of the Fourier transform, measurements made in the frequency domain and transformed to the time domain are equivalent to measurements performed in the time domain. The discrete impulse response profile is collected in the time domain and the discrete transfer function is collected in the frequency domain. The time invariant indoor channel transfer function *H(x,f)* may be represented by the following equation:

$$H(x,f) = \sum_{k=0}^{N_p(x)-1} \alpha_k(x)\, e^{j\theta_k(x)} \bullet e^{j2\pi f \tau_k(x)}$$

The same assumptions regarding linearity and time invariance of the indoor RF time domain channel also apply to the indoor frequency domain channel. The linear filter representation of figure 1.3 can also be used for the indoor frequency channel and is shown in figure 1.4. Note that by defining the

channel in the frequency domain, the received signal, R(f), is now defined as the product of the transmitted signal, S(f), and the channel plus noise. This is computationally more efficient than the convolution introduced in the time domain model given in section 1.2.

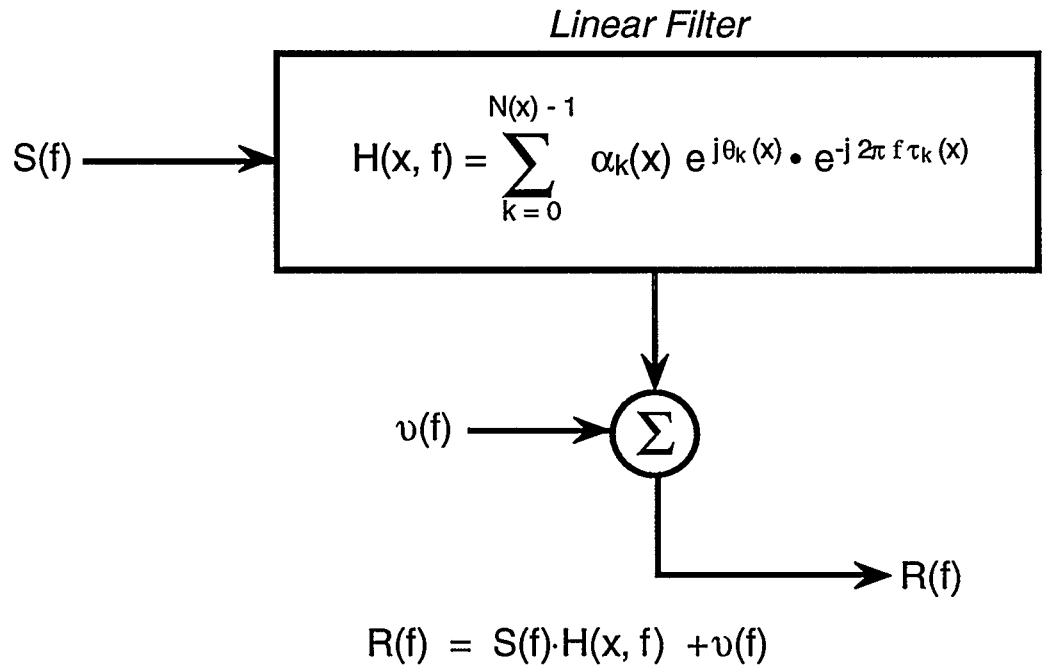

Figure 1.4: A Frequency Domain Indoor RF Propagation Channel Model

Measurements are made by exciting the channel with a signal of variable frequency. The frequency is typically swept from a start frequency to an end frequency and the channel response or transfer function is collected. The Fourier transform gives the bandlimited impulse response of the channel. The frequency resolution defines the length of the time delay profile and the frequency bandwidth defines the temporal resolution of the impulse response.

Frequency measurements have been performed for the outdoor channel [Olivier and Tiffon, 1987; Matthews, Molkdar, and Mohebbi, 1989].

Frequency measurements in the indoor environment are reported by Howard and Pahlavan [Howard and Pahlavan, 1990a]. The measurement system used by Howard and Pahlavan is similar to the measurement system reported in this thesis and was developed independently.

The temporal resolutions of the impulse responses obtained by aforementioned researchers cannot easily be determined as the data was not processed properly before taking the Fourier transform [Zaghloul, Morrison, and Fattouche, 1991a]. The error resulted from not windowing the non-periodic transfer function before applying the discrete Fourier transform which requires periodicity. This oversight causes incorrect impulse response profiles that seriously degrades any subsequent analysis. In the setup used by Howard and Pahlavan, calibration was also ignored. The effects of windowing and calibration will be described in detail in chapter two of this report.

1.6 Scope of the Present Study

The need for better measurement systems has already been justified. This report adds to the current body of knowledge by presenting a new measurement technique that will enable researchers to improve the characterization of the indoor RF propagation channel.

This study is restricted to the introduction, measurement procedure, evaluation, and capabilities of the frequency domain measurement system. This requires the characterization of indoor channel parameters but they are used for validation purposes only and are not intended as a rigorous analysis of the indoor channel.

CHAPTER TWO

THE FREQUENCY DOMAIN MEASUREMENT SYSTEM

2.1 Objective

In this chapter, the frequency domain measurement system is introduced. The experimental setup and procedure is described. Special consideration on data handling and post processing is given as well as a brief discussion on processing alternatives.

2.2 Hardware Configuration

In this section the function of the individual components of the measurement system will be described and the pertinent technical specifications will be given. The basic measurement system configuration is shown in figure 2.1. It consists of a network analyzer with an S-parameter test set, an amplifier, cables, antennas, and a personal computer. Although not shown in the hardware configuration, a spectrum analyzer is also a useful device if available.

2.2.1 HP8753A Vector Network Analyzer

The HP8753A Vector Network Analyzer is an instrument that measures the transfer and/or impedance function of a linear network through sine wave testing. Non-linear testing can also be performed but the focus of this work is on linear systems. Both narrowband (CW) and wideband (swept frequency) measurements from 300 kHz to 3 GHz are possible. The frequency resolution is 1 Hz and the output power is adjustable from -10 dBm to + 24 dBm.

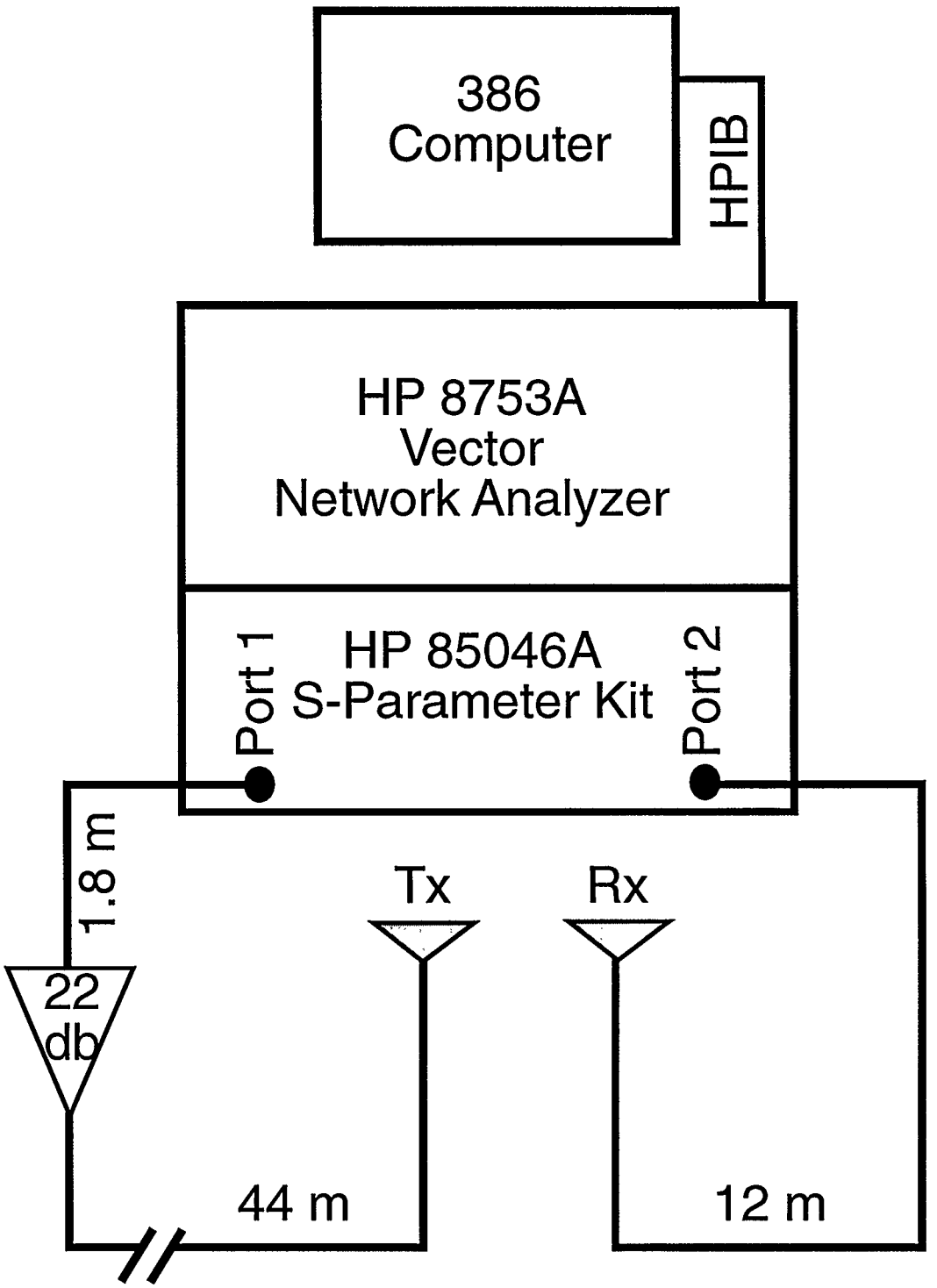

Figure 2.1: Measurement System Configuration.

The dynamic range (limited by input crosstalk) is approximately 80 dB. The network analyzer has a magnitude accuracy of ±1 dB and a phase accuracy of ±3° with -10 dBm at the input. A complete list of specifications is given in the reference [Hewlett Packard, pp. 240-244].

As implied by the word 'vector', the HP8753A can fully characterize a Device Under Test (DUT) by measuring the magnitude and phase of its response to a sine wave stimulus. The magnitude is determined from relative ratio measurements that are usually made in dB. This is the log ratio of the unknown signal (the response of the DUT) with the reference signal (the stimulus). For example, a magnitude of 0 dB means the ratio of the two signals is unity while a ratio of ± 20 dB means a voltage ratio 10:1. Phase measurements are also relative where the reference signal is considered to have zero phase. The analyzer measures the phase difference between the signal transmitted through the DUT and the reference signal.

The HP8753A measures the transfer function of the DUT by stimulating it with a high frequency sweep and sampling its response, so an understanding of how this is accomplished is beneficial. It is not practical to sample the response of the DUT at RF frequencies as this would require very fast sampling which is difficult to accomplish. A simpler method of sampling is to down-convert the RF frequencies to lower frequencies. These frequencies are called Intermediate Frequencies (IF). The IF signal is sampled after it has been filtered. The filter has an adjustable bandwidth from 10 Hz to 3 kHz. The size of the IF bandwidth affects the time it takes to sample the signal (i.e., the lower the IF bandwidth, the longer it takes to sample). For the results reported in this work, an IF bandwidth of 3 kHz was used. This resulted in a sweep

frequency time of 0.5 ms per sample (e.g., a measurement consisting of 801 samples would take 400.5 ms).

The ability of the network analyzer to measure the amplitude ratios and phase differences between the reference signal and the unknown signal (either reflected or transmitted by the DUT) implies a signal separation device. Such devices include directional couplers, bridges, power splitters, and high impedance probes.

2.2.2 HP85046A S-Parameter Test Set

The HP85046A S-Parameter Test Set is a network analyzer accessory that provides the capability to measure reflection and transmission characteristics (including S-parameters) of one or two port devices. It contains two bridges, a power splitter, and a solid-state switch to allow measurements of a two port device in both directions. A complete technical specification is given in the reference [Hewlett Packard, pp. 249]. It is pointed out here that the S-parameter test set introduces a 12 dB loss into the measurement system.

2.2.2.1 S-Parameters

Scattering parameters or S-parameters were developed to characterize linear networks at high frequencies. An excellent discussion of S-parameter design and measurement techniques can be found in the references [S-Parameter Design, 1972]. A brief summary is presented here.

S-parameters are used to characterize n-port devices at high frequencies. The number of parameters depends on the number of ports and is determined by the following relationship:

$$\text{number of S-parameters} = (\text{number of ports in the DUT})^2.$$

Therefore a one port device has one scattering parameter; a two port device has four; and so on. Since the indoor RF propagation channel can be considered as a linear two port network, S-parameters are of interest. Figure 2.2 shows a linear two port network with its associated S-parameters

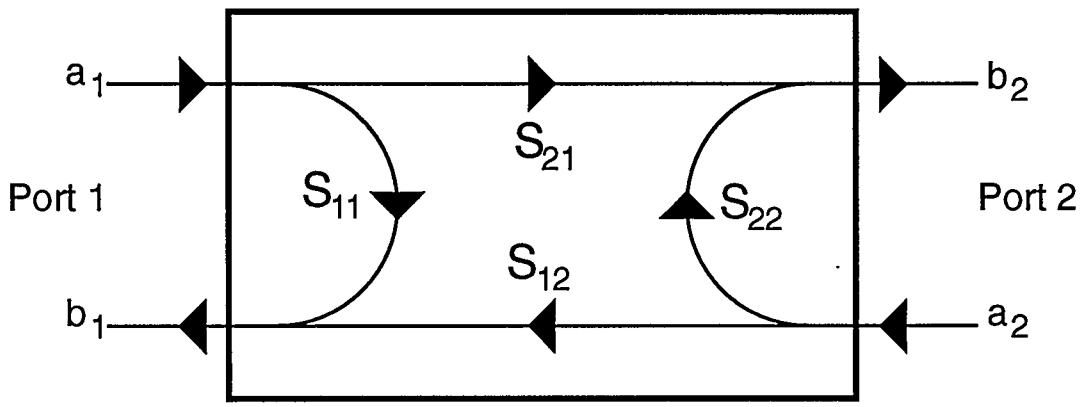

Figure 2.2: S-Parameter Model for a Two Port Linear Network

For a two port device, two linear equations are defined that relate the S-parameters and the input ('a') and output ('b') waves, and are given here:

$$b_1 = S_{11}\, a_1 + S_{12}\, a_2$$

$$b_2 = S_{21}\, a_1 + S_{22}\, a_2$$

Given these equations, any S-parameter can be found in terms of the other known parameters. S_{11} and S_{22} are reflection parameters and S_{21} and S_{12} are transmission parameters. The two S-parameters of interest are S_{11} (for antenna characterization) and S_{21} (for the indoor RF propagation channel characterization). The solution for these parameters is given here:

$$S_{11} = \frac{b_1}{a_1} \Big|_{a_2 = 0}$$

$$S_{21} = \frac{b_2}{a_1} \Big|_{a_2 = 0}$$

An important point to realize is that the 'a' and 'b' waves are measured in terms of voltage. Therefore the power in dB of any S-parameter is determined by 20Log_{10}(S-parameter).

2.2.3 SHL2000 Amplifier

The amplifier shown in figure 2.1 is an SMC SFL-2000 (type 9037). This amplifier has a 1 dB input compression point at -5 dBm and a 1 dB output compression point at +17 dBm. It has a minimum rated gain of 22 dB (that is flat within ± 1.5 dB) and a maximum input voltage standing wave ratio (VSWR) of 1.77 from 10 MHz to 2000 MHz. Its current consumption at +15V is 100 mA. These specifications were verified using the network analyzer and it was found that from 900 MHz to 2000 MHz the amplifier had a gain of 22 dB and was flat to within ± 0.5 dB.

2.2.4 Belden RG400 Cables

Approximately 58 m of RG400 coaxial cable was used in the measurement setup. This cable was used due to its popularity (and therefore availability) in microwave RF measurements and device connections. It is a high quality 50 Ω cable rated with a nominal attenuation of 43 dB per 100 m at 1000 MHz. The velocity of propagation is rated at 0.69c (c is the speed of light).

2.2.5 Discone Antennas

The antennas that were used are shown in figure 2.3. They were manufactured at NovAtel Communications Limited in Calgary Alberta specifically for the measurement system test frequencies described in this report. The discone antenna was chosen because of its ability to propagate signals over a large bandwidth [Saleh and Valenzuela, 1987]. This is essential for swept frequency measurements.

2.2.6 AST Premium 386 Computer

The computer shown in figure 2.1 is an AST Premium 386 MS-DOS based system. It is fitted with a General Purpose Interface Bus (GPIB) card. The GPIB is used for program control of the network analyzer and to transfer data acquired from the measurements to the computer where it can be stored for post processing. The type of computer used is not important; the AST was used because it was the one provided with the measurement system.

2.2.6.1 Data Acquisition Software

The measurement process was highly automated thanks to the software package that was developed and modified upon request by David Tholl of NovAtel Limited. The development language used was *Asyst 2.0* ™ an RPN-like language developed specifically for data acquisition and instrument control.

2.2.6.2 Data Compression

Post processing of measurement data implies a lot of what is known as 'number crunching'.

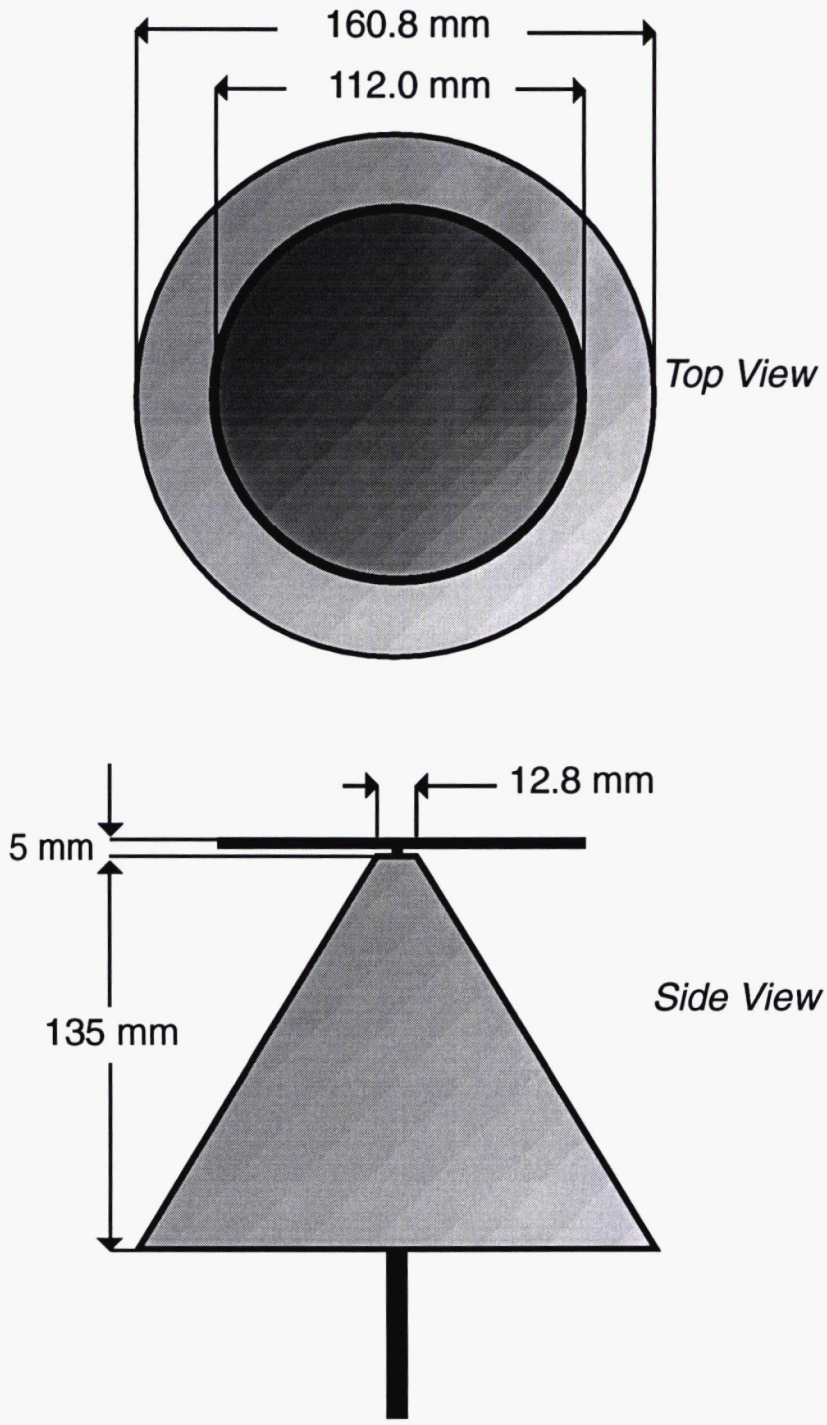

Figure 2.3: Discone Antenna.

Generally, personal computers are not well suited to this task for various reasons (speed being the most prominent). It is therefore better to transfer the measured data to a larger computer (mainframe, workstation, etc.). This suggests that the data should be in a compact form for either quick modem transfers or optimum use of removable media (floppy disks, tapes, etc.). There are many methods of data compression available from residual methods employing linear predictive coding [Press et al., pp. 465-466] to sophisticated Huffman coding techniques [Proakis, pp. 83-86]. Some good compression algorithms can be found in the references [Welch,1984; Ziv and Lempel, 1977, 1978]. Public domain packages like *PKZIP* ™ for DOS machines and *STUFFIT* ™ for Apple computers employ these techniques. Unfortunately, sophisticated data compression can take a long time and therefore may only be practical for archival purposes.

Faster data compression may be accomplished simply by changing the type of data that is stored. The network analyzer measures ratios or differences as discussed in section 2.2.2 which are non-integer numbers. High level computer languages such as C, Pascal, or Fortran support both integer and non-integer numbers. The difference between the two styles of numbers is how many bytes are required for storage. For example, in C, a float (non-integer) is stored in four bytes while a short (integer) is stored in two bytes. It is apparent then that if the numbers from the measured data can be converted into integers, two files can be stored in the space that previously stored one file. Caution must be taken to ensure that no information is lost in this conversion. This can happen if the number that is converted has a greater resolution (dynamic range) than the number it is being converted to. For example, if the number 0.67785 is to be converted to an integer format with all five digits

preserved, it must be multiplied by 100,000 and truncated to remove decimal parts. An integer of 67785 cannot be stored as a two byte integer because it is outside the maximum range of -32767 to 32768.

The two S-Parameters S_{11} and S_{21} are measured from a passive network. This means that the respective I and Q components will be less than one. Also, since the dynamic range of the network analyzer is approximately 80 dB, and the maximum two byte integer has a dynamic range greater than 90 dB, a conversion to a two byte integer is appropriate.

This conversion to two byte integers was performed by scaling the number with the largest absolute value to 32767. The remaining numbers were then scaled by the same ratio and stored in binary format.

2.2.7 HP8561B Spectrum Analyzer

Although not shown in figure 2.1, the HP8561B, 50 Hz to 6.5 GHz, Spectrum Analyzer can be a complementary part of the measurement system. It is accurate to $\pm$ 4 x 10^{-6} of the measured frequency and has a minimum resolution bandwidth of 10 Hz. Primarily it was used for examination of the specific spectral band before and during the measurement process. The purpose of which is to check for potential interference within the band or for measurement validation. The spectrum analyzer is a versatile instrument that has many applications. It is not necessary for the frequency domain measurement system so it was not frequently used.

2.3 Experimental Measurement Procedure

In this section an explanation of the procedure for obtaining measurements is presented. Two types of measurements are discussed as well as calibration considerations for each. These measurements are applied to a

DUT, which for the purposes of this study, is the indoor RF propagation channel or sometimes referred to as the channel. This naming convention will be held throughout this thesis unless specifically stated otherwise.

2.3.1 Swept Frequency Measurements

Swept frequency measurements are performed by collecting the channel response as a function of frequency. This is also referred to as the channel transfer function, H(f), and is given by the following equation:

$$H(f) = \sum_{k=0}^{N-1} H(k)\delta(f - k\cdot\Delta f - f_o)$$

where N is the number of samples, f_o is the initial frequency, and Δf is the frequency step size. The product $N\Delta f$ determines the bandwidth (BW) of the transfer function (i.e., 801 samples where Δf = 0.5 MHz gives a transfer function with a 400 MHz BW). From this it can be seen that swept frequency measurements produce the wideband response of the channel.

The indoor RF propagation channel transfer function is measured by placing the transmit and receive antennas somewhere in the indoor environment. The network analyzer sweeps the channel by transmitting a signal of increasing frequency and collecting from the receive antenna the response to this stimulus. This response is downloaded to a computer for post analysis. The varying frequency signal consists of a sine wave at increasing frequencies where the start and stop frequencies as well as the uniform step size (Δf) are determined by the user. Figure 2.4 shows the magnitude of a typical indoor channel frequency response. The bandwidth is 200 MHz (900 MHz to 1100 MHz) and Δf is 0.5 MHz. A good deal of information can be

abstracted from this type of profile (i.e., path loss, coherence BW, fading statistics, etc.).

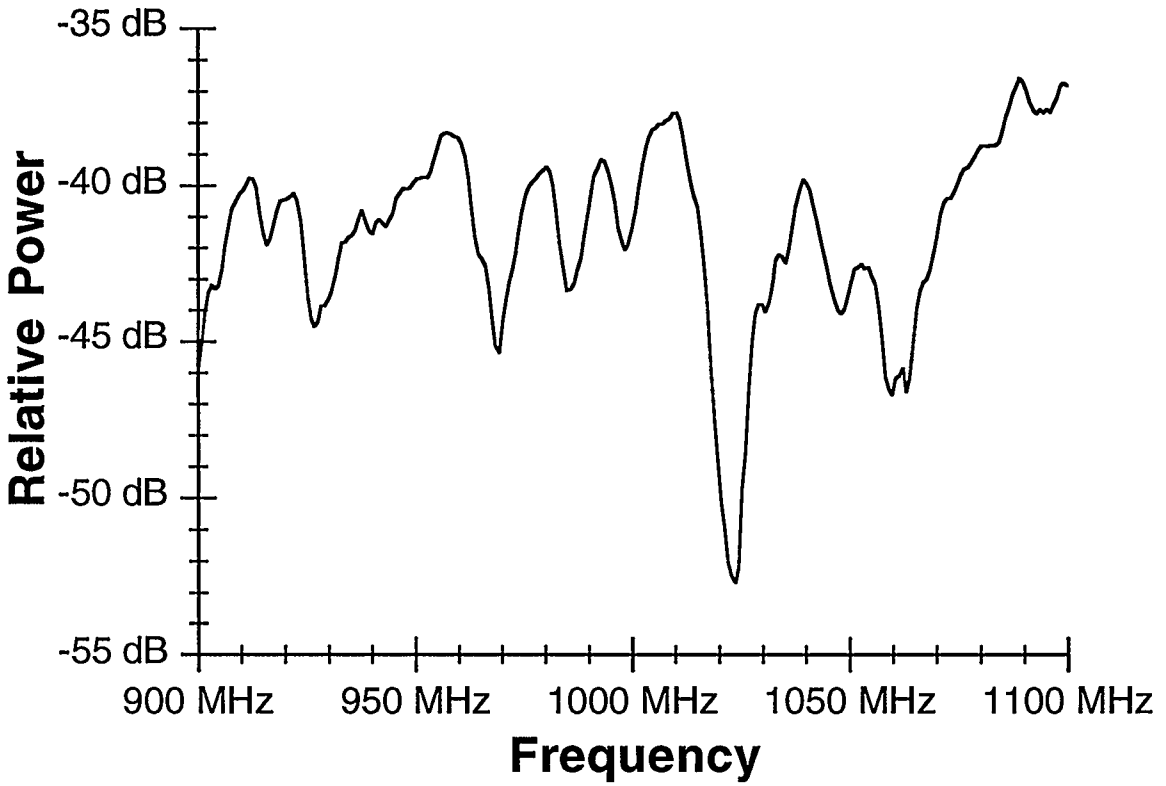

Figure 2.4: Magnitude of a Typical Swept Frequency Measurement.

The associated phase of the frequency response depicted in figure 2.4 is shown in figure 2.5. It can be seen that the phase has a strong linear trend which is expected. The deviation from linearity occurs when the magnitude of the channel response is in a significant null. For purposes here, a significant null can be termed as a null deep enough to affect phase linearity. A more rigorous approach to null definition is found in the references [Zaghloul, Fattouche, Morrison, and Tholl, 1991b].

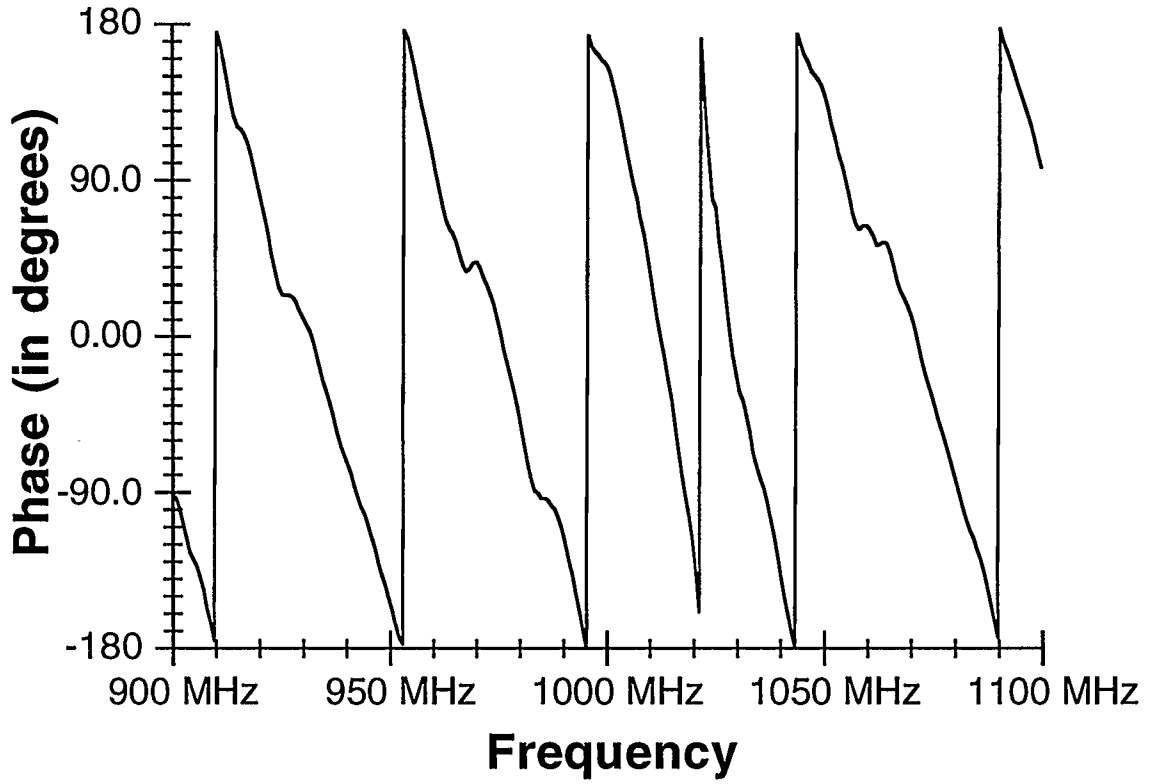

Figure 2.5: Phase of a Typical Swept Frequency Measurement.

2.3.1.1 Calibration

Essential to the reliability of any measurement system is the careful consideration of calibration. This may seem obvious but it has been noted that this important step is not always done [Howard and Pahlavan, 1990a]. Unfortunately, system calibration is quite often ignored and for the other measurement systems described in chapter one, calibration was not reported.

Calibration is a way of removing the unwanted system information from the measured results. The purpose of the measurement system described in this chapter is to obtain a measured response of the indoor channel. However, between port one and port two of the network analyzer with the S-

parameter test kit, there are actually three channels: the cables, amplifier, and transmit antenna; the indoor channel; and the cable and receive antenna. Calibration requires that the effects of any channel that is not the indoor channel be minimized so as to produce a measured response that is close to the 'true' channel. Three methods of calibration were identified and are discussed in the following sections. The basic principal for each of them is the same. Essentially a measurement of all components in the system with the indoor channel removed is performed. This measurement yields the standard channel. Subsequent measurements with the indoor channel in the measurement path are then normalized to this standard channel. The use of S-parameters makes the standard channel normalization easy to implement. To find S_{21} of the indoor channel, simply divide (complex division) the measured S_{21} by S_{21} of the standard channel.

2.3.1.1.1 Anechoic Chamber Calibration

Using an anechoic chamber to define the standard channel produces the best results. This is because a true anechoic chamber provides an environment that has a single path (i.e., the path between the transmit and receive antennas). The standard channel is measured by placing the two antennas far enough apart that the near field effects are negligible and the collecting the response of all components in the measurement system. Then distance between the antennas must be known as it becomes a part of the standard channel. Measurements normalized to this channel will be free of the effects due to cable, amplifier, and antenna characteristics as well as effects due to mismatching. There is one problem associated with this method however, that is a large anechoic is required. In most cases this problem will

eliminate the practicality of this method. Therefore, an acceptable alternate method should be used. Two of these methods will be discussed in the next section.

2.3.1.1.2 Calibration Without Antennas

It is possible to obtain a standard, single-path channel without an anechoic chamber. The first method is accomplished by replacing both antennas with a straight-through connector and measuring the response. This provides a standard, single-path channel that characterizes everything in the system except for the antennas. This is a valid technique providing that the return loss from the antennas is small enough so that their effects are negligible on the measurements when they are in place.

The second method uses the same concept and the same assumptions about the antennas as the first method. The only difference is in the implementation. The first method (and the anechoic chamber method) implies measurement of a standard channel to be used for calibration in post processing. The method described now uses the network analyzers built-in calibration feature for on-the-spot calibration. The antennas are still replaced by a straight-through connector and then the network analyzer uses the measured response of this channel as a reference against subsequent measurements.

Both methods produce the same results so the built-in calibration might be more convenient if a specific study of the standard channel is not required. The researcher should keep in mind however, that the antenna gain varies as $1/\lambda^2$ which may require compensation in large sweeps.

The calibration methods presented in this section were used for the results reported in this study.

2.3.2 Continuous Wave Measurements

Continuous wave measurements are performed by collecting the channel response at a specific frequency as a function of time. This gives the narrowband response of the indoor channel that is given by the following equation:

$$F(\tau) = \sum_{k=0}^{N-1} F(k)\delta(\tau - k\Delta t)$$

where N is the number of samples and Δt is the time increment or sample time. The frequency of interest, number of samples and total time of measurement (thus implying a Δt) can be selected by the user. The network analyzer does not have to change frequencies for this type of measurement, so the sample time (given a 3 kHz BW) can be shorter than that for the swept frequency measurement. The procedure for measuring the narrowband response of the indoor channel is the same as the one described for swept frequency measurements. Calibration can still be performed as described in section 2.3.1 except that for narrowband measurements, it is not as important. This is because narrowband studies focus on ratio measurements (like power law), temporal fluctuations, and fading statistics; all done at a single frequency. They are therefore not very sensitive to system characteristics as are wideband measurements.

The magnitude of a CW measurement is shown in figure 2.6. The profile was collected at 930 MHz while the receive antenna was moved approximately 30 cm relative to an antenna separation of 20 m. 1601 points were collected over a period of 6.5 seconds. It can be seen that the envelope is

subject to severe fading (as much as 30 dB) due to phase cancellation of the multipath components. This type of measurement is typically used in characterizing the channel by fading statistics (distribution, outage time, etc.) or for studying the behavior of the fade itself [Zhang, 1991].

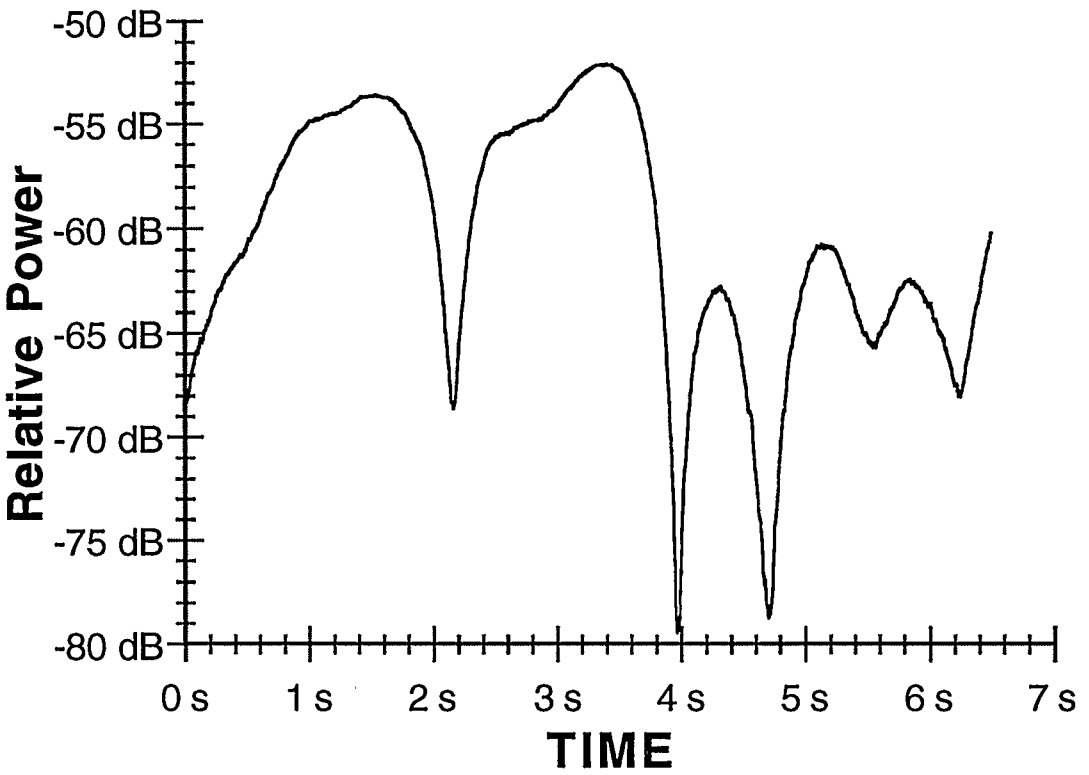

Figure 2.6: Magnitude of a Typical CW Measurement.

The corresponding phase of the CW magnitude shown in figure 2.6 is given in figure 2.7. As expected, the phase changes are more rapid as the envelope approaches, or is in, a null. This information is required in the study of phase distribution, prediction, and minimum/non-minimum phase systems [Fattouche and Zaghloul, 1991].

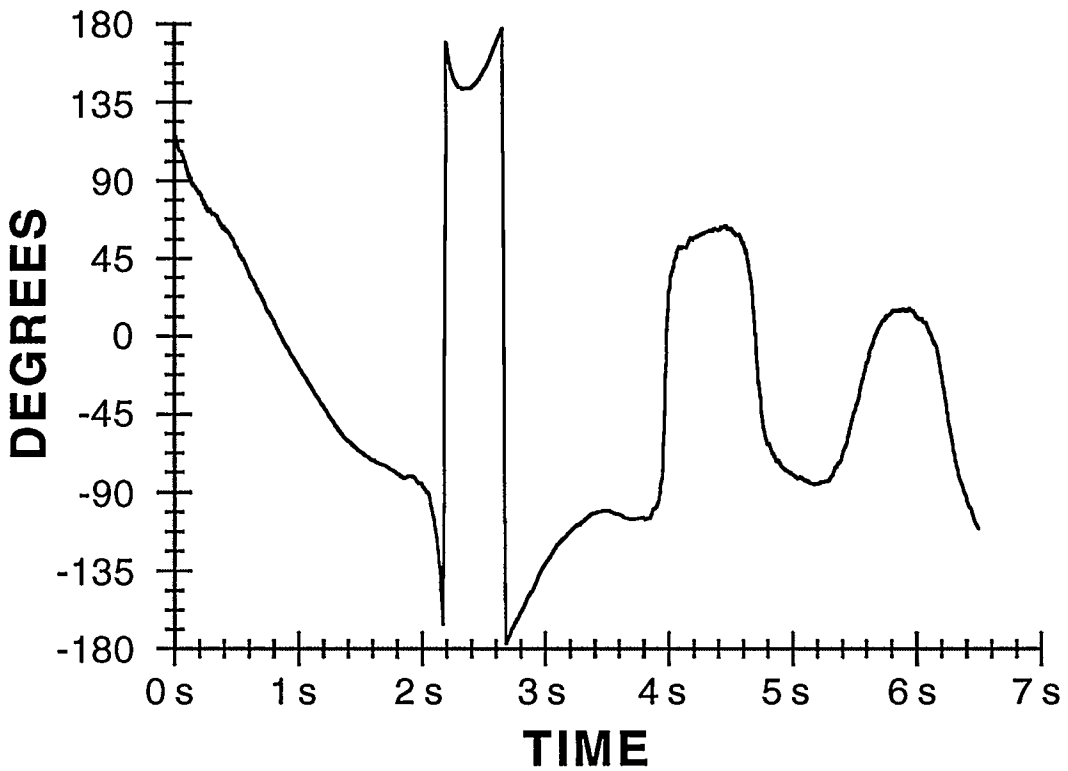

Figure 2.7: Phase of a Typical CW Measurement.

2.4 Data Post Processing

In this section a description of how the measured data is processed. If frequency analysis is required, the data does not need to be processed and can be used directly from the measured results. The processing presented in this section prepares the measured data for temporal analysis.

One of the more popular ways to characterize the indoor channel is through the analysis of its response to an impulse. The wideband impulse response reveals channel characteristics related to specular reflections. Multipath components are resolved by the impulse response profile dependent on the resolution of the characteristic pulse. In other words, a 25 ns pulse (which has a BW of 40 MHz) can only resolve specular reflections separated in time by a minimum of 25 ns. Obviously, the smaller the pulse duration, the

greater the resolving power of the measurement. The thrust in the last few years has been directed at greater resolving power but hardware limitations due to sampling at increasingly higher rates pose a problem.

The measured transfer function of the indoor channel gives an alternate method for determining high resolution impulse responses. By using frequency-time transform methods, a high resolution time domain response that is band limited can be obtained from the wideband frequency response.

2.4.1 The Discrete Fourier Transform

The Discrete Fourier Transform (DFT) plays an important role in many signal processing applications particularly due to the discovery of the Fast Fourier Transform (FFT) which makes computing the DFT an efficient process [Cooley and Tukey, 1965].

The DFT is recognized as a popular method for transforming discrete signals from the time domain to the frequency domain. The transformation of frequency signals to the time domain is referred to as the Inverse Discrete Fourier Transform (IDFT). The familiar equations of this analysis/synthisis pair are given here:

$$DFT \qquad H(k) = \sum_{n=0}^{N-1} h(n)\, e^{-j 2\pi kn/N}$$

$$IDFT \qquad h(n) = \frac{1}{N} \sum_{k=0}^{N-1} H(k)\, e^{j 2\pi kn/N}$$

Obviously since the network analyzer measurements are in the frequency domain, the IDFT is used to transform the data to the time domain. Some insight can be gained into the considerations for processing the measured data by examining each step of the process -- from sampling the channel to transforming the data.

Initially, a channel with some continuous transfer function, H(f), and its associated impulse response, h(t), is to be measured. This is depicted in figure 2.8a.

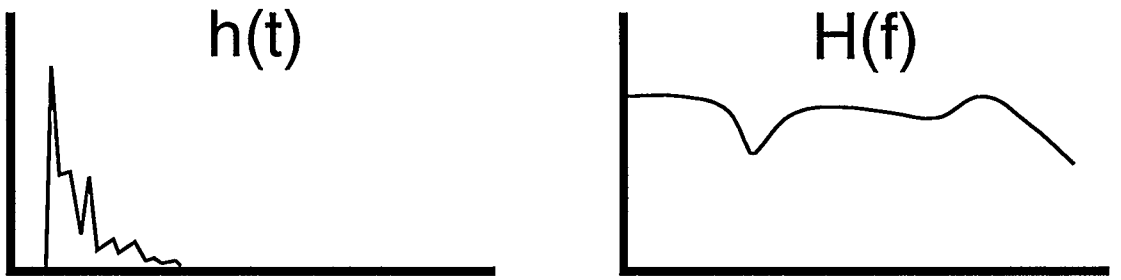

Figure 2.8a: Continuous Time and Frequency Domains

Discrete sampling is equivalent to multiplying the continuous spectrum with a comb function (sometimes referred to as a delta train). Figure 2.8b shows the frequency domain representation, X(f), and the time domain representation, x(t), of a comb function. The sampling is spaced in frequency by Δf. This sampling interval determines the period, T, in the time domain by the relationship: $T = 1/\Delta f$. An important consideration must be noted in this step. Due to the periodic nature of the IDFT, aliasing in the time domain can take place if Δf too large (i.e., T is smaller than the excess delay of the channel).

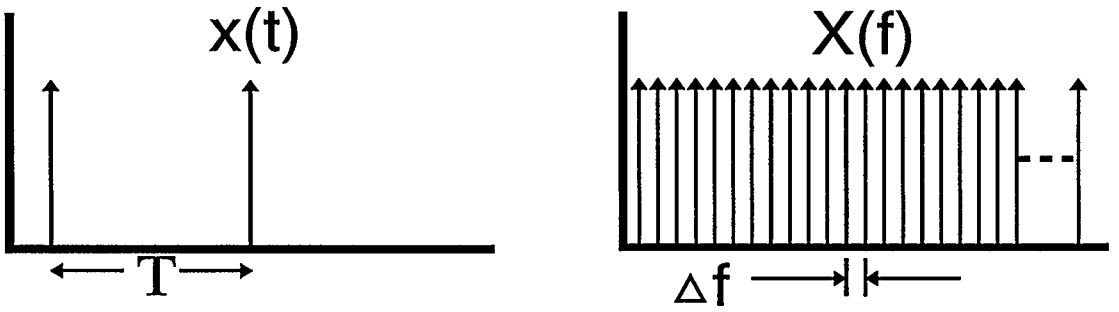

Figure 2.8b: Comb Function Time and Frequency Domains

Figure 2.8c depicts the result of sampling the frequency domain. The continuous frequency spectrum is quantized by the relationship X(f)H(f). The time domain representation of the comb function is convolved with the impulse response of the channel (h(t)*x(t)). From this it is apparent that if the excess delay of the channel is greater than the period of x(t), aliasing will occur. This implies that some knowledge of the channel delay spread is needed before measurements are performed. The only reliable way to find this is to measure the channel with a small Δf and observe the excess delay.

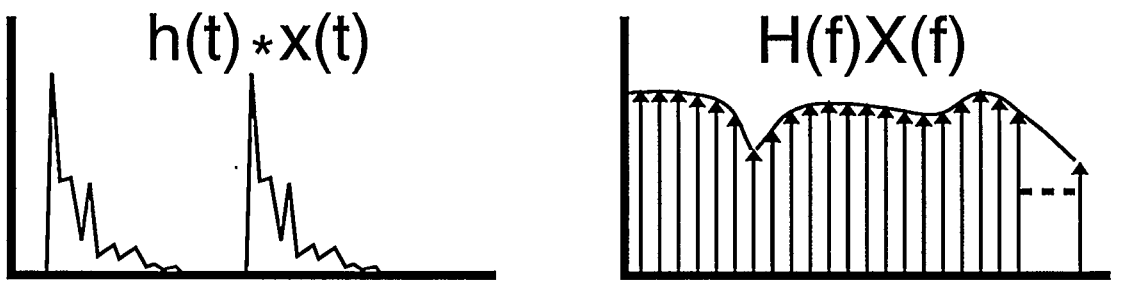

Figure 2.8c: Sampled Frequency Domain and Corresponding Time Domain

Experimental data is necessarily finite. This places an implied window on the data. In other words, the finite frequency data can be interpreted

as part of an infinitely long data record contained within a window that is rectangular by default. This window, W(f), (in the frequency domain) and its associated time domain representation, w(t), are given in figure 2.8d. The bandwidth, B, of the window is the bandwidth of the sampled frequency response. This has a direct relationship to the resolution of the associated impulse response. For example, if the bandwidth of the window is 200 MHz, the resolution of its IDFT is 1/B or 5 ns.

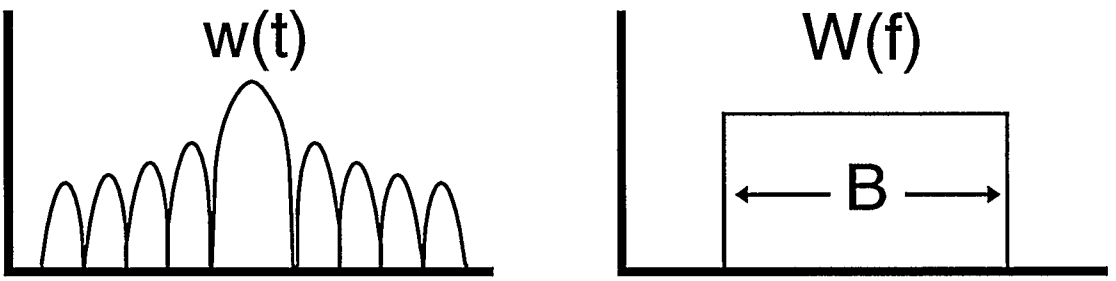

Figure 2.8d: Window Function Time and Frequency Domain

Figure 2.8e demonstrates the final result of this process. The sampled, windowed transfer function is given by the expression H(f)X(f)W(f). The time domain representation is a bandlimited impulse response given by h(t)*x(t)*w(t) (which is difficult to depict graphically). A second important consideration needs to be pointed out here. The IDFT of windowed data is equivalent to the Fourier Transform of an infinitely long data set convolved with the Fourier Transform of the window. Therefore, caution must be exercised when processing the data to ensure that the time domain function of the frequency window does not significantly distort the data.

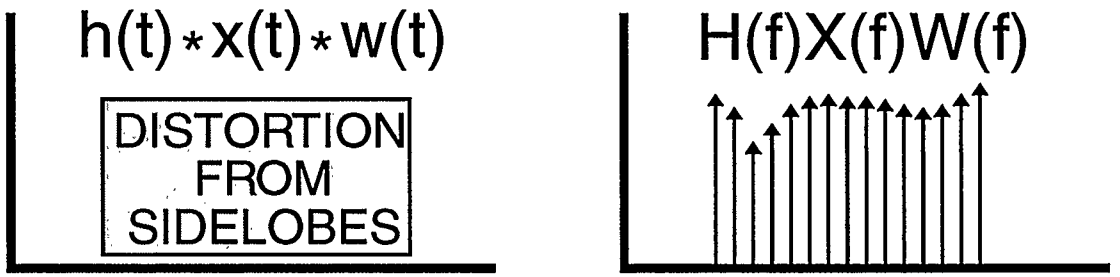

Figure 2.8e: Sampled, Band Limited Frequency Domain and Time Domain Representation

2.4.2 Windows For DFT

Window functions play an important role in minimizing the convolution effects of the DFT. It was shown in section 2.4.1 that finite data has a rectangular window by default. This window in the frequency domain (refer to figure 2.8d) can be expressed by the following:

$$W(n) = \begin{cases} 1 & n = 0, 1, 2, \cdots, N-1. \\ 0 & otherwise \end{cases}$$

The IDFT of this function yields a sinc function that is expressed by the following equation:

$$w(n) = \frac{B}{2\pi} sinc\left(\frac{B}{2} n\right) \qquad n \neq 0$$

This sinc function is shown in figure 2.9. By convention [Harris, 1978] we define the resolving bandwidth of a window sinc function as the width of the mainlobe 6 dB below its peak. The smaller the mainlobe width -- the greater the resolving power of the function. The resolution of an impulse response obtained from a windowed frequency response is the inverse of $N\Delta f$

(the bandwidth of the sampled transfer function) times the resolving bandwidth of the convolving sinc function.

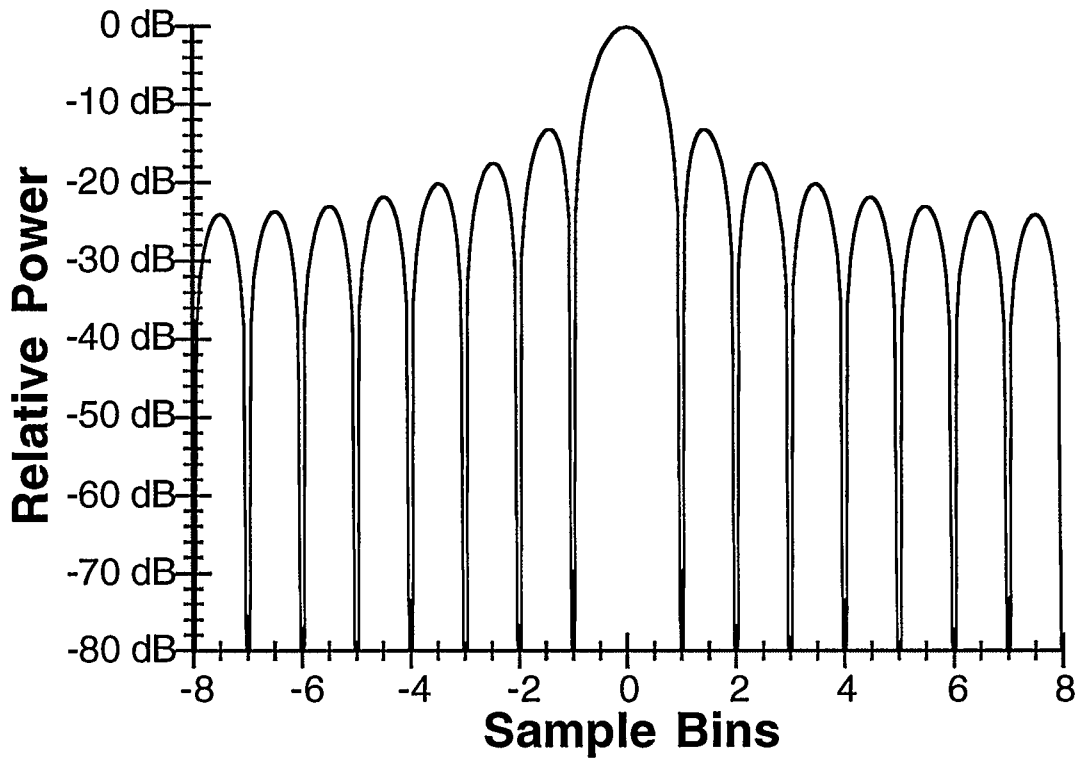

Figure 2.9: Sinc Function of a Rectangular Window.

The sinc function from a rectangular window has an excellent resolving power of 1.1 bins but it can be seen from figure 2.9 that the first sidelobe is approximately 13 dB down from the mainlobe peak. This means that frequency domain data multiplied by a rectangular window can lead to truncation artifacts (spectral leakage) in the time domain response that can be misinterpreted as additional reflections.

These artifacts can be reduced by the application of a window with smoother edges than the sharp rectangular window. However, smooth

windows increase the main lobe width of the convolving sinc function which leads to a loss in resolution. Clearly, the choice of an appropriate window involves a careful tradeoff between sidelobe reduction and loss of resolution. Indeed, there is a large variety of window functions to choose from [Harris, 1978; Oppenhiem and Shafer, Ch. 11.].

It was found that the IDFT of the measured results had a large dynamic range. This required the use of a window function whose convolving sinc function had very low sidelobe levels. The minimum 3-term Blackman-Harris window was chosen as a good candidate for the results presented in this thesis. A complete description of this window is found in the literature [Harris, 1978] and is summarized here.

The frequency domain representation of the minimum 3-term Blackman-Harris window is shown in figure 2.10 and is expressed by the following:

$$W(n) = a_0 - a_1 \bullet \cos\left[\frac{2\pi}{N\text{-}1} n\right] + a_2 \bullet \cos\left[\frac{2\pi}{N\text{-}1} 2n\right]$$

$$a_0 = 0.42323,\ a_1 = 0.49755,\ a_2 = 0.07922,$$
$$n = 0, 1, 2, \cdots, N\text{-}1.$$

Clearly this window is smoother than the rectangular window but there is an associated loss in resolution in the time domain due to the increase in mainlobe width of the convolving sinc function.

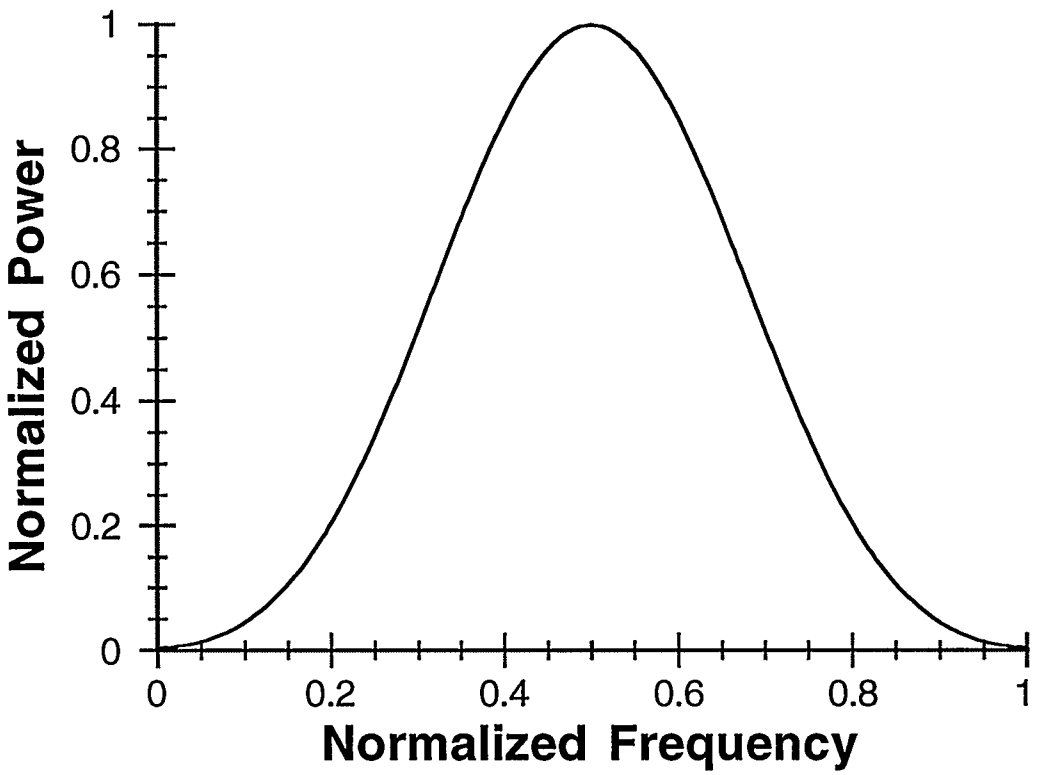

Figure 2.10: Frequency Domain Representation of a Minimum 3-Term Blackman Harris Window.

The IDFT of figure 2.10 is shown in figure 2.11 and is given by the following expression:

$$w(n) = (W\text{-}1)\ sinc\left[\frac{(W\text{-}1)n}{2}\right] \bullet \left[a_0 - \left[\frac{a_1 \bullet ((W\text{-}1)\ n)^2}{((W\text{-}1)\ n)^2 - (2\pi)^2}\right] - \left[\frac{a_2 \bullet ((W\text{-}1)\ n)^2}{((W\text{-}1)\ n)^2 - (4\pi)^2}\right]\right]$$

$$a_0 = 0.42323,\ a_1 = 0.49755,\ a_2 = 0.07922,$$
$$n = 0, 1, 2, \cdots, N\text{-}1.$$

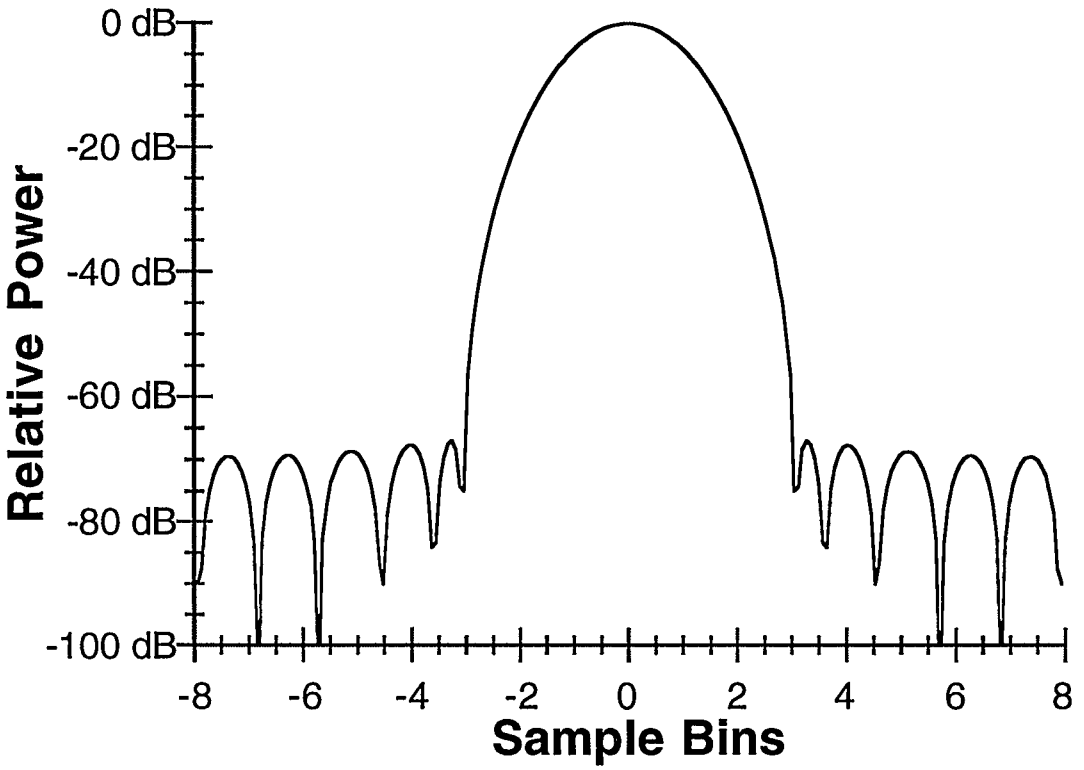

Figure 2.11: Sinc Function of a Minimum 3-Term Blackman-Harris Window.

From figure 2.11 it can be seen that the first sidelobe levels are approximately 70 dB below the mainlobe peak and that the resolving bandwidth is 2.3 bins (an apparent typographical error exists in the literature [Harris, 1978] that states the resolving bandwidth to be 1.81 bins). An impulse response obtained from a 200 MHz frequency response that is convolved with this function has a 6 dB resolution of 11.5 (5 ns x 2.3). This is the case for the windowed impulse response shown in figure 2.12. For comparison, an unwindowed (rectangular windowed) and uncalibrated impulse response from the same frequency response profile (shown in figure 2.4) that was centered at 1.0 GHz is shown on the same axis. This figure shows the importance of calibration and windowing. For the case of the unwindowed profile, the high

sidelobes of the rectangular window add significant distortion to the impulse response. This is especially obvious due to the precursor (which cannot physically exist) that is 13 dB below the peak of the first arrival. Also, the dynamic range of the profile has been greatly reduced.

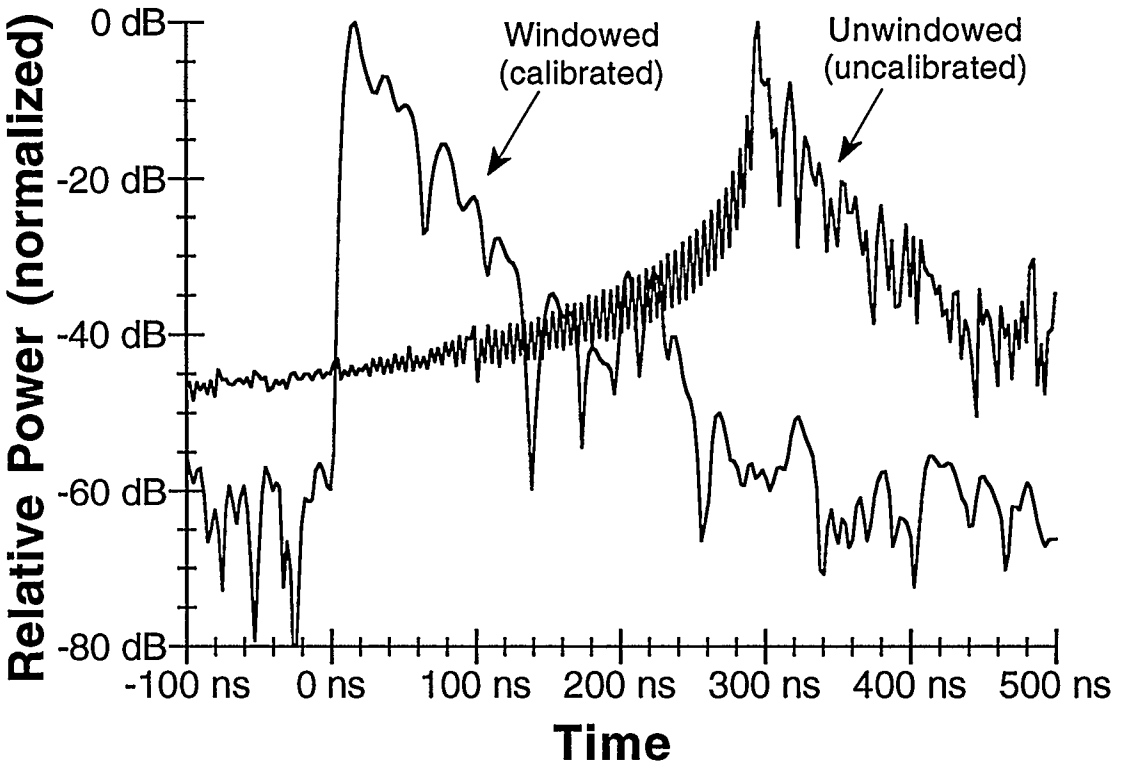

Figure 2.12: Comparison of Windowed and Unwindowed Impulse Responses with Calibration Effects.

The effects of calibration are also plainly seen. An uncalibrated profile is delayed in time due to the delays in the measurement system. The measurement that produced the information for the profiles in figure 2.12 was done by placing both antennas 5 m apart. The calibrated profile shows the first arrival at 17 ns. This agrees well with the 16.7 ns it would take an EM wave to travel through free space (i.e., 5 m / c — 5 meters divided by the speed of light).

This reveals an important point about the measurement system — the absolute phase reference in the frequency domain gives an accurate time reference in the time domain that is useful in determining the distance of the direct and reflected paths between the two antennas. This feature is not found in the measurement systems described in section 1.5.1.

2.4.3 Modeling as an Alternative

The resolution loss in the impulse response profile associated with windowing the frequency data can be overcome by modeling.

Modeling is equivalent to estimating the "true" spectrum of an infinite series of data samples from a finite subset of the data. It therefore avoids the windowing associated with necessarily finite size from experimental data. This is an appropriate alternative to calculating the IDFT/window spectrum. There are many types of models and algorithms that can be used for the type of data that is presented in this report. An example of a suitable Auto Regressive Moving Average (ARMA) algorithm is the Transient Error Reconstruction Analysis (*TERA)* developed at the University of Calgary. The *TERA* modeling method reintroduces data that cannot be modeled which is crucial if the model is not entirely correct This method is described in detail in the references [Smith et al., 1986; Smith and Nichols, 1990] and briefly summarized here. First, the data is modeled as the output of an IIR filter. This requires estimating the transfer function from the finite data set. The AR and MA portions are determined individually. Second, the IDFT of the infinite data sequence is estimated from the AR and MA coefficients by an implicit extrapolation of the finite data sequence. For the case of the swept frequency data, the model

estimates the infinite transfer function from the measured data and the impulse response is determined from the model coefficients.

A modeled and an IDFT/windowed impulse response determined from a 900 MHz to 1100 MHz sweep is shown in figure 2.13 and another example is given in the reference [Morrison et al., 1991]. The model order is two which is consistent with previously reported results that used an AR process [Howard and Phalavan, 1990b]. It can be seen that the modeled impulse response has a greater resolution (5 ns for the modeled profile and 11.5 ns for the windowed profile).

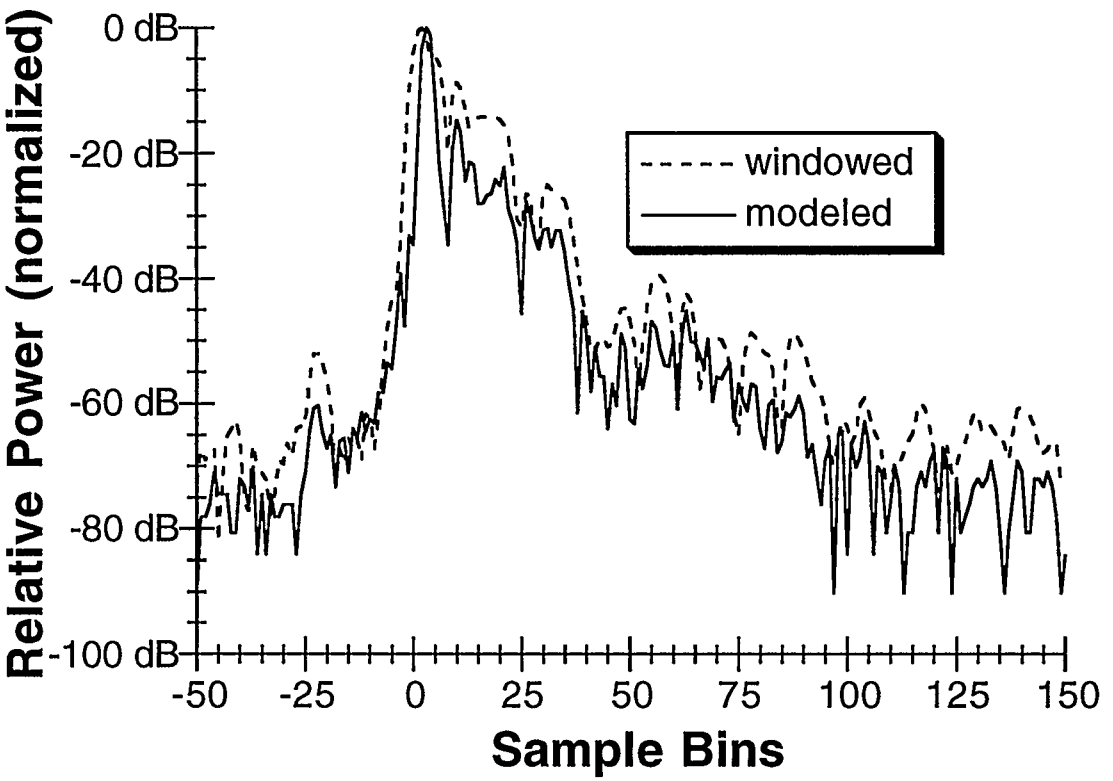

Figure 2.13: Modeled verses. Windowed Impulse Response.

Modeling improves the resolution over the traditional Fourier techniques but it is not always a familiar or convenient technique. Also, to some extent, the resolution can be arbitrarily increased by sweeping a larger frequency band. Obviously there are limitations due to available bandwidth and hardware constraints.

CHAPTER THREE

MEASUREMENT SYSTEM EVALUATION

3.1 Objective

The purpose of this chapter is to examine certain characteristics of the measurement system that might be detrimental to the quality and accuracy of the measured results. As with any experimental system, there are certain limitations that are inherent to its individual components. In the following sections, limitations due to bandwidth, interference, and dynamic range are examined. The procedures used for the individual tests are briefly discussed in the appropriate sections.

3.2 Cable Effects

In this section, potential problems that might arise from using a long cable in the measurement system are addressed.

3.2.1 Cable Position

Guided energy along a cable can lead to reflections that are not due to the measured environment. If this effect occurs, it is dependent on cable position. In other words, moving the cable will change the path of the guided energy that in turn, will produce a different effect on the measured results.

Tests were performed to quantitatively check if cable position affected the signal. These measurements were performed with the instrumentation inside a shielded room and outside a shielded room. The justification for this was to make sure that if guided energy was present, it would

be terminated in the ground plane of the shielded room before reaching the measurement instrumentation. This would allow for easier identification of guided energy in the profiles that were taken outside the shielded room.

The measurements were taken with cables in different positions (wound around a metal object, draped over lab benches, etc.) in an attempt to maximize the possibility of getting guided energy along the cables. Tests were performed several times and the worst case results are presented here.

3.2.1.1 Frequency Domain

Figure 3.1 shows the magnitude of the channel frequency response from two different cable positions.

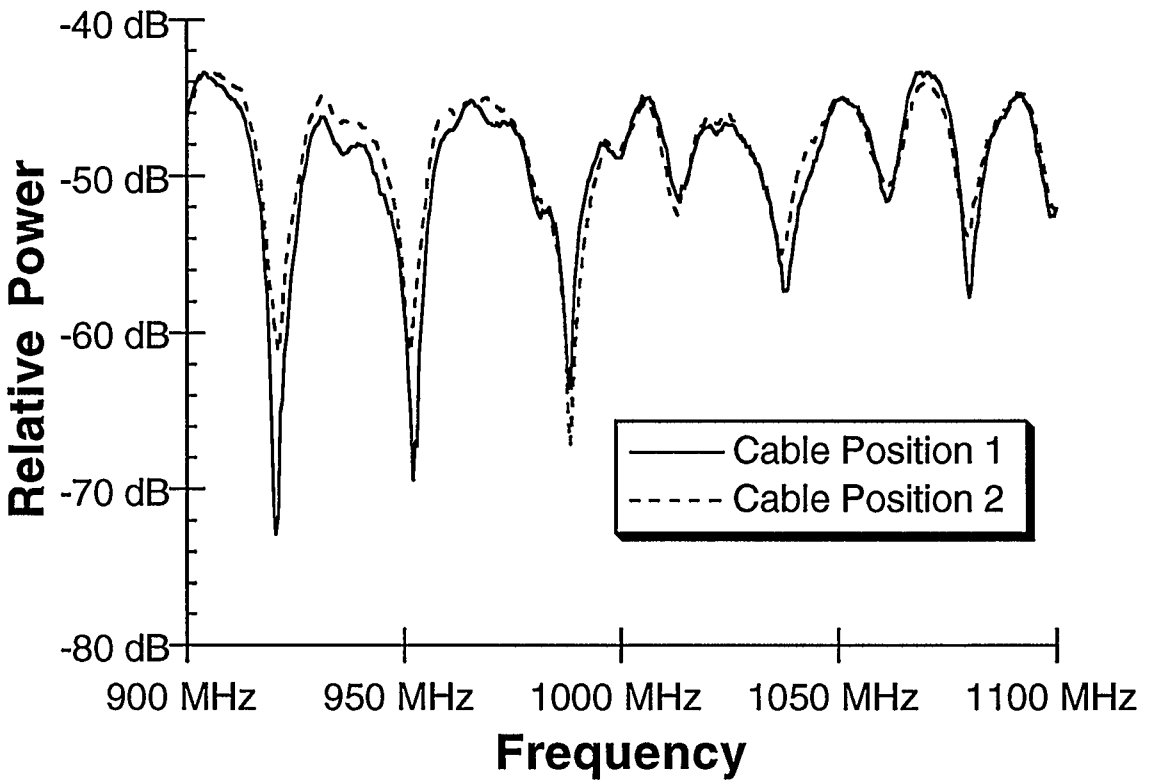

Figure 3.1: Comparison of Frequency Response Magnitude from Two Different Cable Positions.

The null depth varied whenever it approached the noise level. This is expected due to the spurious nature of noise spikes. Otherwise, the signals were the same within ± 2.5 dB. Although the measurements appear to have a marginal sensitivity to the cable position, there was sufficient time in-between the measurements (the elapsed time between measurements varied from 8 to 12 minutes) for the channel to vary. Further measurements as a function of time (not cable position) indicated that when the magnitude of the frequency response is not in a null, variations of ± 3 dB can occur. The same order of null depth deviation due to noise was observed.

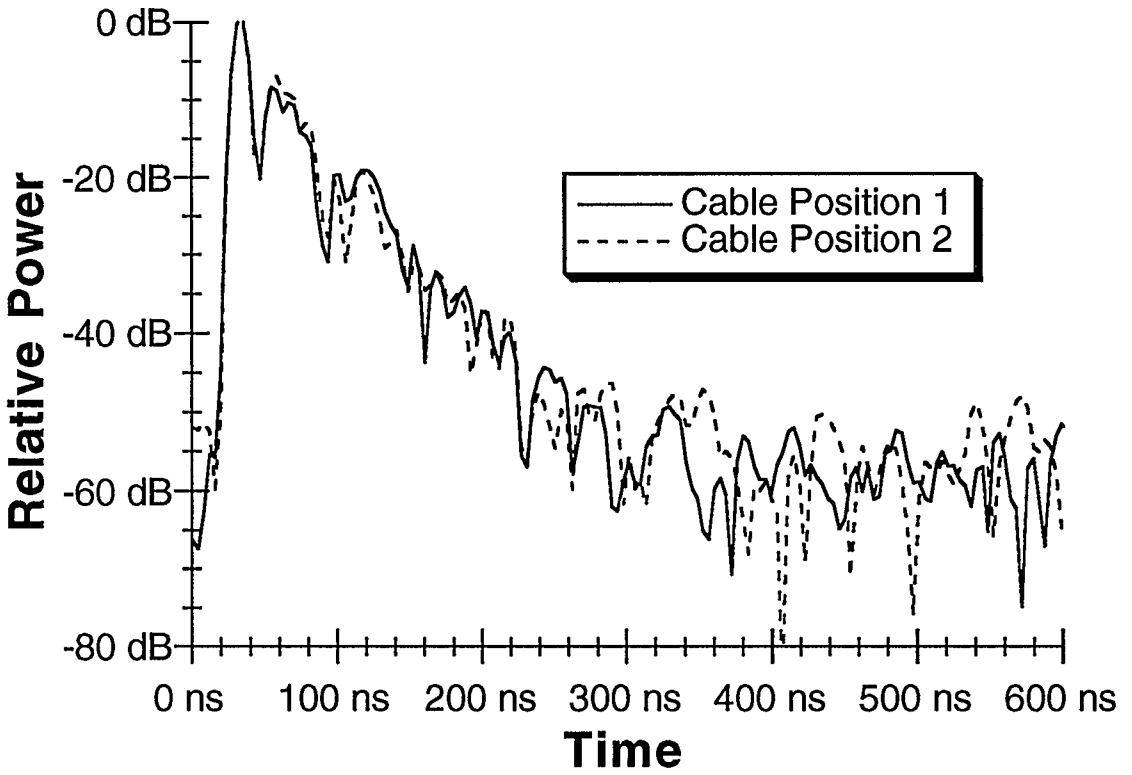

Figure 3.2: Comparison of Impulse Response Magnitude from Two Different Cable Positions.

3.2.1.2 Time Domain

Figure 3.2 shows the magnitude of the impulse response obtained from the corresponding frequency profiles. Again, variations of ± 2.5 dB occurred but the general character of the profiles are the same. This means that statistically the excess delay and τ_{rms} of the profiles are the same. The impulse response profiles from the tests done as a function of time (as described in 3.2.1.1) showed the same order of variation.

3.2.1.3 Interpretation of Cable Position Experiment

The results from both frequency and time domain profiles demonstrated that channel variations are a consequence that must be expected. The important result was that these variations appear to be related to the physical nature of a dynamic environment and not any detrimental effect due to the cable.

3.2.2 Cable Coupling

Coupling is a phenomenon that can exist in any RF system. In particular, a system with long cable runs may be especially susceptible. The cable used in the frequency domain measurement system is a high quality shielded cable specifically manufactured for UHF propagation. However, this does not exclude the possibility of the transmit cable from coupling with the receive cable.

Tests were performed to measure the ability of the transmitting cable to couple with the receiving cable. To maximize the potential for coupling, the tests were performed with the transmit and receive cables intertwined and parallel to each other. Also, tests were done with the transmitting cable

matched (50Ω load), mismatched (75Ω load), and open circuited. The receive cable was always terminated by the antenna.

3.2.2.1 Frequency Domain

Figure 3.3 depicts the magnitude of the frequency response for the test using the mismatched load. The average level of the signal is approximately -85 dB which is approaching the lower sensitivity limits of the measurement system. Even though there are spikes 25 dB stronger than the average signal level, there appears to have no correlated information. This would be expected if the profile was due to noise.

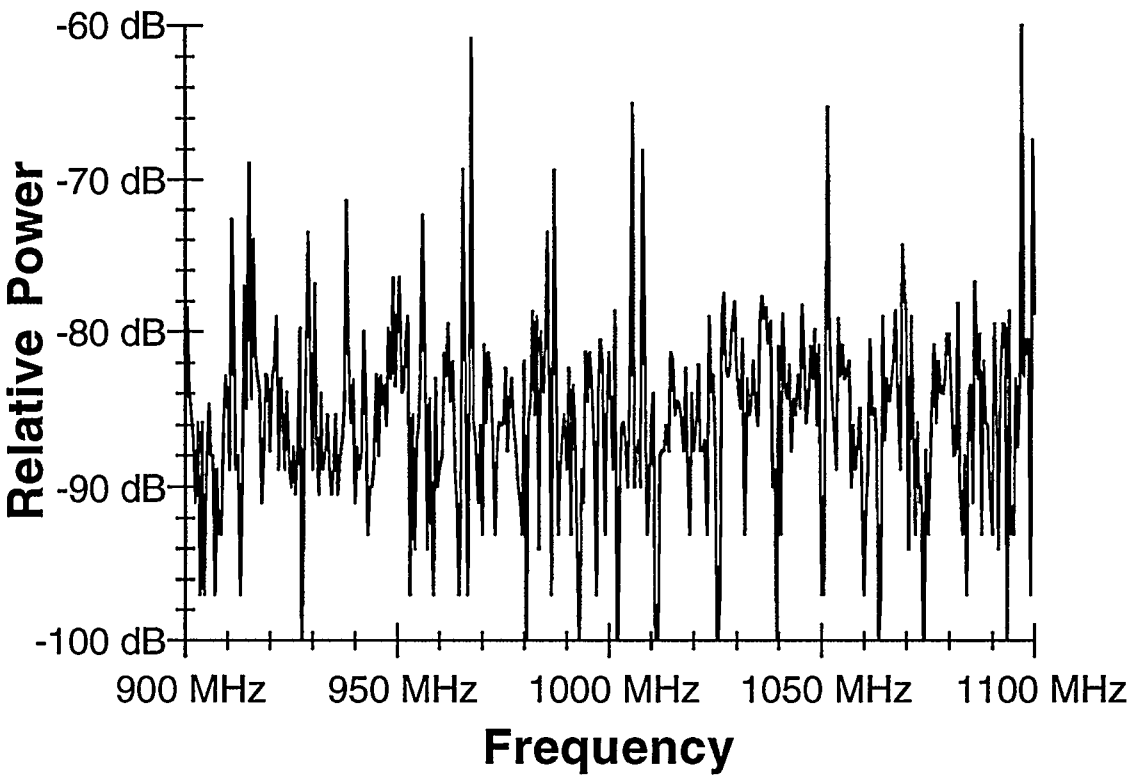

Figure 3.3: Frequency Response Magnitude from Coupling Experiment.

3.2.2.2 Time Domain

Figure 3.4 shows the magnitude of the corresponding impulse response profile. It can be seen that the same dynamic activity is present and again there appears to be no correlated information.

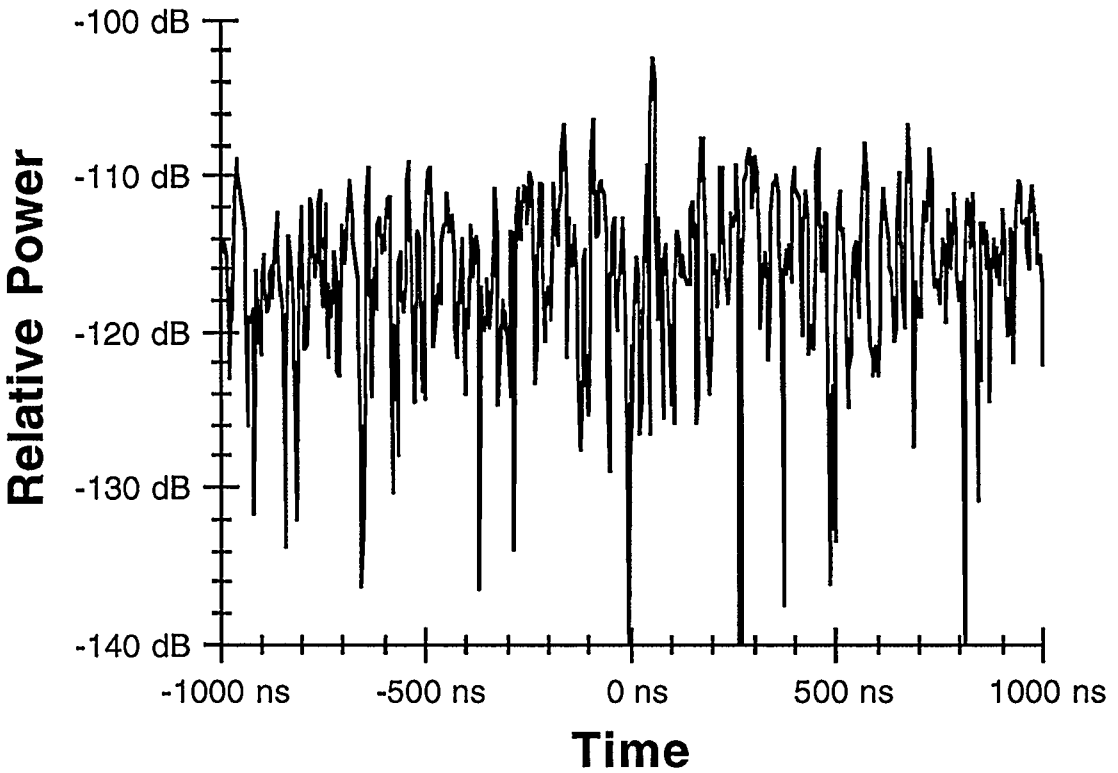

Figure 3.4: Impulse Response Magnitude from Coupling Experiment.

For completeness, an impulse response from a different experiment is shown in Figure 3.5. Note the precursor at -200 ns. This phenomenon was thought to be a result of aliasing. Further tests using different frequency sampling intervals (Δf) indicated that the precursor was not a result of an aliased distant reflector (i.e., the precursor had the same relative time of approximately -200 ns for different sampling intervals).

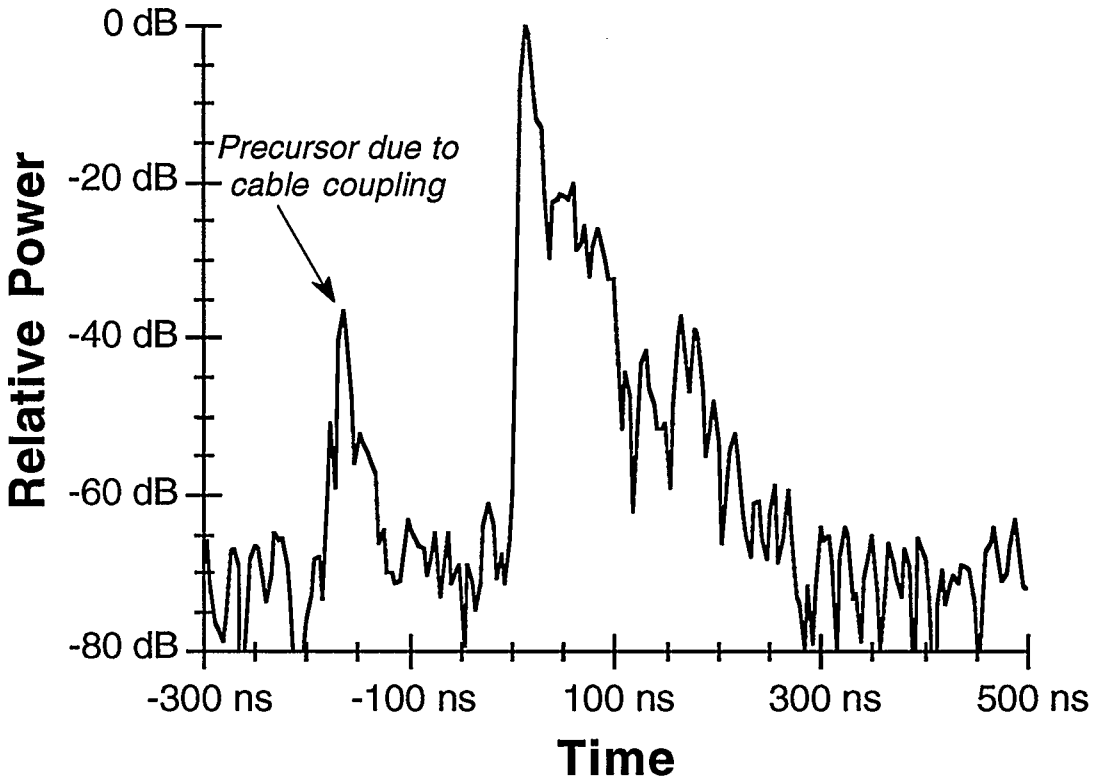

Figure 3.5: Impulse Response Magnitude Showing Cable Coupling.

3.2.2.3 Interpretation of Cable Coupling Experiment.

The results from tests designed specifically to introduce coupling indicate that the transmit cable does not couple with the receive cable. The results shown here are for the case of the mismatched load. Results from the matched and open loads were similar. It was shown in figure 3.5 however, that coupling can occur. This phenomenon will always appear as a precursor to the first arrival due to the method of system calibration. It should be noted that a precursor can be present due to an aliased distant reflector (which was ruled out for the information presented here). Fortunately, this coupling, when it appears (which is rarely), is not detrimental to the data. This is because the

precursor's position and power do not affect the part of the profile that is studied providing that Δf is small enough to avoid aliasing back into positive time.

3.2.3 Bandwidth of Cable and Amplifier

Bandwidth limitations are important to know before measurements are performed. Measurements taken outside the system's usable bandwidth are invalid primarily due to severe or non-linear attenuation. One method for determining the presence of non-linear distortion in a linear system is to analyze the phase distortion. This can be accomplished by finding the group delay (τ_g) which will be explained in the following section.

Tests were performed by measuring the transfer function of the amplifier and cables between the range of 900 MHz and 2000 MHz.

3.2.3.1 Group Delay

Group delay is defined as the derivative of the phase response with respect to the frequency. That is, the rate of change of the phase response as a function of frequency. The equation for group delay is given here:

$$\tau_g = \frac{d\phi}{d\omega} = Lim_{\Delta f \to 0} \frac{\Delta\phi}{2\pi \cdot \Delta f}$$

where

ϕ is in radians,

ω is in radians/sec,

Δf is in Hz,

$\Delta\phi$ is in radians,

τ_g is in seconds.

A perfectly linear phase shift would have a constant rate of change with respect to frequency and therefore a constant group delay. This results from the differentiation process that reduces the linear portion of the phase response to a constant value and transforms the deviations from linear phase into deviations from constant group delay. The units for group delay are seconds. This means that group delay is a measure of transit time through the DUT for a particular frequency. A linear system will exhibit a constant group delay at all frequencies within the usable bandwidth.

Figure 3.6 shows the attenuation and group delay of the cable and amplifier.

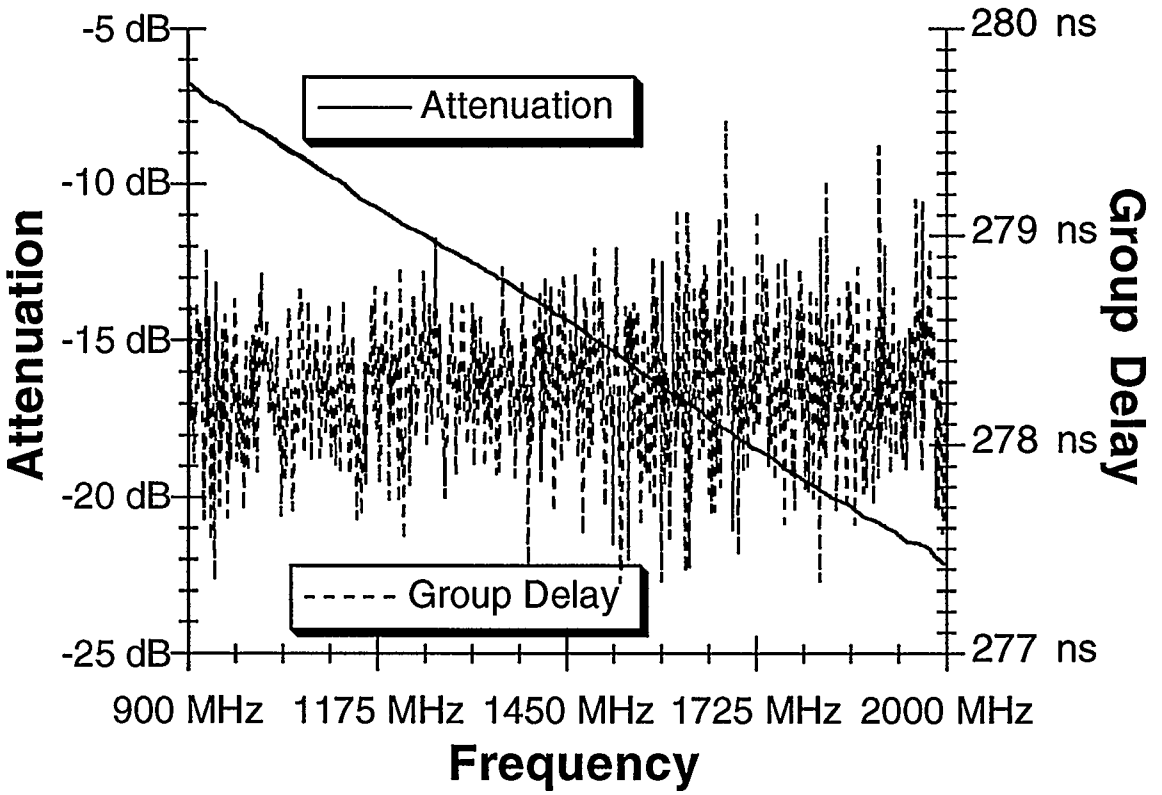

Figure 3.6: Group Delay and Attenuation of Cable and Amplifier.

The results from figure 3.6 are summarized here:

i) The attenuation varied linearly as a function of frequency and can be expressed as follows:

$$\alpha = mf + b$$

where

m ≅ -13.7 dB/GHz,

b ≅ -5.4 dB,

f is in GHz,

α is in dB.

ii) The group delay is virtually constant across the band; τ_g has a mean of 278.27 ns and a standard deviation of 0.31 ns. This agrees well with the presence of 58 m of cable (58 m / (0.695 c) = 278.2 ns).

3.2.3.2 Interpretation of Bandwidth Experiment

The nearly constant value of group delay and the linearity of the attenuation, confirms that the amplifier and cables are linear within the desired bandwidth.

3.3 Antenna Return Loss

The antenna return loss, S_{11}, is closely associated with the problem of usable bandwidth (i.e., the return loss of the antenna will be small outside of its usable bandwidth). The return loss was examined to justify the calibration method described in section 2.3.1.1.2. S_{11} was measured from 0.9 GHz to 2.0 GHz for both antennas and the VSWR was determined by the following expression:

$$VSWR = \frac{||S_{11}| + 1|}{||S_{11}| - 1|}$$

where

S_{11} is a voltage ratio,

VSWR is a voltage ratio.

The return loss response for both antennas is shown in Figure 3.7. The VSWR in the frequency band of interest had a maximum of 1.45 corresponding to a return loss of approximately -15 dB.

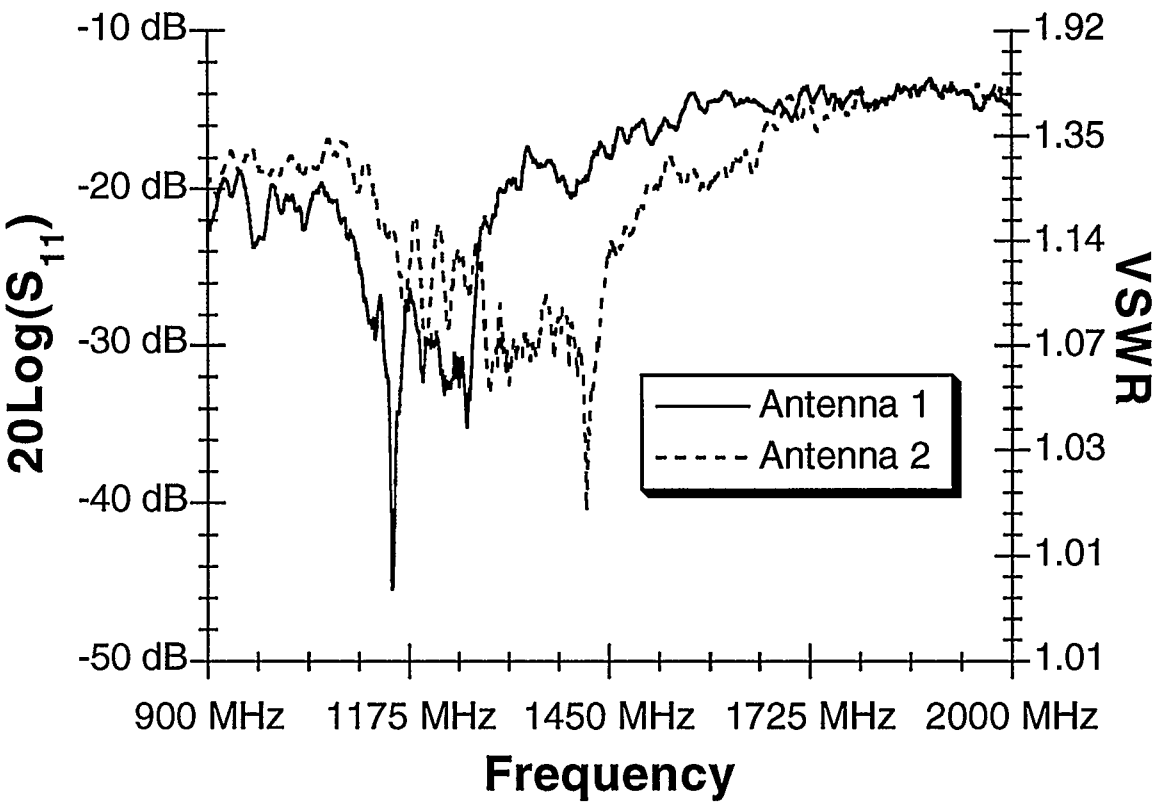

Figure 3.7: Antenna Return Loss Ratios.

3.3.1 Interpretation of Antenna Return Loss Experiment

It was assumed that a VSWR of less than 2:1 would be sufficient for the calibration method discussed in chapter two [McGirr, 1990]. This would result in a transmit power loss of 0.5 dB. The actual maximum VSWR of 1.45:1 results in a power loss of approximately 0.2 dB. This is considered to be acceptable for removing the antennas in the calibration procedure as described in section 2.3.1.1.2 (i.e., the antenna bandwidth is usable in the range of 900 MHz to 2000 MHz).

3.4 System Sensitivity to Interference

The network analyzer collects the channel transfer function by sweeping a specified frequency band, so the measurement may be corrupted by interfering signals. This interference would be mostly due to strong in-band signals, but since there is no bandpass filtering at the receive antenna, out-of-band signals can also result in interference.

Tests were performed by transmitting a single tone interferer in the environment while a frequency sweep measurement was being performed. The frequency sweep was done from 900 MHz to 1100 MHz and the interfering signal tone was deliberately set to 968.5 MHz (a sampled frequency point) to maximize its effect. The level of the interfering signal was changed by 5 dB increments from approximately 50 dB above the mean level of the network analyzer's receive power to 20 dB below it. The effect of the interferer on a single sweep as well as on the average of ten sweeps was examined. A reproduction of a plot showing the interferer and the channel transfer function as measured by a spectrum analyzer is shown in figure 3.8. The x-axis is

divided into a 30 MHz per division grid that starts at 850 MHz and ends at 1150 MHz. The y-axis is divided into a 10 dB per division grid. The marker at 968.5 MHz shows the maximum interference level.

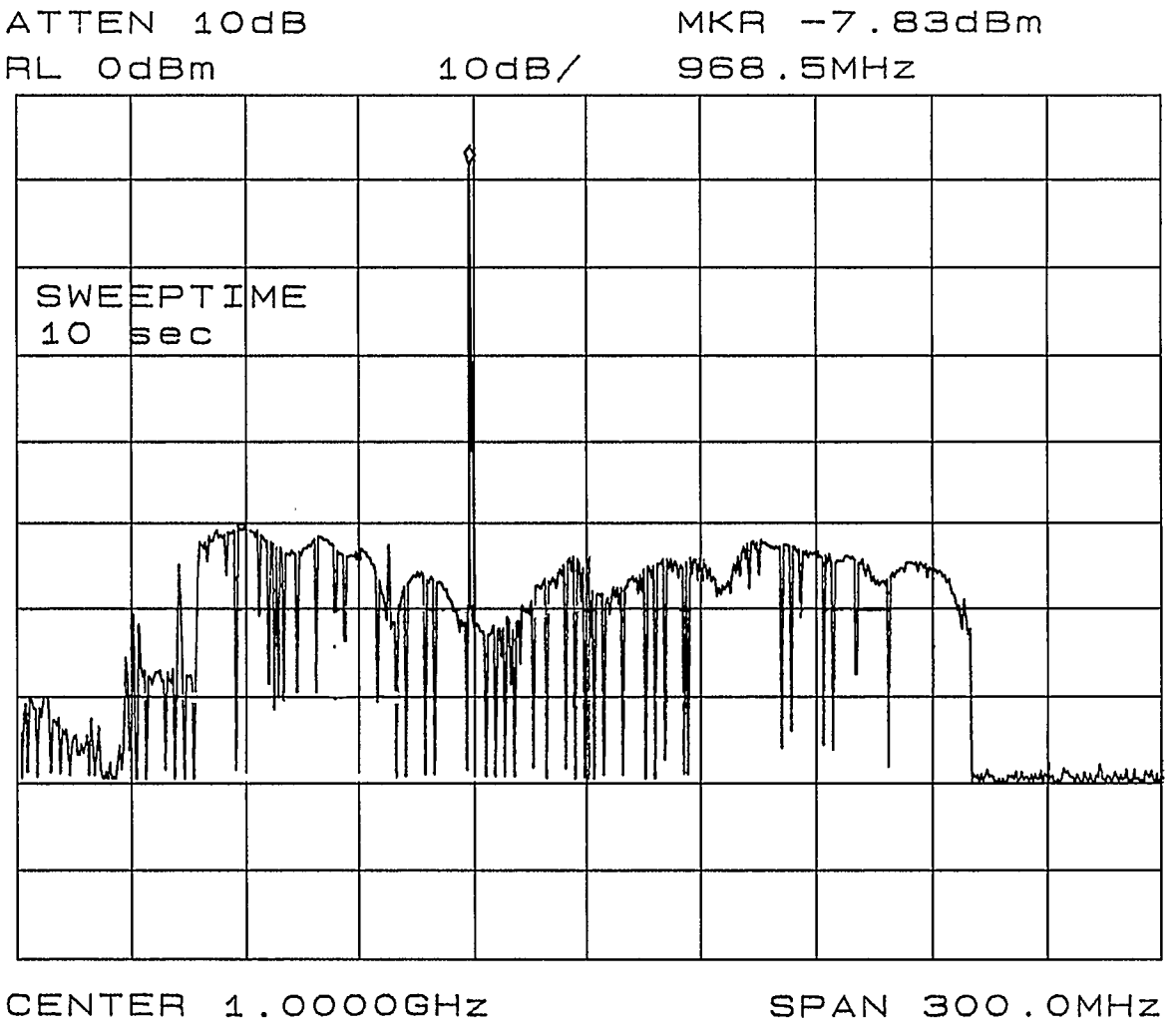

Figure 3.8: A Spectrum Analyzer Plot Showing the Channel Transfer Function with the Maximum Interfering Signal Present.

3.4.1 Frequency Domain - Single Sweep

Figure 3.9 shows a 200 MHz frequency sweep starting at 900 MHz and the effects from the interference which is 25 dB above the network analyzer's

receive power level. There is an interference spike at 968.5 MHz as expected, but it is approximately 12 dB above the transfer function power level instead of 25 dB. This improvement is a consequence of the interferer not being coherent with the network analyzer due to instantaneous phase differences. This results in some interference rejection.

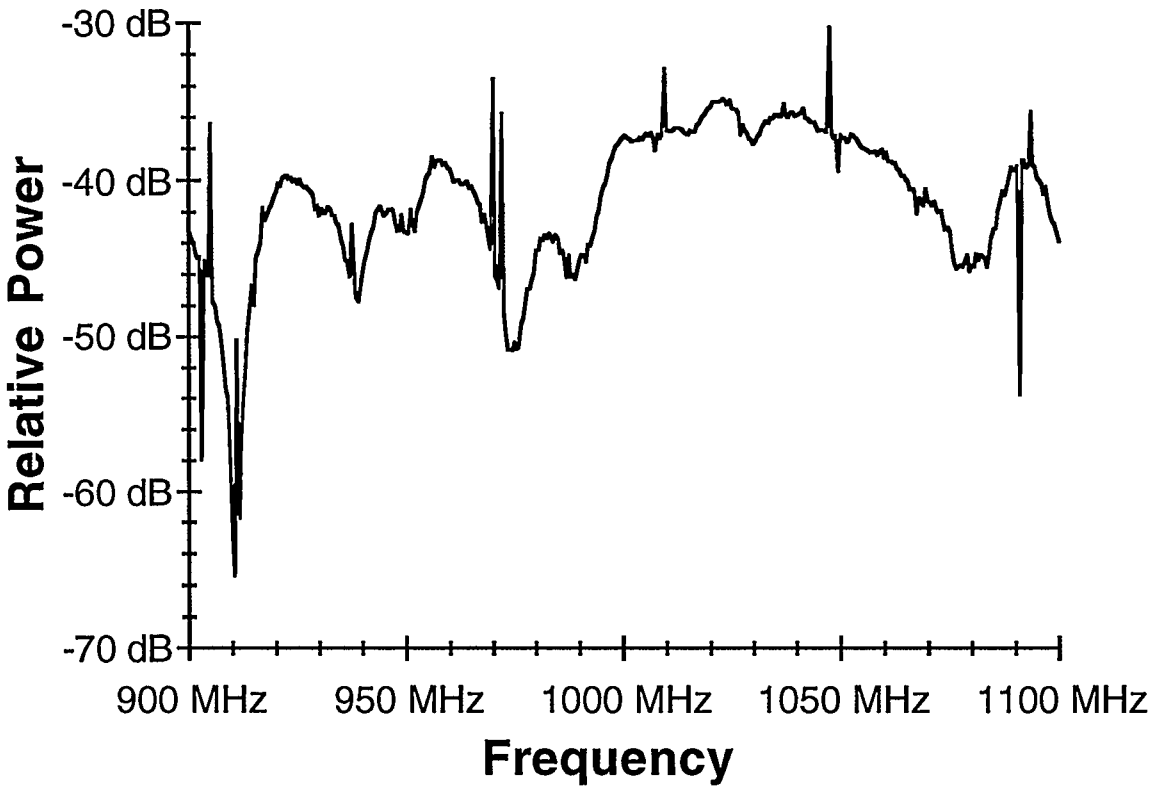

Figure 3.9: Frequency Response Magnitude of a Single Sweep with Interferer Present

There are other interference spikes present in the profile — some as large as 15 dB. This is due to intermodulation products present in the network analyzer that cause a single interferer to create tones across the measured profile. This would seem to magnify the effect of the interference.

However, it should be noted that the interference spikes are quite distinct making their identification and subsequent removal straightforward.

3.4.2 Time Domain - Single Sweep

It is recognized that the post removal of interference would result in an impulse response that would be nearly identical to one with no interference. The interest of this evaluation however, is in examining the effects of interference in the time domain as well.

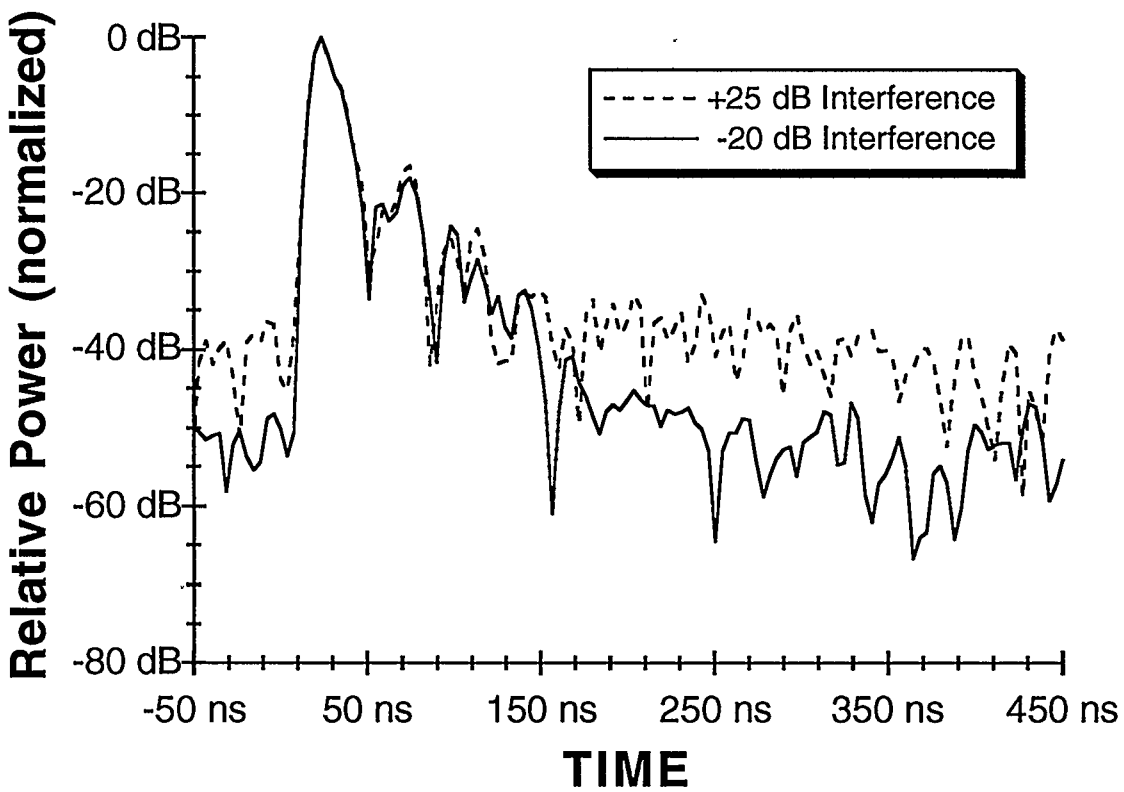

Figure 3.10: Impulse Response Magnitude of a Single Sweep with Interferer Present.

Figure 3.10 shows the impulse response from frequency sweeps where the interferer was 25 dB above the network analyzer's receive power and

20 dB below it. This results in two profiles: one with strong interference effects, and one with essentially no interference effects. The profile that contains interference effects demonstrates two distinct characteristics that differ from the profile with no interference effects.

First, the deviations in the profile above the noise level are as much as 5 dB. The reduction in deviation with respect to those in the frequency domain can be attributed to the Fourier transform which tends to minimize interference effects by spreading them across the band. This result is sometimes used to advantage in smoothing algorithms [Press et al., pp. 514-516].

Second, the mean value of the noise floor has been increased from -53.0 dB to -38.5 dB. This resulted in a small effect on τ_{rms}. The profile with interference has a τ_{rms} of 11.0 ns and the profile without interference has a τ_{rms} of 10.7 ns.

3.4.3 Results from Averaging Profiles

At this point, a discussion of temporal averaging is in order. Temporal averaging is sometimes employed as a method for improving the SNR in a measurement. This is because the noise between any two measurements is generally uncorrelated whereas the signal is correlated. Temporal averaging reduces the mean value of the noise floor, N_f, by the following expression:

$$\Delta N_f = 20 log_{10}(\sqrt{\eta})$$

where η is the number of profiles that are averaged.

In other words, if ten profiles are averaged, the mean value of N_f in the averaged profile would be reduced by 10 dB with respect to the mean value of N_f in the individual (unaveraged) profiles.

Experiments were conducted by measuring ten individual frequency sweeps in succession in the same location. These profiles were then averaged to produce a single profile. This is analogous to the averaging done by the network analyzer that measures a specified number of sweeps and stores the averaged result. The network analyzer takes 0.5 ms per sample, so ten measurements consisting of 201 points would take 1 s to complete. The delay characteristics of the individual sweeps as well as the averaged sweep were examined.

It was found that the first arrival occurred in the same sample bin for all individual sweeps and consequently, for the averaged sweep. It was also found that τ_{rms} of the individual impulse responses had little variation. The ten individual sweeps had an average τ_{rms} of 19.40 ns with a standard deviation of 0.60 ns. This agrees well with a τ_{rms} of 19.53 ns for the impulse response of the averaged profile. These results tend to justify averaging as a method for reducing noise.

3.4.3.1 Frequency Domain - Average of Multiple Sweeps

Figure 3.11 shows a 200 MHz frequency profile starting at 900 MHz that results from the average of ten consecutive sweeps. The effects of the interferer (still +25 dB above the network analyzer's received power level) are still noticeable but the interference spikes have been significantly reduced to approximately 2 dB. Also, the frequency response appears smoother due to the suppression of noise. A comparison with figure 3.9 shows that the transfer

function shape and power level have not been affected by averaging as expected.

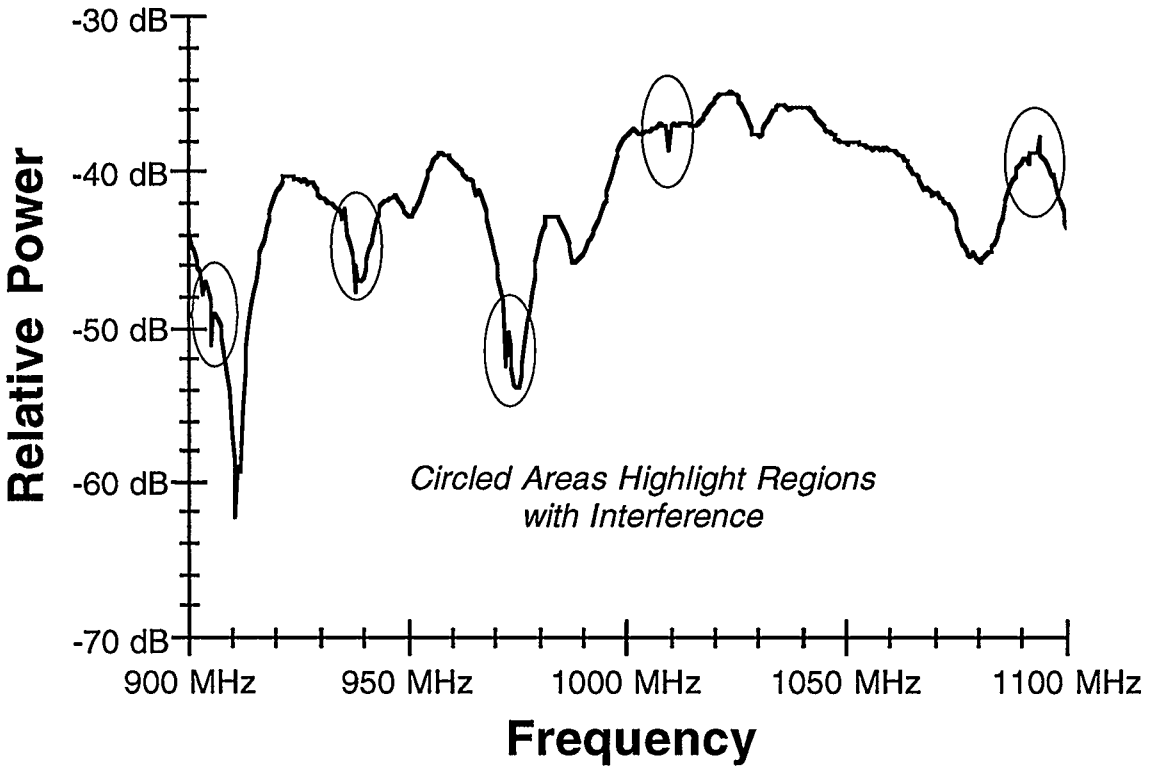

Figure 3.11: Averaged Frequency Response Magnitude with Interferer Present.

3.4.3.2 Time Domain - Average of Multiple Sweeps

Figure 3.12 shows the impulse responses (with and without the +25 dB interferer) from the averaged frequency responses. Again there are deviations between the two profiles but the dynamic aperture has been increased by approximately 10 dB.

The noise floor of the profile with the interferer present has a mean value of -49.7 dB. The noise floor of the profile without interference effects has a noise floor with a mean value of -63.4 dB. The τ_{rms} values of the profile with

interference effects and for the profile without interference effects are 11.3 ns and 10.1 ns.

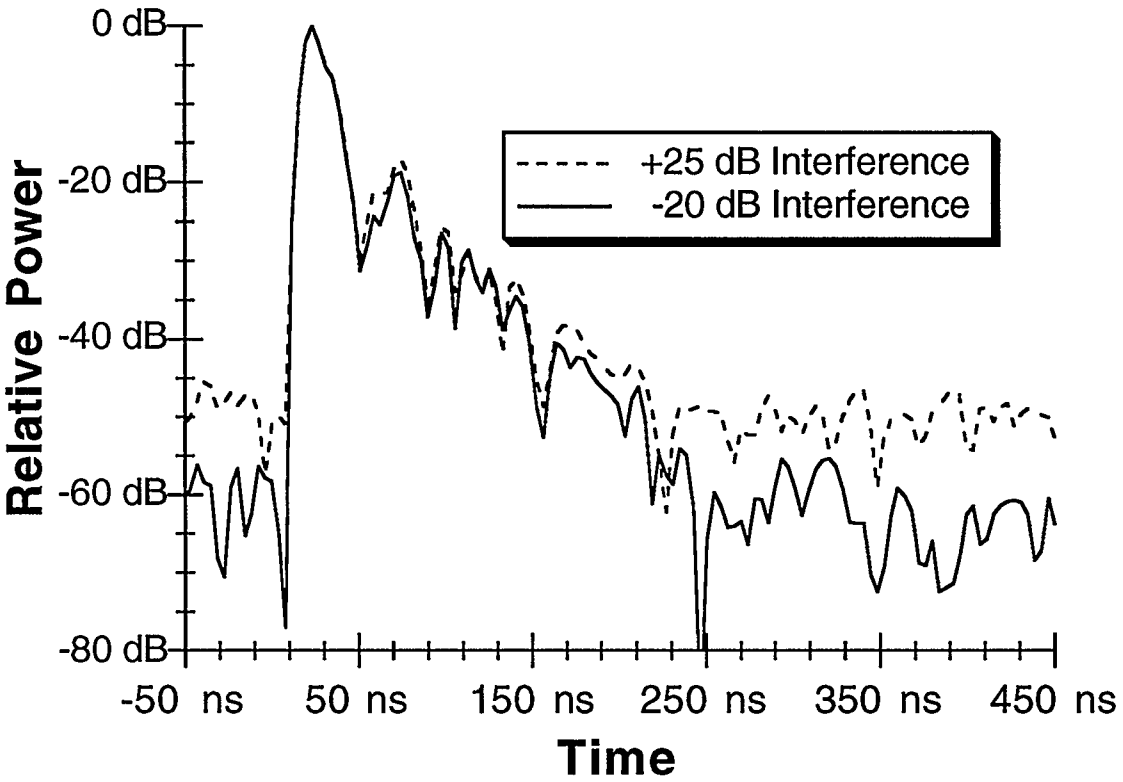

Figure 3.12: Impulse Response Magnitude (from Averaged Frequency Responses) with Interferer Present.

3.4.4 Interpretation of Interference Experiment

The experiment reported in this section was designed to produce worst case interference. In other experiments conducted for varying reasons, interference was not present (at least it was unnoticable). Also, the spectrum analyzer was used to examine the measured spectrum before testing was done. Again, interference was not a problem. This is not to say that interference will not occur, but simply that it doesn't appear to be problematic.

There are two remarkable results exposed in the experiment which are explained by the following points:

1. The system is quite robust when it comes to interference rejection. The reasons for this are as follows: i) The interference is not usually coherent with the measurement signal due to instantaneous phase differences. ii) The frequency sweep is usually slow compared to an interfering transmission (this is related to (i) but not exclusively the same thing). This improves the possibility of the network analyzer being blind to the interferer.
2. Averaging gives an increased SNR and therefore reducing the effects of interference.

These results suggest that the system, although not immune to interference, shows capabilities that have strong interference rejection. Results obtained in the presence of strong interference are still valid and are therefore very useful.

3.5 Dynamic Range

In this section, the dynamic range of the system is formally defined. The dynamic range of the frequency response is different from that of its associated impulse response. The reasons for this and the tests identify the dynamic range are explained.

Tests were performed by placing a variable attenuator in the transmit path (before the amplifier). The antennas were placed 3 m apart and the frequency response as a function of added attenuation was collected. This was accomplished by attenuating the transmitted signal by 5 dB steps (from 0

dB to 45 dB) and observing the effects on both the transfer functions and their associated impulse responses.

3.5.1 Frequency Domain

Figure 3.13 shows the frequency responses as a function of added attenuation: 0 dB, 15 dB, 30 dB and 45 dB (the graph legend is shown in Figure 3.14).

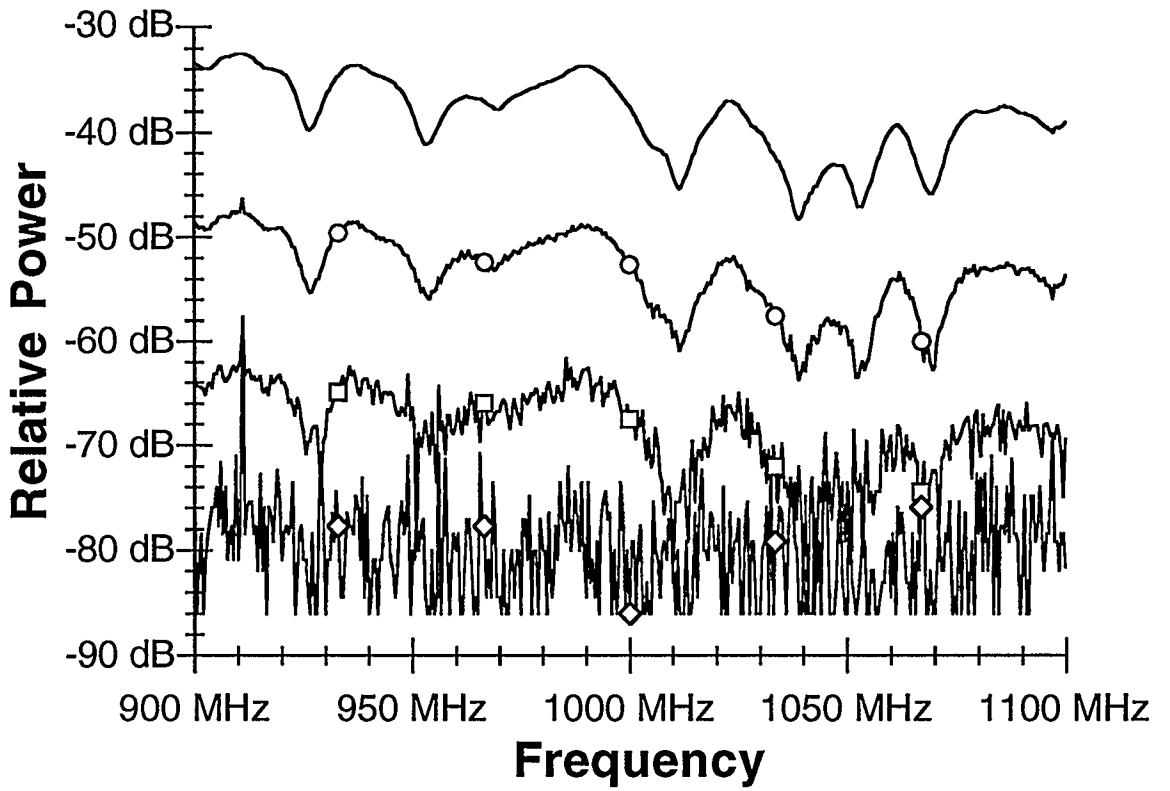

Figure 3.13: Frequency Response Magnitude as a Function of Added Attenuation.

The profiles are similar to each other except attenuated, as expected. An introduction of 0 dB attenuation shows the channel transfer function. Progressive attenuations of 15 dB and 30 dB result in transfer

functions that look similar except for more noise and greater path loss. An introduced attenuation of 45 dB results in a noisy frequency profile that is dissimilar from the expected transfer function. The profile also appears to have little information content (the lower limit truncation is due to instrumentation limits). This dynamic range can be explained as follows: the network analyzer has a dynamic sensitivity, D_N, of 80 dB, and there is a relative path loss, P_L, associated with free space transmissions. The 0.5 dB per meter loss in the cables is compensated for by the amplifier and effects from both are removed by calibration. The dynamic range of the frequency response, D_F, is give by the following expression:

$$D_F = D_N + |P_L| \approx 80\,dB + |P_L|$$

This explains the apparent loss of information when the transmit signal was attenuated by 45 dB. The path loss at 1.0 GHz is approximatly 40 dB so an additional loss of 45 dB places the signal level at the noise level of the network analyzer. It should not be forgotten that temporal averaging also plays a role in dynamic range analysis but its most significant effects are demonstrated in the time domain.

3.5.2 Time Domain

Figure 3.14 shows the corresponding impulse responses from the attenuated frequency responses. Again, the profiles were similar but with reduced dynamic ranges as the attenuation was increased. However, the dynamic range of the impulse response is larger than its respective frequency response. Note for example, that the impulse response from the frequency

response that was attenuated by 45 dB still contains approximately 26 dB of information.

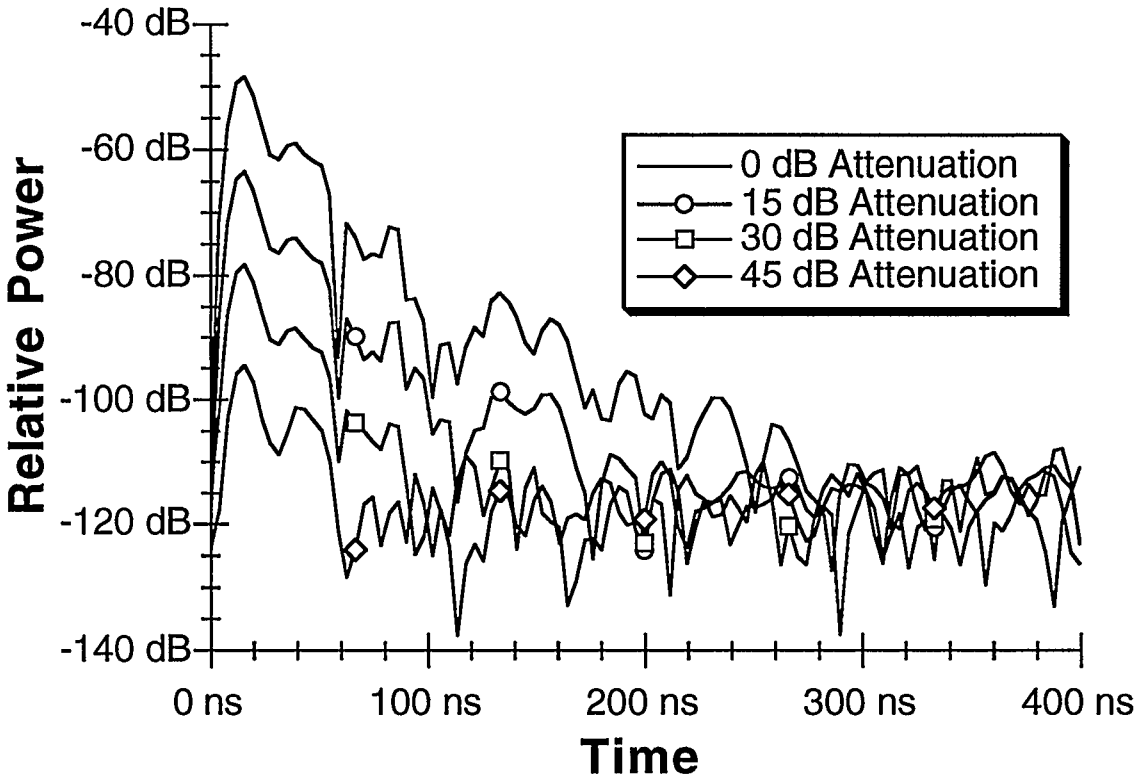

Figure 3.14: Impulse Response Magnitude from Attenuated Frequency Responses.

This enhanced dynamic range is partly due to the noise bandwidth reduction property, N_B, of the Fourier transform [Goldman, pp. 80-81; Harris, 1978] which is given by the following equation:

$$N_B = 10LOG_{10}(ENBW)$$

where,

$$ENBW = \frac{\left[\sum_{n=0}^{N-1} w[n]\right]^2}{\sum_{n=0}^{N-1} w[n]^2}$$

and $w[n]$ are the window coefficients.

Essentially, this states that the mean value of N_f of the impulse response will be lowered by N_B. Therefore, an impulse response profile that was obtained from a 401 point sweep will have its dynamic aperture increased by 26 dB. When this is combined with temporal averaging as described in section 3.4.3, the dynamic aperture is increased by 36 dB. This is not a trivial result as the dynamic aperture that results from N_B and averaging alone equals or surpasses the dynamic range of the other measurement systems described in section 1.5. The dynamic range of D_F must also be added in along with a minor processing loss, W_L, due to windowing. A Minimum 3-sample Blackman-Harris window has a processing gain of 0.42 [Harris, 1978] that results in a loss of approximately 4 dB. The dynamic range of the impulse response, D_I, is given by the following expression:

$$D_I = D_F + |N_B| - |W_L| + 20LOG_{10}(\sqrt{\eta})$$

Impulse response profiles from the measurements showed this relationship to be true. For example, in the case where the frequency response

was not attenuated, P_L at 1.0 GHz (the center frequency) is approximately 40 dB. Therefore,

$$D_I \approx 80\,dB - 40\,dB + 26\,dB - 4\,dB + 10\,dB$$
$$\approx 72\,\text{dB}.$$

This closely agrees with the dynamic range of the unattenuated impulse response in figure 3.14 of 68 dB (from a peak of -47 dB to the mean value of N_f of -115 dB).

3.5.3 Interpretation of the Dynamic Range Experiment

The experiment demonstrated a very powerful aspect of acquiring impulse responses from measured transfer functions. The resulting available dynamic range is large. The greatest reduction in dynamic range is due to P_L which can be compensated for by amplification and therefore increasing the dynamic range further. As in the case of interference rejection, the benefit from acquiring an impulse response by taking the Fourier transform of the transfer function is significant.

3.6 Channel Stationarity

Although not specifically a part of the system, channel stationarity is presented here for completeness.

The HP network analyzer requires a finite time interval to sweep a frequency band (i.e., 0.5 ms per sample), so the issue of channel stationarity is raised. The results of this thesis assume the indoor channel to be slowly time varying, (i.e., it does not change significantly during a measurement sweep). This assumption is also used by other researchers [Yegani and McGillem, 1989;

Ganesh and Pahlavan, 1989; Saleh and Valenzuela, 1987]. Furthermore, measurements were performed at times (nights and weekends) when there were no moving objects in the channel and in most cases, ten consecutive sweeps were made at each location and the averaged result was used. Figure 3.15 shows the Doppler spectrum from a 1.0 GHz continuous wave measurement made during these times. The bin resolution after windowing is 0.46 hertz (0.2 hertz * 2.3 from using a minimum 3-term Blackman-Harris window). The entire spectrum is contained within one bin which indicates that the assumption of stationarity is valid. Measurements taken at different frequencies and for different time intervals showed the same result (i.e., the Doppler spectrum was contained within one sample bin).

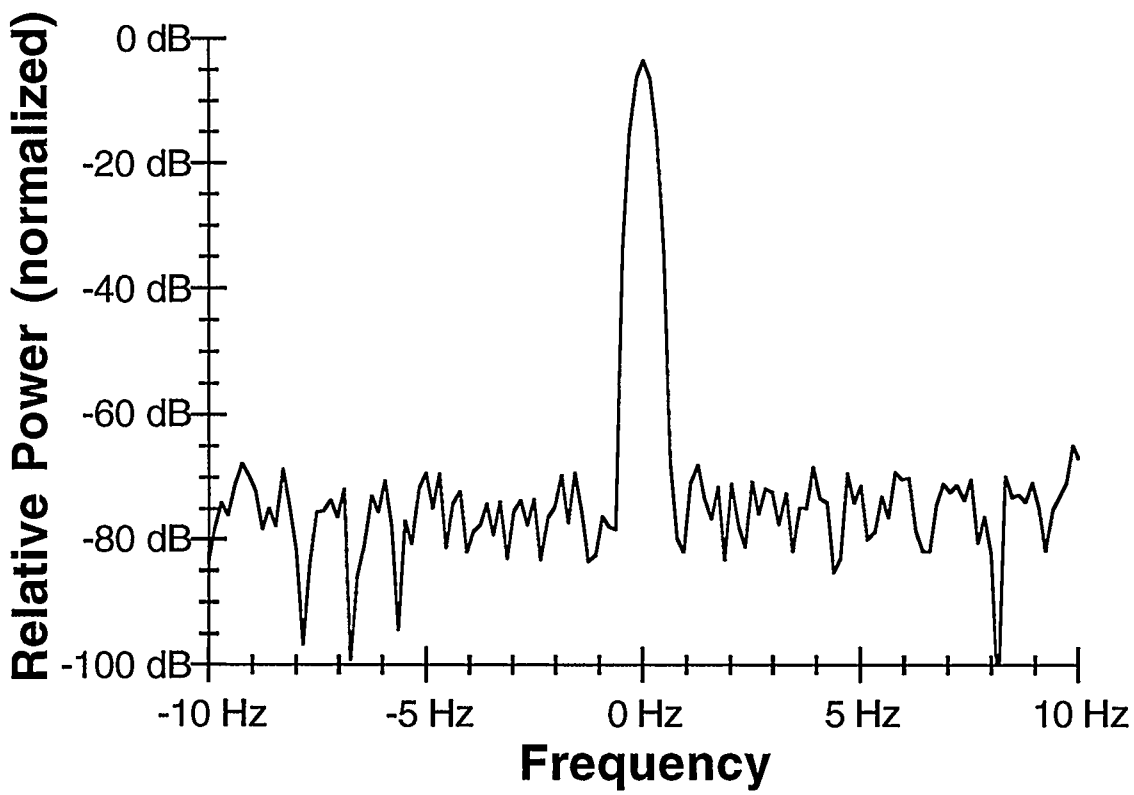

Figure 3.15: Doppler Spectrum of a 1.0 GHz CW Measurement.

CHAPTER FOUR

MEASUREMENT RESULTS

4.1 Objective

In this chapter, results for different types of measurements are documented. The results are not presented with a rigorous analysis but are given to demonstrate the various types of channel characterization techniques the measurement system is capable of doing.

Channel characterization is done by different methods where each method has an associated analysis technique. Researchers choose the best type of analysis based on the measured data available and the required output of the analysis. Popular analysis methods are described in section 1.3.

It will be shown in this chapter that the frequency domain measurement system is capable of producing results that are equivalent or better than the current time domain systems as described in section 1.5.

4.2 CW Measurements

As mentioned in section 1.3.1, narrowband or CW measurements are used primarily to find fading statistics and the distance/power law gradient. It has been shown that the envelope of a CW signal typically has a Rayleigh or a Rician fading depending on whether there is a line-of-sight (LOS) transmission or not [Proakis, Ch. 7]. The fading distribution (implying depth of nulls) is normally what is characterized.

The power law is another useful characterization method as it indicates how rapidly a signal's power will decrease with distance. A relationship to estimate the rate of decay of a transmitted signal that predicts the

median power of a signal at a given distance is found in the literature [Cox,Murray,and Norris, 1983,1984] and is given here:

$$P = \frac{1}{D^m}$$

or

$$P(dB) = -m \log_{10} D$$

where:

P is the power of the received signal

m is the gradient

D is the distance between the transmit and receive antennas

Results from some of the CW measurements presented here have been reported in the literature [Zaghloul et al., 1990a].

4.2.1 Fixed Antenna Separation Measurements

In this section, results from measuring a 945 MHz CW signal with an obstructed path (OBS) are given. The selection of 945 MHz was arbitrary. The receive bandwidth of the signal was 3 kHz but the network analyzer is capable of smaller bandwidths if desired.

Figure 4.1 shows the magnitude of a CW signal with a moving reflector. The measurement was accomplished by fixing the transmit-receive antenna separation and walking through the environment during a transmission. The transmit time for this measurement was 60 s in which 1601 samples were collected. Since this is an OBS measurement, it is assumed that the fading follows a Rayleigh distribution. Some valuable observations can be

made without determining the distribution parameters, however. First, fade levels vary depending on where the mobile reflector is in relation to the antennas and signal degradation can be significant (25 dB at 40 s for example). Second, the moving reflector does not always result in fading but can give an increased received power level (3+ dB at 11 s).

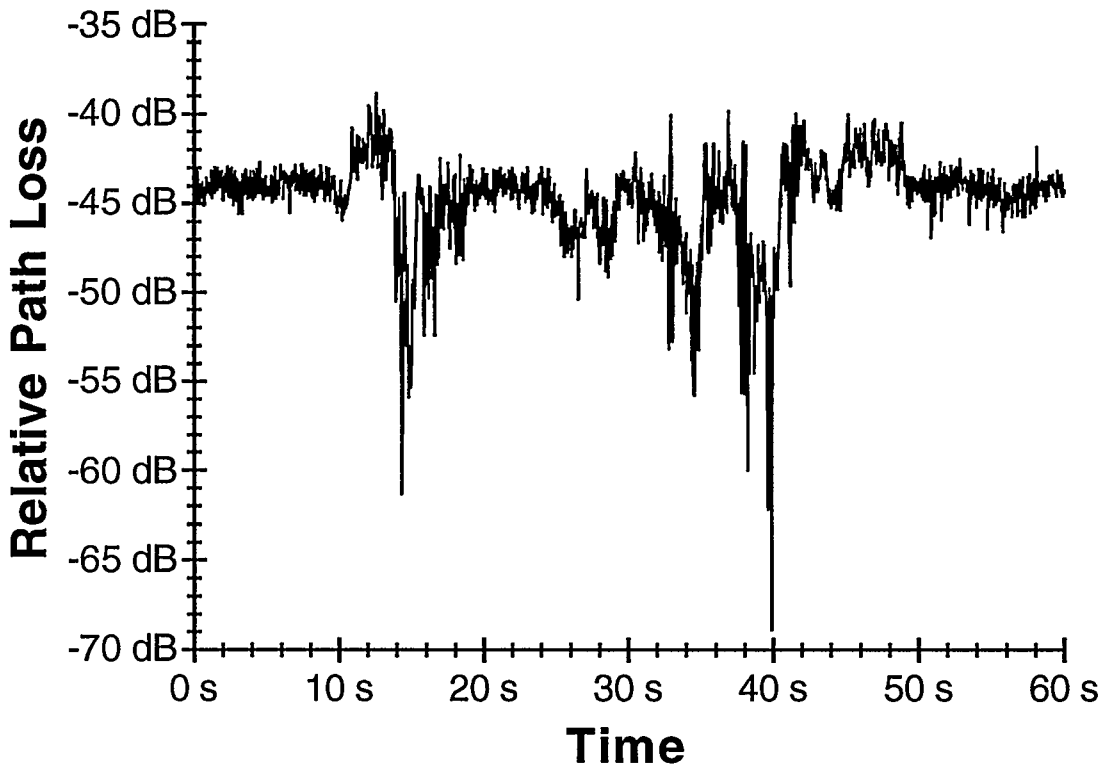

Figure 4.1: Magnitude of a 945 MHz CW Measurement with a Moving Reflector.

Figure 4.2 shows the corresponding phase of the signal in figure 4.1. As expected, there are rapid phase variations whenever the signal magnitude is in a null. CW systems typically yield information about the envelope and then the phase distribution is assumed. The network analyzer measures the complex envelope so phase distributions can be empirically

determined. This would produce a more accurate characterization that may lead to a deeper understanding of phase cancellation in the indoor environment.

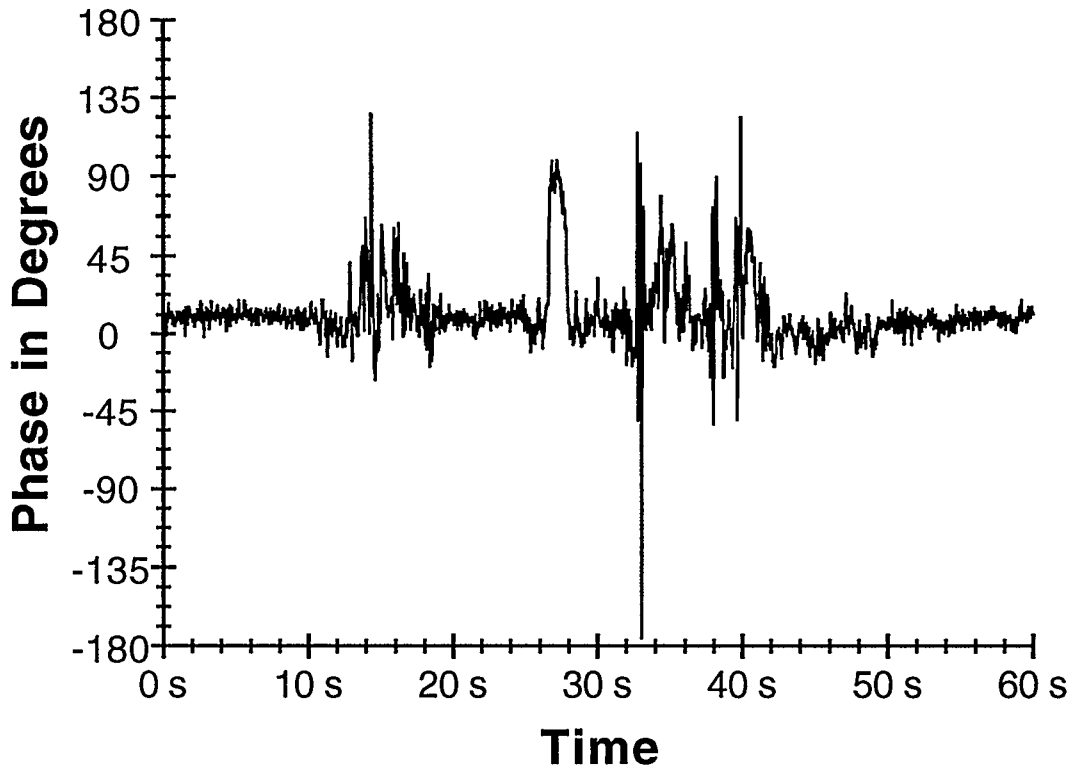

Figure 4.2: Phase of a 945 MHz CW Measurement with a Moving Reflector.

4.2.2 Variable Antenna Separation Measurements

In this section, results from measuring a 945 MHz CW signal with a line-of-sight path are given.

Figure 4.3 shows the signal magnitude of a CW signal as a function of distance. This type of measurement is useful in determining the power law of the channel. The measurement was accomplished by moving the

transmit antenna away from the receive antenna at a speed of approximately 1 m per second for 30 seconds.

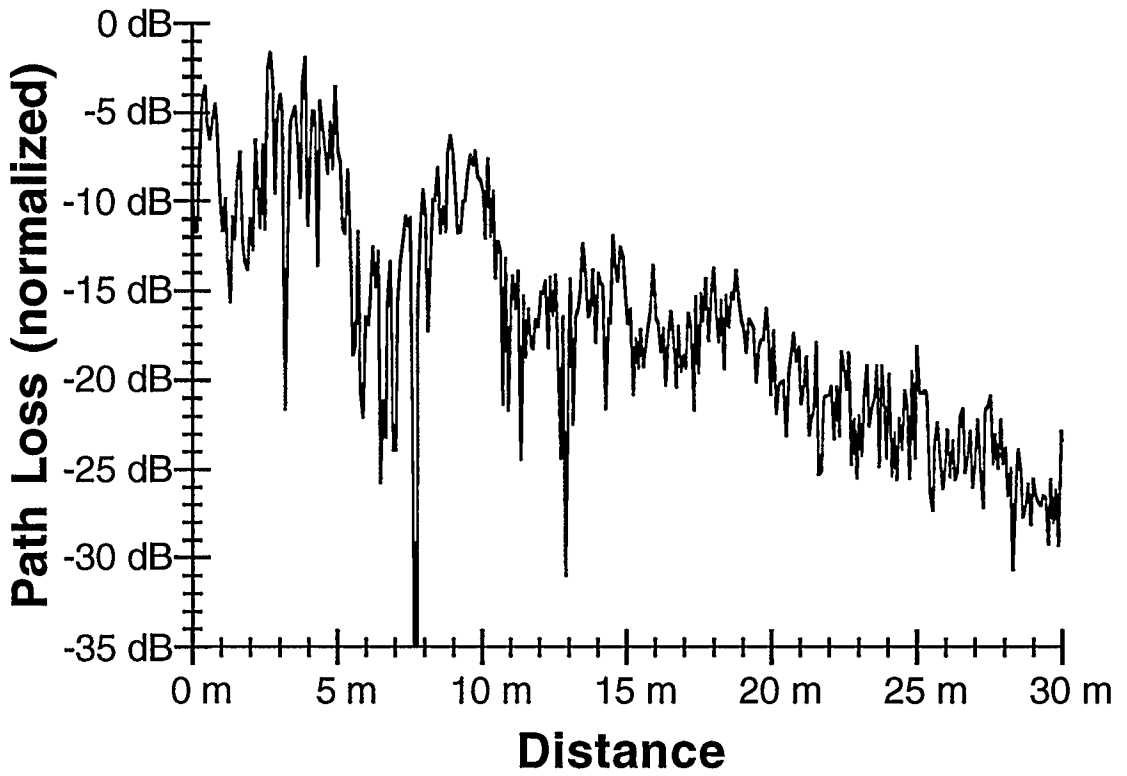

Figure 4.3: Magnitude of Path Loss as a Function of Distance.

This measurement suggests that there is a region of small separations between the transmitter and the receiver where the received amplitude is showing exponential decay with a standing wave pattern superimposed on it. This region is followed by the region of range clamping [Zaghloul et al., 1990b] where the standing wave pattern disappears and only a slower exponential decay persists. The region in the 0 to 2 meter range appears to have a different standing wave characteristic. This may be attributed to near field effects of the two antennas.

Figure 4.4 shows the power law associated with the indoor channel in the NovAtel building. Several measurements were made and the averaged result was used.

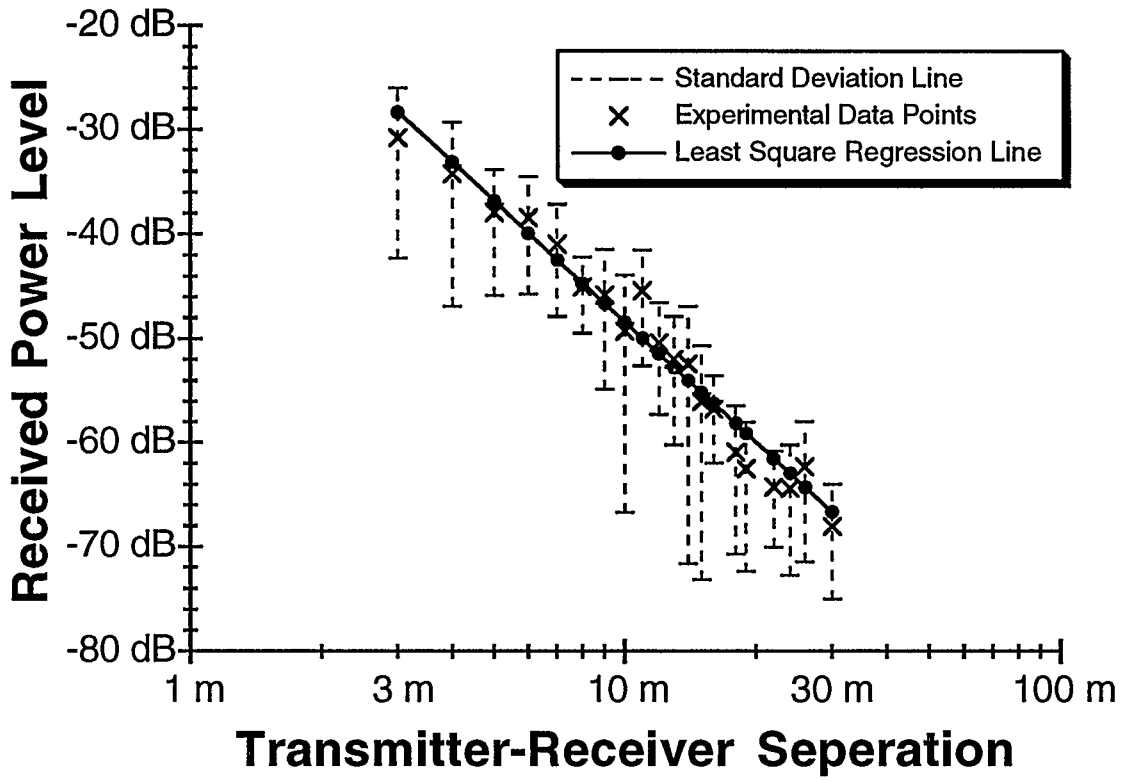

Figure 4.4: Path Loss as a Function of Transmitter-Receiver Separation.

The vertical lines on the plot represent one standard deviation above and below the mean value. The measurements were fitted to a straight line on a log-log scale by least squares regression. The Pearson's correlation coefficient is 0.97 and the slope is -38.35 suggesting that the power law is proportional to the following expression:

$$P = \frac{1}{D^4}$$

This result is consistent with range of power laws found by several other researchers [Molkdar, 1991].

4.3 Swept Frequency Measurements

As discussed in section 1.3.2, swept frequency measurements are used to characterize the wideband response of the channel. The coherence bandwidth of the channel is proportional to the inverse of τ_{rms}. This is useful in determining the minimum separation between frequencies that can be used in frequency diversity and in determining the maximum bit rate that can be transmitted on the channel without equalization. Also, investigation of the frequency response of the channel for different antenna separations can lead to estimating the correlation bandwidth as a function of transmitter-receiver separation. For example, analysis of data taken from the NovAtel building showed that the correlation bandwidth is larger than 1 MHz [Zaghloul et al., 1990a].

Unlike traditional time domain measurement systems that operate at a single frequency, the frequency domain measurement system can easily determine τ_{rms} for different frequencies. This can be done by sweeping a large band (say 1.0 to 2.7 GHz) and then truncating the data using a moving window (say 320 MHz wide). This smaller bandwidth sample is used to determine the impulse response at its center frequency. The value for τ_{rms} is determined for that frequency. The window is then moved to the next frequency point and the process is repeated. This type of analysis may be useful in determining the choice of frequency band for indoor wireless products.

4.3.1 Delay Spread Results

Measurements from 1.0 GHz to 2.5 GHz were evaluated from two different buildings (in Calgary: NovAtel 3rd floor, and AGT 19th floor). Each measurement consisted of 1601 points and was windowed by a 320 MHz band. The frequency sweeps were analyzed by studying τ_{rms}; starting from the lowest 320 MHz possible, calculating τ_{rms}, increasing the center frequency, f_c, by 20 MHz and repeating until the entire 1.0 to 2.5 GHz band was covered. It should be noted that the amplifier in figure 2.1 was removed and the network analyzer's built-in amplifier was used.

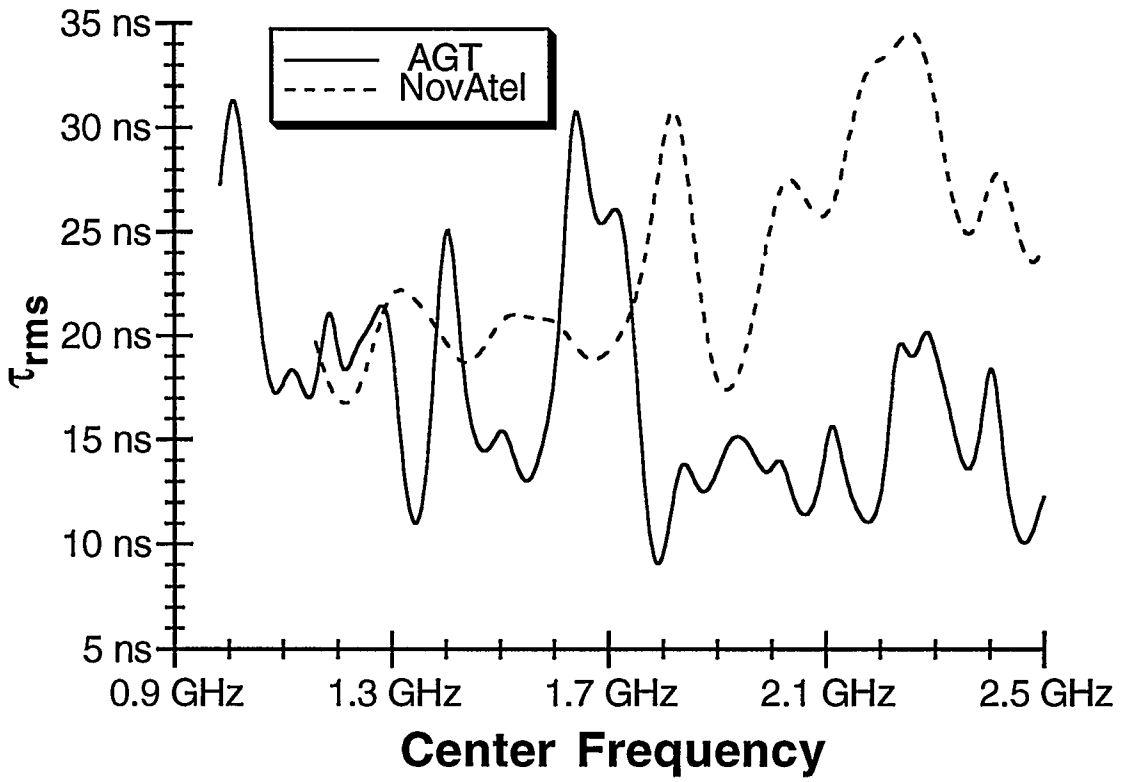

Figure 4.5: τ_{rms} as a Function of Center Frequency for a Single Location.

Figure 4.5 shows τ_{rms} as a function of f_c for a single location. This suggests that τ_{rms} is dependent on frequency at any given location. Values can range between 10 ns and 35 ns.

Figure 4.6 shows τ_{rms} as a function of f_c when the average of 25 locations was used. It can be seen that the values for τ_{rms} are tending toward a mean value (somewhere between 15 ns and 25 ns). This result would indicate that although τ_{rms} can largely vary at any given location, it will have some average value. This would also suggest some stochastic distribution of τ_{rms} as a function of location. The result for an average τ_{rms} is consistent with other researchers' findings [Hawbaker and Rappaprt, 1990; Bultitude, Mahmoud, and Sullivan, 1989].

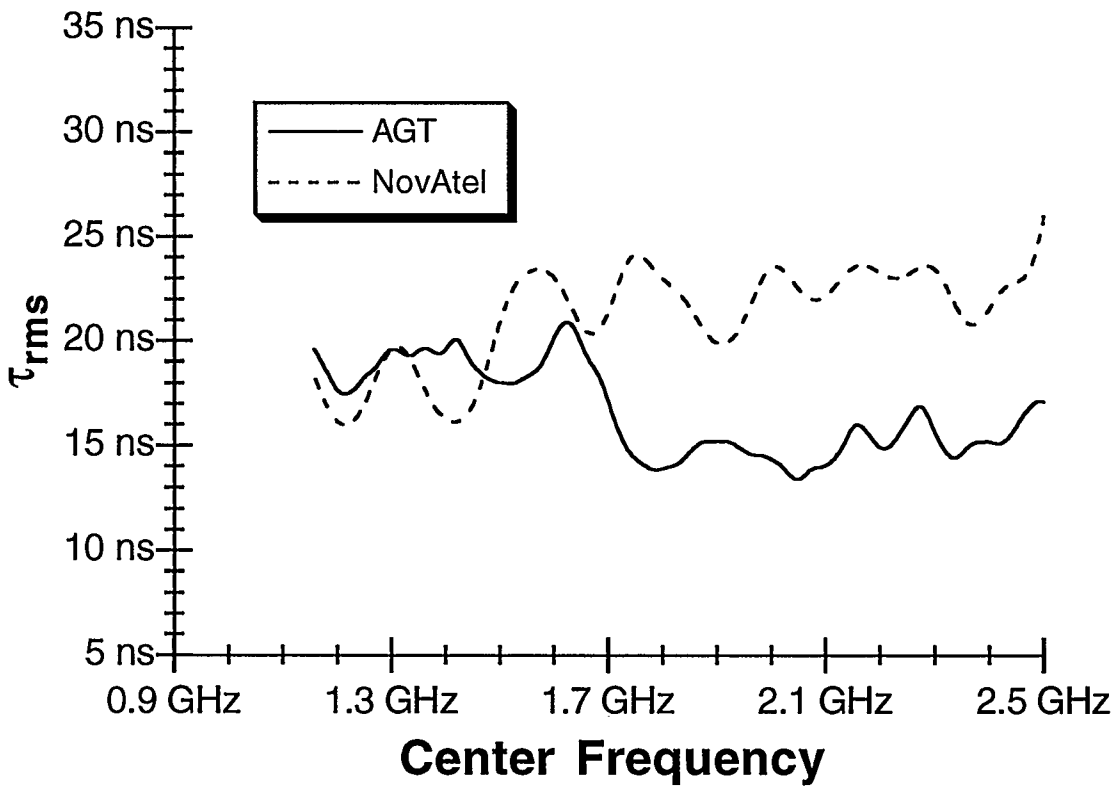

Figure 4.6: τ_{rms} as a Function of Center Frequency — the Average of Several Locations.

Results shown here are for the case of a LOS.transmisson. The results for OBS transmisson show similar results with τ_{rms} having more variations [Zaghloul et al., 1991b].

4.3.2 Frequency Selectivity

The frequency selective nature of a channel is directly related to its delay spread which is related to the data rate that can be transmitted without equalization. This would indicate that a study of the frequency selective nature may be useful. This type of study is easily accomplished with a frequency measurement system.

The number of nulls per frequency band is inversely proportional to the coherence bandwidth (assuming a uniform distribution of nulls across the measured band) which is proportional to the reciprocal of τ_{rms} [Proakis, Ch. 7]. Therefore, the number of nulls per frequency band is a valid characterization of the frequency response. Observation of the frequency response in two different bands suggests that the average number of nulls is different (i.e., the coherence bandwidth may vary).

Measurements were performed by sweeping a 200 MHz band centered at 1.0 GHz and 1.6 GHz with LOS transmitter-receiver separations varying from 10 m to 30 m in 0.5 m steps. The number of nulls per frequency band was determined as follows:

i) The mean level of a single frequency response was determined.

ii) A specified dB level below this mean was chosen as the null depth.

iii) The number of times the frequency response crossed below the null depth was determined.

iv) The average number of such nulls was obtained over all profiles.

Table 4.1 gives the number of nulls in the 1.0 GHz and 1.6 GHz band for various null depths. It can be seen that the overall average number of nulls in the 1.6 GHz band is more than 3 times the number of nulls in the 1.0 GHz band.

Null Depth → *Frequency Band* ↓	**0 dB**	**2 dB**	**4 dB**	**6 dB**	**8 dB**	***Over all Average***
1.0 GHZ	23	4.7	1.0	0.53	0.28	5.9
1.6 GHz	34.2	29.3	20.5	14.0	9.7	21.5

Table 4.1: Average Number of Nulls per 200 MHz Band for Different Null Depths.

A similar analysis can be done in the time domain. For this case, a study of the number of peaks in each impulse response at 1.0 GHz and 1.6 GHz is done. The number of peaks per profile was determined as follows:

i) The level of the largest peak (the first arrival) in a single profile was determined.

ii) A specified dB level was chosen.

iii) The number of peaks within this level and the largest peak level was determined.

iv) The average number of such peaks was obtained over all profiles.

The results from this experiment are reported in table 4.2 which shows the average number of peaks for different peak levels in the two frequency bands. It was found that the average number of peaks in the 1.6 GHz band is 1.6 times greater than that of the 1.0 GHz band.

Peak Level → *Frequency Band* ↓	**-28 dB**	**-24 dB**	**-20 dB**	**-16 dB**	**-12 dB**	***Over all Average***
1.0 GHZ	3.9	2.7	1.8	1.2	1.1	2.1
1.6 GHz	4.2	3.9	3.7	2.9	2.2	3.4

Table 4.2: Average Number of Peaks for Different Peak Values

These results indicate that the RF propagation channel is more dynamic in the 1.6 GHz band than in the 1.0 GHz band. This can be explained as a result of the greater resolving power at higher frequencies. In other words, the small wavelength of higher frequencies can resolve finer structures within the channel. The dynamic nature tends to increase with an increase of either the number of nulls in a frequency response or the number of reflections in an impulse response.

4.3.3 200 MHz and 1000 MHz Bandwidth Measurements

The measurements reported thus far have mostly been for transfer functions with a 200 MHz bandwidth. Based on the antenna, amplifier, and cable results reported in sections 3.2.3 and 3.3, it is apparent that a transfer function with a larger bandwidth can be collected. The purpose of doing this is

to obtain an impulse response that has a better time resolution. Section 2.4 showed that the time resolution of an impulse response is equal to the inverse of the transfer function's bandwidth times the bin-width of the windowing function. This means that transfer functions with 200 MHz and 1000 MHz bandwidths would give impulse responses with time resolutions of 11.5 ns and 2.3 ns respectively. This is an important result as an increase in the time resolution will reveal more spectral features of the channel. Currently, time domain systems that can measure a coherent channel impulse response have reported resolutions of 25 ns [Bulitude, 1989]. Time domain systems that can measure the impulse response envelope only have reported resolutions of 7.8 ns [Rappaport, 1989].

Tests were performed to show the frequency domain technique's ability to produce high resolution impulse responses. Measurements were done for both LOS and OBS paths. Profiles were collected as a function of bandwidth where the bandwidth was increased around a fixed center frequency from 200 MHz to 1000 MHz in 200 MHz steps. This is equivalent to measuring a 1000 MHz sweep and truncating it to 200 MHz at the center frequency.

4.3.3.1 Line of Sight Path

Figure 4.7 shows two impulse response profiles obtained from LOS measurements at 200 MHz and 1000 MHz. The ability of the wider band measurement to resolve multipath reflections in greater detail is apparent. The first arrival lobe (a single path) of the impulse response obtained from a 200 MHz sweep is approximately 35 ns wide at - 20 dB. Within that same width, the impulse response from 1000 MHz sweep contains information about 5 paths. Due to their time resolutions, these paths could not be resolved with current

time domain systems. Because these profiles are from LOS measurements, the first arrival (the direct path) is the dominant peak (i.e., it has the greatest power). This figure also demonstrates an expected result — namely, the reflections in low resolution impulse response profiles are the vector sum of multiple reflections.

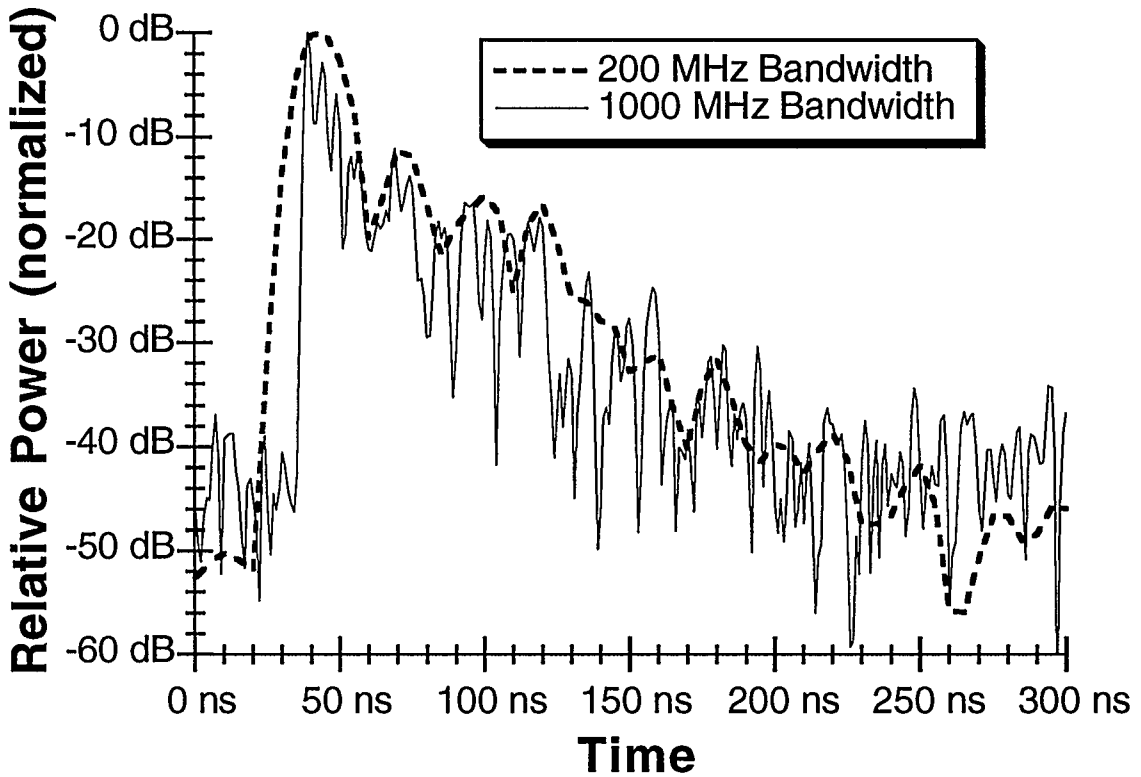

Figure 4.7: LOS Impulse Responses from 200 MHz and 1000 MHz Sweeps.

4.3.3.2 Obstructed Path

Figure 4.8 shows two impulse response profiles obtained from OBS measurements at 200 MHz and 1000 MHz. The results are similar to the LOS case with an interesting exception. The first arrival is no longer the strongest arrival. Indeed, it can be seen that there are several weaker impulses before

the strongest signal arrives. This is a consequence of the direct (and therefore the shortest path) being obstructed. The measurement was performed in a cluttered environment where a bookcase was used to obstruct the antenna's line-of-sight. It is difficult to determine which path caused the strongest reflection except to say that it has an additional 6 m (20 ns * c = 6 m) associated with it. This detail has not been reported by other researchers.

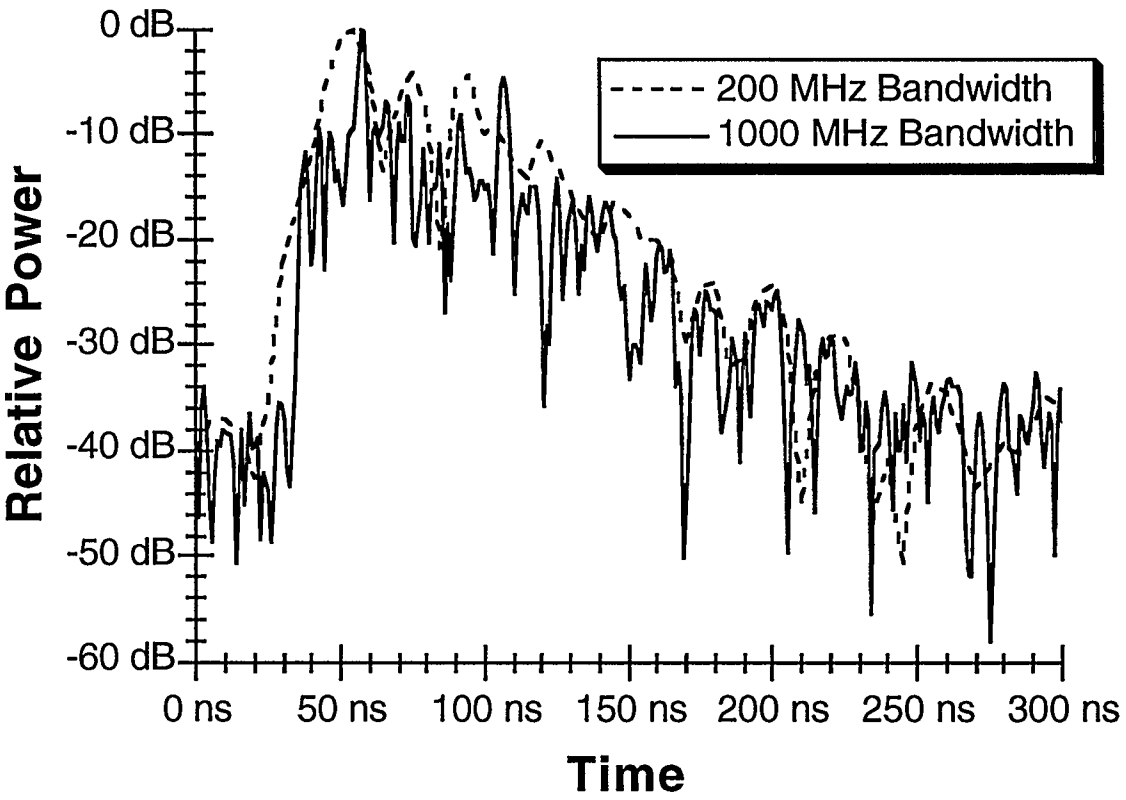

Figure 4.8: OBS Impulse Responses from 200 MHz and 1000 MHz Sweeps.

4.4 Sliding Correlator Measurement Comparison

During the period of research for this report, there was an opportunity to compare the frequency domain measurement technique with a

well known time domain system. The measurements were performed independently at the Communications Research Center (CRC) in Ottawa, Ontario. The experiment was conducted by Dr. Robert Bultitude of CRC and David Tholl of NovAtel Limited and the results were made available.

The measurement was done by placing the antennas in approximately the same locations for both systems. The channel response in 120 different locations was collected (the transfer function was collected using the network analyzer and the impulse response was collected with the sliding correlator). The transfer function was collected over a 100 MHz bandwidth so that the resolution of the resulting impulse response (after windowing) would closely match that of the sliding correlator.

The dynamic range of the frequency domain system was shown in section 3.5 to be limited by the cross talk rejection of the network analyzer. This is quite different for the sliding correlator that has a dynamic range limitation of $20\log_{10}(L)$, where L is the code length. The sliding correlator system in this experiment used a code length of 63 giving a dynamic range of 36 dB.

The 30 dB half-window resolution (the width from the peak to the first null of the window function at 30 dB) of the frequency domain system is 2.4(1/B). B is the bandwidth of the frequency sweep which in this case, is 100 MHz giving a 30 dB resolution of 24 ns. The theoretical half window resolution of the sliding correlator is 1/R, where R is the chip rate of the code which, in this case, is 40 MHz giving an approximate 30 dB resolution of 25 ns.

The time of data acquisition of the frequency domain system has been presented which is 0.5 ms per point. The data acquisition time per bit of the sliding correlator is $1/f_d$, where f_d is the difference frequency which is 4 kHz giving an acquisition time of 250 μs. The total acquisition time for the

experiment here is as follows: the network analyzer collected 10 sweeps of 201 points each requiring 1 s (100 ms per sweep), the sliding correlator collected 3 measurements of 63 bits each requiring 47.25 ms (15.75 ms per measurement).

Figure 4.9 shows the comparison of the resulting impulse response from a typical measurement. The sliding correlator response does not give a relative time base so the profiles were aligned by using the first arrival as a reference. The time base from the network analyzer method was preserved.

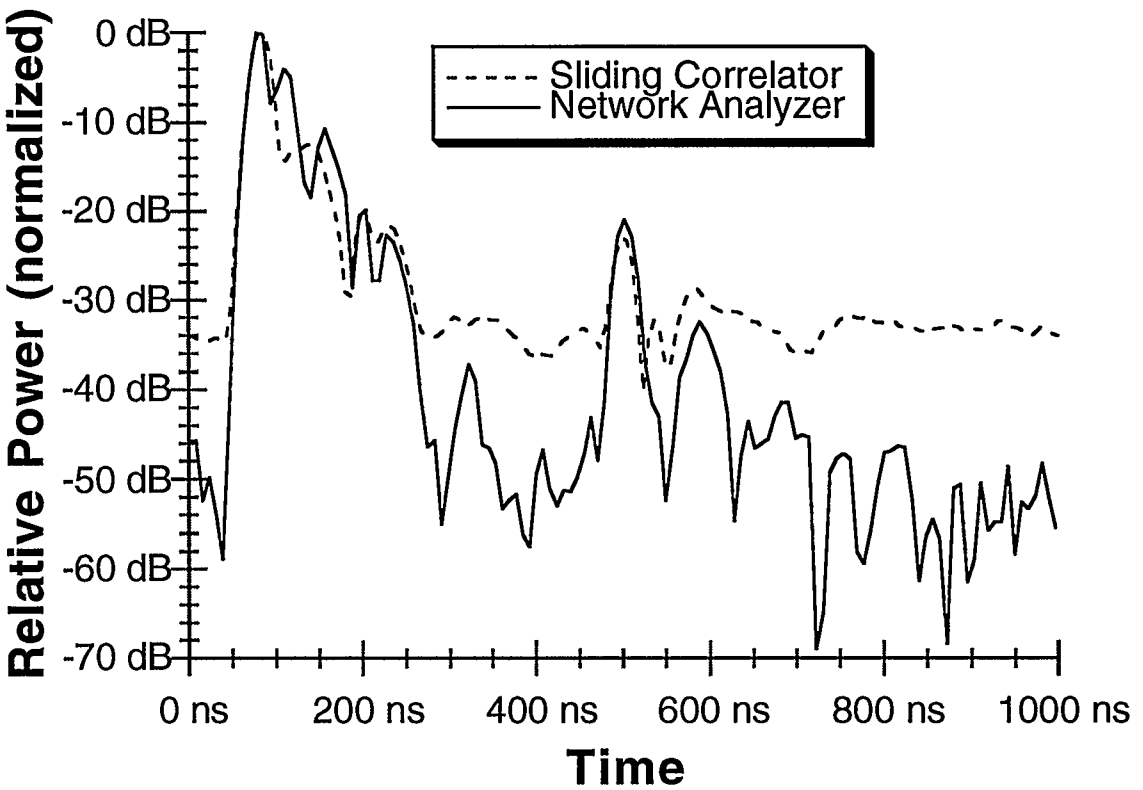

Figure 4.9: Comparison of Impulse Responses Obtained from a Sliding Correlator and a Network Analyzer.

It can be seen that the two profiles match closely except that the impulse response obtained from the frequency domain system has a larger dynamic range. Variation in the profiles peaks and nulls can be attributed to the

setup time between the measurements (up to 1 hour). An interesting feature that can be seen in these profiles is the presence of a distant reflector with an excess delay of approximately 420 ns. This means the path of the reflector is approximately 64 m longer than the path of the first arrival. The largest dimension of the building in which the measurements were taken is 38 m — so the reflector is external to the building. This result confirms that indoor communications can be influenced by external surroundings.

Clearly there are many tradeoffs between the two systems. The sliding correlator is much faster at data acquisition which makes it better for measurements where channel stationarity might be a concern (the network analyzer may not be the optimal frequency collection device for data acquisition speed). However, the frequency domain system can be easily implemented and provides a straight forward method for getting an impulse response with high resolution and excellent dynamic range.

4.5 Channel Reciprocity

Channel reciprocity studies are performed when the channel is charaterized for wireless duplex communications. Although it is generally assumed that reciprocity holds for indoor channels, findings of other researchers indicate that this phenomenon may not always be observed [Lafortune and Lacours, 1990].

A problem associated with reciprocity measurements is the need to reverse the order of transmisson while the channel is relatively stationary without changing the location of the antennas. In other words, what was the receive antenna becomes the transmit antenna and vice-versa.

The network analyzer is excellent for this type of measurement as it can perform S_{12} as well as S_{21} measurements. This means that channel transfer functions from these two parameters can be quickly collected one after the other without changing the system setup (note that the amplifier in figure 2.1 was removed before performing any measurements). Frequency and impulse responses from both measurements can then be compared [Morrison et al., 1991b].

Figure 4.10 shows the impulse responses from S_{21} and S_{12} measurements. It can be seen that the measured channel is observed to be reciprocal down to the noise level.

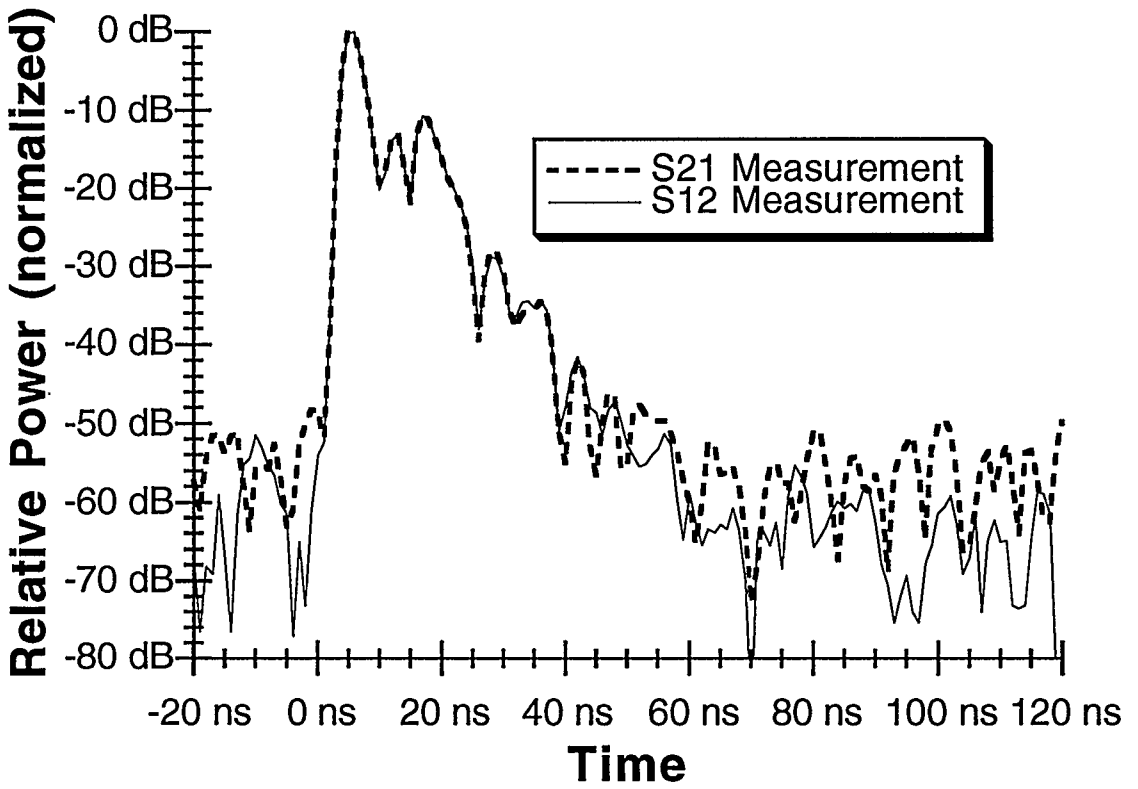

Figure 4.10: Impulse Responses from S_{12} and S_{21} Measurements.

4.6 Linear Array Simulation

Linear antenna arrays are used in determining the direction of a moving reflector or to determine the angle-of-arrival (AOA) spectrum of incident EM waves. Ideally, an antenna array consists of several antennas followed by individual receivers. This is a very costly experimental setup. By making the assumption that channel variations are not significant over a period of time, it is possible to evaluate the AOA spectrum in a channel illuminated by a single source.

The procedure for conducting this type of measurement is simply to collect the channel transfer function at one location, move the receive antenna in a straight line to the next location and repeat the process.

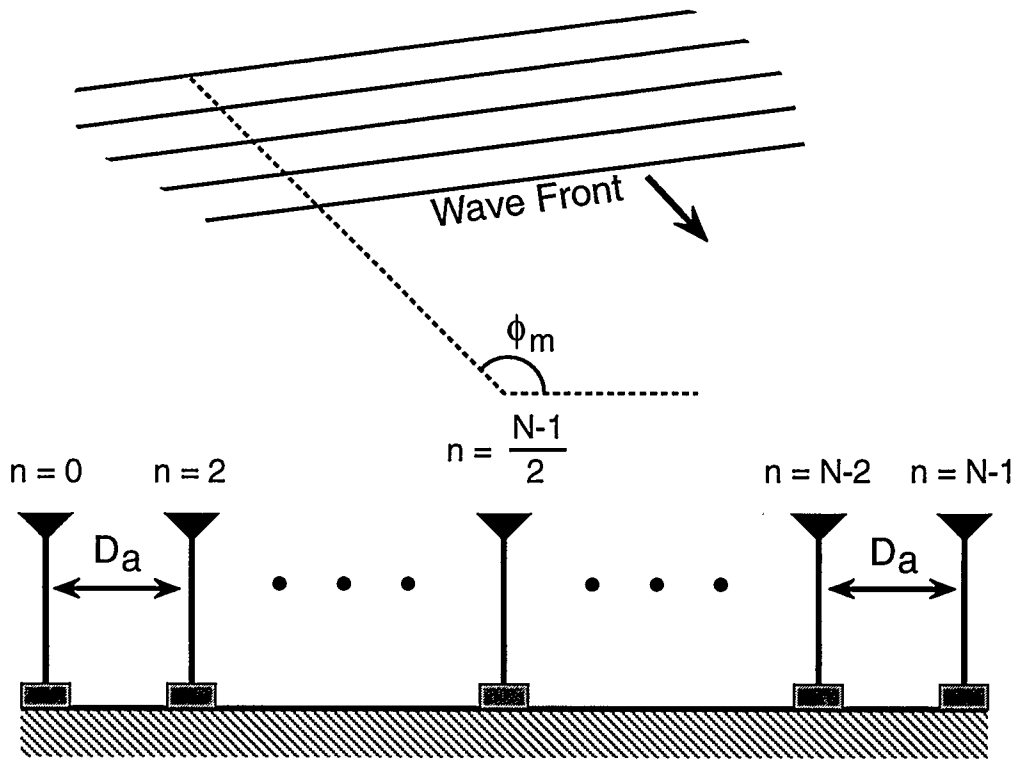

Figure 4.11: A Linear Antenna Array

Figure 4.11 shows the concept of of a linear antenna array. The array consists of N elements (antennas) that are equally spaced. The illuminating plane wave is received by each element for processing.

A detailed development of the theory is given in the references [Haykin, pp. 194-289; Tsui, pp. 235-265] and is summarized here. The signal at the *nth* element of an array by the *mth* plane wave may be described as

$$s(n,m) = a_m \exp\left[j\left(n - \frac{N+1}{2}\right)\theta_m\right]$$

where:
a_m is the signal amplitude
N is the number of elements in the array
θ_m is the electrical phase angle

θ_m is expressed by the following:

$$\theta_m = \frac{2\pi D_a}{\lambda} \cos \phi_m$$

where:
D_a is the interelement distance
λ is the received wavelength
ϕ_m is the AOA of the *mth* plane wave

The Fourier transform of the spatial series $s(n,m)$, is the angle spectrum $S_m(\phi)$, which is defined by the following expression:

$$S_m(\phi) = a_m \sum_{n=1}^{N} \exp\left[-j\left(n - \frac{N+1}{2}\right)(\phi - \phi_m)\right]$$

In words, the same sample bin from the impulse responses of each element is collected and the angle spectrum is found from the Fourier

transform. This can be viewed as taking the Fourier transform across the array of the individual impulse responses.

Measurements were performed on the 3rd floor of the NovAtel building when no other persons were present. OBS path measurements were performed by sweeping the channel from 1.6 GHz to 1.8 GHz and moving the receive antenna 1 cm for every sweep. A typical AOA spectrum from this measurement is shown in figure 4.12.

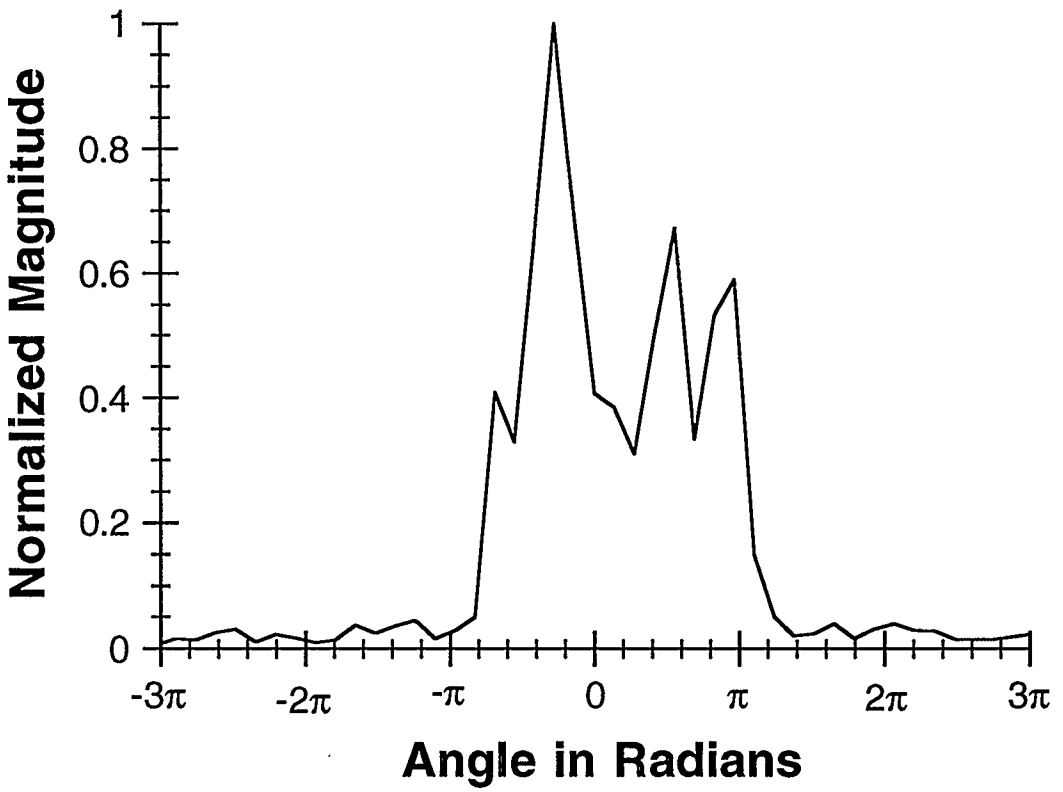

Figure 4.12: An Angle-of-Arrival Spectrum.

Note that the entire spectrum is between $\pm\pi$ as it should be. It can be seen that this spectrum contains direction information about 4 dominant plane waves. A 5th plane wave is also evident from the inflection point at

approximately $\pi/5$. Similar data was reported in the literature [Fattouche et al., 1990] where it was used to model the indoor environment for the purpose of simulating a digital cellular system with diversity.

CHAPTER FIVE

CONCLUSIONS

5.1 Experimental Results

This thesis presented a system for measuring the transfer function of the indoor RF propagation channel. The complex impulse response was obtained from the Fourier transform of the measured frequency response. Measurements were evaluated in both the time and the frequency domains to determine the operating parameters and overall performance of the system. Results for frequency domain measurements are scarce in the published literature and therefore traditional time domain analysis was invoked for most studies. Due to the equivalence of frequency and time, the frequency domain system reported in this study can also be considered as an impulse response determination system. Therefore, time domain analysis techniques are appropriate.

There are numerous indoor RF propagation studies that use time domain measurement systems so some expectations were formed prior to performing frequency domain measurements. These studies served as a benchmark for early system evaluation. The early analysis was encouraging as the results conformed to expectations. This led to more measurements being performed for both indoor channel characterization and system evaluation.

It was found that the system performed well and was robust to potential trouble areas like RF interference. Typical channel characterization measurements such as path loss and delay spread gave results that were comparable to those in the literature.

5.2 Viability of the Frequency Domain Measurement System for Indoor Channel Characterization

Indoor RF propagation studies have been ongoing for more than a decade and most characterization issues are still unresolved. This is not a result of improper research techniques but is a testament to the complex nature of the indoor RF propagation channel. This problem can be solved by: i) developing a flexible measurement system that enables a more detailed study of the indoor RF environment, and ii) encouraging a larger number of studies by making measurements more accessible to a larger number of researchers.

It will be shown in section 5.2.2 that the frequency domain measurement system addresses both points thus making it a valuable contribution to the field of indoor RF communications.

5.2.1 System Disadvantages

Perfect measurement systems do not exist so naturally there will be disadvantages. Problems that are common to all RF measurement systems are not considered disadvantages because they are not system specific. Two problems unique to the frequency domain measurement system are presented in this section.

1. The requirement of a long cable connection is not necessarily a disadvantage but it does limit the system to strictly indoor measurements. In most cases, this also confines both the transmit and the receive antenna to the same floor. It should be noted that the cable system is largely responsible for the accurate phase measurements which takes the guess work out of finding the distance of the direct and reflected paths.

2. The sweep time for wideband measurements may be slow for rapidly varying channels. This problem is overcome by performing measurements at times (e.g., nights and weekends) when the environment is less time varying.

Neither of the disadvantages discussed here is deemed serious as both can be managed by careful planning of the measurement experiment.

5.2.2 System Advantages

Like the previous section, this section is concerned with areas that are considered unique to the frequency domain measurement system. Highlighted here are eight points that are believed to be the strengths of the system.

1. The implementation of the system is straight forward. Although the HP network analyzer is a complex piece of equipment, it reduces the overall equipment count of the measurement system. In current time domain systems the individual transmit and receive sections each require several discrete components.
2. The system is accessible to a large number of researchers. This is because a network analyzer is a standard piece of test equipment in RF laboratories. This implies that the system is not dedicated for one purpose and therefore presents an economical method for channel characterization studies. This is not true for the specialized or complicated measuring systems used in time domain systems.
3. The system is very flexible as it is not restricted to either narrowband or wideband measurement studies. Additionally, it is

not limited to a specific frequency or sampling bandwidth. This is convenient for studies at different frequencies and for those requiring narrowband and wideband statistics on the same channel.

4. The system yields both magnitude and phase information. The phase information gives, among other things, an accurate estimation of the separation between the transmit and receive antennas. This is not found in other systems and is useful when direct measurement of the separation is not possible.
5. Interference rejection in wideband measurements is good. This may not be true for systems transmitting a narrow pulse at a specific frequency.
6. Reciprocity studies can be conducted quickly and conveniently without changing the experimental apparatus. This is a consequence of the S-parameter test set

7. A consequence of determining impulse responses from the Fourier transform results in an extended dynamic range. The available dynamic range is superior to that in current time domain measurement systems. In most cases, an increased dynamic range of two to three times over what was previously available can be achieved.
8. The impulse response of a channel can be obtained with a temporal resolution that has not been achieved by current time domain systems. Time domain systems that yield magnitude and phase information have reported resolutions of 25 ns

[Bultitude,1989]. Systems with magnitude information only have reported resolutions of 5 ns [Hawbaker and Rappaport, 1990]. In section 4.3.3 an impulse response with a 2.3 ns resolution is given. This is not the limit of the available resolution as it can be increased by sweeping a larger frequency band or by modeling (see section 2.4.3).

The advantages of the frequency domain measurement system are significant as they represent an advance in some aspects of current inbuilding measurement techniques. Consideration must be given to the pros and cons of any measurement system or technique. The fact that the advantages of the frequency domain measurement system weigh heavily against its disadvantages makes it an attractive system for indoor RF propagation studies.

5.3 Further Research

Over the past several years, measurement and characterization of the indoor RF propagation channel has been a topic of vigorous research. To date there are a number of unresolved issues and a number of uninvestigated areas that demand further measurement and modeling efforts. Some of these topics are presented here.

Due to the nature of traditional time domain measurement systems, frequency based models are unknown. A frequency model would be an asset as it may be represented in a more compact form than an impulse response model. In section 2.4.3 it was shown that a second order ARMA process produced an excellent fit of the measured data. This suggests the development of a statistically based empirical model.

The assumption of a uniform phase distribution (section 1.5) in the indoor environment is a carry-over from mobile communications in the outdoor channel. This assumption is based on a random distribution of scatterers which may not be correct for the indoor environment as the large-scale structure of buildings is highly patterned — usually cubical. As of yet, there has been no empirical verification of this phenomenon. This is most likely a result of the unavailability of measurement systems that yield phase information.

There are differing conclusions about path loss models reported in the literature [Alexander, 1983; Akerberg, 1988]. Additionally, the parameters of a given model have large variations depending on the environment. This dependence is not well understood.

Some reports show a relationship between τ_{rms} and transmitter-receiver separations [Devasirvatham, 1986; Zaghloul et. al. 1990b] and others' reports have found no relationship [Rappaport , 1989; Saleh and Valenzuela, 1987]. An established dependence of this parameter would greatly influence system design and therefore further investigations would be worthwhile.

Angle-of-Arrival modeling for the indoor channel has not been done. This type of modeling would most likely be statistically based and would be valuable for microcellular diversity studies [Fattouche et. al., 1990].

The issue of spatial and temporal correlations between path variables has not been addressed. Determination of any correlated relationships may have a significant influence on system design.

Current methods of analysis and modeling are based on correlation statistics that are phase blind. This may not be appropriate when phase information is available. Recent development of fast algorithms in higher order statistical analysis [Nikias and Raghuveer, 1987] has made extended

statistical modeling accessible. Mendel, who is a leading expert in the field of higher order statistical modeling, has stated that nearly all previous modeling methods would benefit from extended statistical analysis [Mendel, 1991].

The topics presented in this section can be mostly resolved through the analysis of a large data base. During the spring of 1991, a large data set using the frequency domain measurement system was collected. This data set consisted of 12,000 measurements from two dissimilar office buildings; 6000 measurements were made on the 19th floor of the AGT building in downtown Calgary and 6000 measurements were made on the first and third floors of the NovAtel building in Calgary. This is the largest collection of indoor measurements made to date. It is believed that a thorough analysis of this data base would yield an important contribution and further the understanding of indoor RF propagation behavior.

REFERENCES

Akerberg, "Properties of a TDMA Pico-Cellular Office Communication System," *Proceedings of IEEE Globecom'88*, December 1988, pp. 1343-1349.

Alexander S. E., "Radio Propagation within Buildings at 900 MHz," *Electronic Letters*, Vol 18, No. 21, 1982, pp. 913-914.

Alexander, S. E., "Characterizing Buildings for Propagation at 900 MHz," *Electronic Letters,* Vol. 19, No. 20, 1983, pp. 860.

Bultitiude, R. J. C., Mahmound, S. A., and Sullivan, W. A., "A Comparison of Indoor Radio Propagation Characteristics at 910 MHz and 1.75 GHz," *IEEE Journal of Selected Areas in Communications*, Vol. 7, No. 1, 1989, pp. 20-30.

Bultitude, R. J. C., "Measurement, Characterization, and Modeling of Indoor 800/900 MHz Radio Channels for Digital Communications," *IEEE Communication Magazine*, Vol. 25, No. 6, June 1987, pp. 5-12.

Cooley, J. W. and Tukey, J. W., "An Algorithm for the Machine Calculation of Complex Fourier Series," *Mathematics of Computation,* Vol. 19, 1965,.pp. 297-301.

Cox, D. C., "Delay Dopler Characteristics of Multipath Propagation at 910 MHz in Suburban Mobile Radio Environment," *IEEE Transactions on Antennas and Propagation,* Vol. 20, No. 5, September 1972, pp. 625-635.

Cox, D. C., Murray, R. R., and Norris, A. W., "800 MHz Attenuation Measured in and Around Suburban Houses," *AT&T Bell Laboratories Technical Journal,* Vol. 63, No. 6, July-August 1984, pp. 921-954.

Cox, D. C., Murray, R. R., and Norris, A. W., "Antenna Hieght Dependence of 800 MHz Attenuation Measured in Houses,"*IEEE Transactions on Vehicular Technology*, Vol. 34, No. 2, May 1985, pp. 108-115.

Cox, D. C., Murray, R. R., and Norris, A. W., "Measurements of 800 MHz Radio Transmission into Buildings with Metallic Walls," *The Bell System Technical Journal*, Vol. 62, No. 9, November 1983, pp. 2695-2717.

Devasirvatham, D. M. J., "Time Delay Measurements of Wideband Radio Signals within a Building," *Electronic Letters*, Vol. 20, No. 23, 1984, pp. 950-951.

Devasirvatham, D. M. J., "Time Delay Spread and Signal Level Measurements of 850 MHz Radio Waves in Building Environments," *IEEE Transactions on Antennas and Propagation*, Vol. 34, No. 11, November 1986, pp. 1300-1305.

Durante, J. M., "Building Penetration Loss at 900 MHz," *Proceddings IEEE Vehicular Technology Conference,* 1973, pp.1-7.

Fattouche, M., Morrison, G., Zaghloul, H., and Petherick,L. "Diversity for Indoor Radio Communications", *Proceedings of the 33rd IEEE Midwest Symposium on Circuits and Systems*, August 12-14, 1990, pp. 415-417.

Fattouche, M., Zaghloul, H., "Estimation of Phase Differential of Signals Transmitted Over Fading Channels," *Electronic Letters,* Vol. 27, No. 20, September 26, 1991, pp. 1823-1824.

Ganesh, R. and Pahlavan, K., "On the Modeling of Fading Multipath Indoor Radio Channels," *Proceedings of Globcom'89*, November 1989, pp. 1346-1350.

Goldman, S. J., *Phase Noise Analysis in Radar Systems Using Personal Computers.* New York: John Wiley and Sons, 1989.

Harris, F. J., "On the Use of Windows for Harmonic Analysis with the Discrete Fourier Transform," *Proceedings of the IEEE,* Vol. 66, No. 1, January 1978, pp. 51-83.

Hashemi, H., "Simulation of the Urban Radio Propagation Channel," *IEEE Transactions on Vehicular Technology*, Vol. 28, August 1979, pp. 213-224.

Hawbaker, D. A. and Rappaport, T. S., "Indoor Wideband Radiowave Propagation Measurements at 1.3 GHz and 4.0 GHz", *Electronic Letters*, vol 26, No. 21, 1990, pp 1800-1802.

Haykin, S., Editor, *Array Signal Processing*, Englewood Cliffs, New Jersey: Prentice-Hall Inc., 1985.

Hewlett Packard Test and Measurement Catalog, Santa Clara, California: Hewlett Packard Company, 1991.

Hoffman H. H. and Cox, D. C., "Attenuation of 900 MHz Radio Waves Propagating into a Metal Building," *IEEE Transactions on Antennas and Propagation*, Vol. 30, No. 4, July 1982, pp. 808-811.

Howard, S. J. and Pahlavan, K., "Measurement and Analysis of the Indoor Radio Channel in the Frequency Domain," *IEEE Transactions on Instrumentation and Measurement,* Vol. 39, No. 5, October 1990a, pp. 751-755.

Howard, S. J. and Pahlavan, K., "Statistical Autoregressive Models for the Indoor Radio Channel," *Proceedings of IEEE GLOBCOM'90*, 1990b, pp. 1000-1006.

Kiyoyuki, T., Kuwabara, M., "Cordless Telephone System and its Propagation Charateristics," *IEEE Transactions on Vehicular Technology*, Vol. 26, No. 4, November 1977, pp. 367-371.

Lafortune, J., Lecours, M., "Measurement and Modeling of Propagation Losses in a Building at 900 MHz", *IEEE Transactions on Vehicular Technology*, vol 39, No.2, May 1990, pp. 101-108.

Lee, W. C. Y., *Mobile Communications Engineering.* New York: McGraw-Hill, 1982.

Matthews, P. A., Molkdar, D., and Mohebbi, B., "Direction of Arrival and Frequency Response Measurements at UHF," *Proceedings of IEE 5th International Conference on Mobile Radio and Personal Communications,* December 11-14, 1989, pp. 43-47.

McGirr, A., NovAtel Communications Limited, Antennas and Propagation Group, Calgary, Alberta, Canada. Private Communications, 1990.

Mendel, J. M., "Tutorial on Higher-Order Statistics (Spectra) in Signal Processing and System Theory: Theoretical Results and Some Applications," *Proceedings of the IEEE*, Vol. 79, No. 3, March 1991, pp. 278-305.

Molkdar, D., "Review on Radio Propagation into and within Buildings," *IEE Proceedings,* Vol. 138, No. 1, February 1991, pp. 61-73.

Morrison, G., Fattouche, M., Zaghloul, H., Tholl, D., "Frequency Measurements of the Indoor Channel", *Proceedings of Wireless'91*, July 8-10, 1991b.

Morrison, G., Zaghloul, H., Fattouche, M., Smith, M., and McGirr, A., "Frequency Measurements of the Indoor Channel: System Evaluation and Post Processing Using IDFT and ARMA Modeling," *IEEE Pacific Rim Conference on Communications, Computers, and Signal Processing,* vol. 1, May 8-10, 1991a, pp. 71-74.

Nikias, C. L., "Bispectrum Estimation: A Digital Signal Processing Framework," *Proceedings of the IEEE*, Vol 75, No. 7, July 1987, pp. 869-891.

Olivier, P. and Tiffon, J., "Transfer Function Measurement as a Characterization of the Urban Mobile Radio Channel," *Proceedings of IEE International Conference on Antennas and Propagation*, April 1987.

Oppenhiem, A. V., Schafer, R. W., *Discrete-Time Signal Processing.* Englewood Cliffs, New Jersey: Prentice-Hall Inc., 1989.

Press, W. H., Flannery, B. P., Teukolsky, S. A., and Vetterling, W. T., *Numerical Recipies in C — The Art of Scientific Computing*, Cambridge: Cambridge University Press, 1988.

Proakis, J. G., *Digital Communications 2nd edition.* New York: McGraw-Hill, 1989.

Rappaport, T. S., "Characterization of UHF Muiltipath Radio Channels in Factory Buildings," *IEEE Transactions on Antennas and Propagation,* Vol. 37, No. 8, August 1989, pp. 1058-1069.

Rappaport, T. S.and McGillem C. D., "Characterizing the UHF Factory Radio Channel," *Electronic Letters*, VOl. 23, No. 19, 1987, pp. 1015-1017.

Rice, L. P., "Radio Transmission into Buildings at 35 and 150 MHz.," *The Bell System Technical Journal*, Vol. 38, No. 1, January 1959, pp. 197-210.

S-Parameter Design, Hewlett Packard Application Note 154, April 1972.

Saleh, A. A. M., and Valenzuela, R. A., "A Statistical Model for Indoor Multipath Propagation," *IEEE Journal on Selected Areas in Communications*, Vol. 5, No. 2, February 1987, pp.128-137.

Seidel, S. Y. and Rappaport, T. S., "Simulation of UHF Indoor Radio Channels for Open-Plan Building Environments,"*Proceddings IEEE Vehicular Technology Conference,* 1990, pp.596-602.

Shefer, J., "Propagation Statistics of 900 MHz and 450 MHz Signals Inside Buildings," *Microwave Mobile Radio Symposium*, Boulder, Colorado, March 7-9, 1973.

Slekys, A.G., "What's Ahead Worldwide for Digital Cellular," *Mobile Radio Technology*, Vol. 8, Issue 5, May 1990, pp.25-58.

Smith, M. R. and Nichols, S. T., "A comparison of models use as alternative magnetic resonance image reconstruction methods," *Magnetic Resonance Imaging*, Vol. 8, 1990, pp. 173-183.

Smith, M. R., Nichols, S. T., Henkelman, R. M., and Wood, M. L., "Application of autoregressive moving average parametric modeling in magnetic resonance image reconstruction," *IEEE Transactions on Medical Imaging,* Vol.5, No. 3, September 1986, pp. 132-138.

Suzuki, H., "A Statistical Model of Urban Multipath Propagation," *IEEE Transactions on Communications*, Vol. 25, July 1977, pp. 673-680.

Tsui, J., *Digital Microwave Receivers — Theory and Concepts*, Norwood Massachusetts: Artech House Inc., 1989.

Turin, G. L., Clapp, F. D., Johnston, T. L., Fine, S. B., and Lavry, D., "A Statistical Model of Urban Multipath Propagation," *IEEE Transactions on Vehicular Technology*, Vol. 21, February 1972, pp. 1-9.

Turin, G. L., "Communication Through Noisy, Random, Multipath Channels," *IRE Convetion Record*, 1956, part 4, pp. 154-166.

Welch, T., "A Technique for High-Performance Data Compression," *IEEE Computer Magazine*, Vol. 17, No. 6, June 1984, pp. 8-18.

Yegani, P. and McGillem C. D., "A Statistical Model for the Obstructed Factory Radio Channel," *Proceedings of Globcom'89*, November 1989, pp. 1351-1355.

Young, W. R., "Comparison of Mobile Radio Transmission at 150, 450, 900, and 3700 Mc.," *The Bell System Technical Journal*, Vol. 31, No. 6, November 1952, pp. 1068-1085.

Zaghloul, H., Fattouche, M., Morrison, G., and Tholl, D., "Comparison of Indoor Propagation Channel Characteristics at Different Frequencies", *Electronic Letters*, Vol. 27, No. 22, October 24, 1991b, pp. 2077-2079.

Zaghloul, H., Morrison, G., Fattouche, M., "Frequency Response and Path Loss Measurements of the Indoor Channel", *Electronic Letters*, vol 27, No. 12, June 6, 1991a, pp. 1021-1022.

Zaghloul, H., Morrison, G., Tholl, D., Davies, R. J., and Kazeminejad, S., "Frequency Response Measurements of the Indoor Channel", *Proceedings of Antem'90*, August 15-17, 1990b, pp. 267-272.

Zaghloul, H., Morrison, G., Tholl, D., Fry, M., and Fattouche, M., "Measurements of the Frequency Response of the Indoor Channel," *Proceedings of the 33rd IEEE Midwest Symposium on Circuits and Systems*, August 12-14, 1990a, pp. 405-407.

Zhang, H., "*A New Fading Model for Digital Mobile Communications* ", MSc. Thesis, University of Calgary, 1991.

Ziv, J. and Lempel, A., "A Universal Algorithm for Sequential Data Compression," *IEEE Transaction on Information Theory,* Vol. 23, No, 3, May 1977, pp. 337-343.

Ziv, J. and Lempel, A., "Compression of Individual Sequences via Variable-Rate Coding," *IEEE Transaction on Information Theory,* Vol. 24, No, 5, September 1978, pp. 5306.